© Copyright 2021

Xiasen Wang

Optimal Deployment of Public Charing Infrastructures in Transportation and Power Network

Xiasen Wang

A dissertation

submitted in partial fulfillment of the

requirements for the degree of

Doctor of Philosophy

University of Washington

2021

Reading Committee:

Don MacKenzie, Chair

Xuegang (Jeff) Ban

Xin Wang

Program Authorized to Offer Degree:

Civil and Environmental Engineering

University of Washington

Abstract

Optimal Deployment of Public Charing Infrastructures in Transportation and Power Network

Xiasen Wang

Chair of the Supervisory Committee:
Dr. Don MacKenzie
Civil and Environmental Engineering

Battery Electric Vehicles (BEVs) can reduce the emission of air pollution and greenhouse gas. One difficulty in promoting the usage of PEVs is the availability of charging infrastructures. Currently, the PEVs can be recharged at home and in public charging stations. A recharging method still under development and experiment is called dynamic wireless charging lanes. This method could charge the electric vehicles while driving on the road, so it is more time-efficient than charging stations.

This paper represents the first attempt to develop an optimal deployment design of charging lanes and fast charging stations, considering the traffic flow and electricity generation network simultaneously. Since the charging lane is still under experiment, we first designed a stated preference (SP) survey to seek the most attributes to influence BEV drivers' charging choice.

Next, given a transportation network and the corresponding power grid, we build a bi-level optimization frame so the user cost of BEV drivers could be minimized. We first assume that one BEV can only use one type of charging method. Based on this assumption, we build a traffic assignment model given the demand and location of charging facilities and combined it with the prediction model based on our stated-preference survey results. Then we design a two-stage solution algorithm to solve the prediction model and the traffic assignment model simultaneously.

However, because the two-stage algorithm is too slow to converge, we release the assumption that all the BEVs can only use one charging method. Then we reformulate the lower-level optimization problem. Given the path between each driver's origin and destination, the objective function is to minimize user costs. The decision variables include charging time at charging stations and charging lanes and the state-of-charge (SOC) at each node. The upper level is to minimize the transportation cost and electricity generation cost. The decision variables include the locations of charging lanes and charging stations and the electricity generated in each bus.

We use Karush–Kuhn–Tucker conditions (KKT) to turn the bi-level optimization problem into a single-level optimization, and finally using binary variables to turn it into a mixed-integer optimization problem. A numerical study and a sensitivity analysis are conducted with an integrated transportation-power network.

TABLE OF CONTENTS

LIST OF FIGURES

LIST OF TABLES

GLOSSARY

AC: Alternating Current

BEV: Battery Electric Vehicle

BPR: Bureau of Public Roads

CLRLM: Capacitated Flow Refueling Location Model

DCFC: Direct Current Fast Charging

EMF: Electro-Motive Force

FCLM: Flow-capturing Location Allocation Model

FRLM: Flow Refueling Location Model

ICE: Internal Combustion Engines

KAIST: Korea Advanced Institute of Science and Technology

KKT: Karush–Kuhn–Tucker conditions

NCP: Nonlinear Complementarity Problem

OD: Origin-Destination

OLEV: Online Electric Vehicle

PSRC: Puget Sound Regional Council

SMFIR: Shaped Magnetic Field in Resonance Transfer

SOC: State of Charge

SOP: Singe OD Problem

SP: Stated Preference

SVM: Support Vector Machine

UE: User Equilibrium

V2G: Vehicle-to-grid

VOT: Value of Time

WAEV: Wireless Advanced Electric Vehicles

WPT: Wireless Power Transfer

ACKNOWLEDGEMENTS

First, I would like to gratefully thank my advisor, Dr. Don MacKenzie, for his guidance, understanding, encouragement, patience, support, and help throughout the years. He is a great advisor, mentor, and friend to me in my Ph.D. period. I feel honored and fortunate to be his student and to work with him.

I would also show my special thanks to Dr. Xin Wang. He always gives me insight suggestions when I have problems, no matter in life and research. Without him, I would not finish my study. It is a pleasant and rewarding time to discuss my research with him. I want to thank Dr. Xuegang Ban and Dr. Shan Liu for being on my committee and their valuable guidance and comments. Their advice and support give me power in my Ph.D. study.

I also need to show my thank to my friends, Dr. Yang Zhou, Dr. Ruimin Ke, and Zhiyong Cui. They give me great help and suggestions in research and my life. I also would like to thank my Ph.D. colleagues Parastoo, Elyse, Tianqi, Chintan, Moein, Borna, and Zack. I wish you all the best in your research.

Last but most importantly, I would thank my parents for their support. Without them, I can never overcome the difficulties in my Ph.D. study.

DEDICATION

To my parents.

Chapter 1. INTRODUCTION

1.1 BACKGROUND

1.1.1 *Battery Electric Vehicles*

Battery electric vehicles (BEVs) are vehicles powered by electricity and can be recharged by external electricity sources. The electricity could be stored in battery packs in the vehicles. Instead of using internal combustion engines (ICE), BEVs' propulsion engines are electric motors and motor controllers operated in the charge-depleting model. In recent years, more and more interests in BEVs have increased dramatically because of the development of battery technology and the rising price of fossil energy [1][2]. Almost every car producer is developing BEVs. As of August 2020, BEVs' cumulative total sales are 1.6 million in the US [3], which is the world's third-largest stock of plug-in passenger cars after China and Europe [4]. The US market share of BEVs increased from 0.14% in 2011 to 1.9% of the total market in 2019 [5].

The advantages of BEV include four aspects:

- Low operating and maintenance cost
- Intense air pollution and greenhouse emission
- Less dependence on imported oil
- Vehicle-to-grid (V2G) system.

BEVs' operation and maintenance costs are lower because internal combustion engines (ICE) have low efficiency in converting fossil fuel energy to propulsion. The energy is wasted when idling and heating. However, BEVs have higher efficiency at converting the stored energy

to propel because they do not consume energy while at rest. Moreover, BEVs could capture and reuse as much as one-fifth of energy consumption during baking through the regenerative braking system. Specifically, gasoline engines' efficiency is only 15% to turn the fuel energy to propel the vehicle and accessories; the diesel engines' efficiency is 20%, but the efficiency of electric drive vehicles typically has as high as 80% [6].

The BEVs could generate less air pollution and greenhouse gas than conventional gasoline vehicles. BEVs operating using electricity emit no harmful pollutants such as carbon monoxide, ozone, lead, and various nitrogen oxides. This benefit of clean air is usually local because air pollution happens in the generation plants' location. From the perspective of life cycle analysis, the electricity generated to recharge BEVs should be from renewable or clean sources such as wind, solar, or nuclear power. If BEVs use electricity generated from coal-fired plants, they may emit slightly more waste gas than ICE vehicles [7].

Furthermore, many countries with a dependence on foreign oil have concerns about the oil supply and price. Besides, another matter is the national security of the most proven oil reserving countries. Therefore, the development of PEVs could be a solution to these problems. The last advantage of BEV is that this kind of technology allows drivers to sell the electricity in their batteries back to the power grid (called a vehicle-to-grid (V2G) system). This system takes advantage that most vehicles' parking time is much longer than the driving time [8].

There are also disadvantages of BEVs:

- Higher cost of batteries and ownership
- Risks of noise
- Security issues

- Availability of charging infrastructures
- The potential overload of the electricity grid.

The cost of BEV with battery racks is more expensive than the conventional ICE of gasoline vehicles due to their Lithium-ion battery pack's higher cost. Furthermore, a study published in 2011 claimed that the energy saving of BEVs could not offset their higher price compared with conventional gasoline vehicles without government subsidies [9].

Another issue is the risk associated with noise reduction. BEVs are operated by electricity, which reduces the noise compared with ICE vehicles. Although the harmful noise could be reduced, people with vision disorder may be in dangers because they may not see and hear the BEVs when they drive near. The security is another problem to promote the usage of BEVs, which includes the risk of a battery fire. Because Lithium-ion batteries may suffer thermal runaway and cell rupture when it is overcharged, or even combustion in some extreme cases [10].

The fourth issue of BEVs is the availability of charging infrastructures. It is widely assumed that the plug-in recharging happens overnight at home. But for residents living in places without an available charging power outlet may be less likely to buy a BEV. Because the public charging stations are the only charging choice for them [11]. Therefore, the public charging places should also guarantee the BEV drivers to complete their trip demands without their batteries running out. The deployment of charging infrastructures is a significant obstacle in promoting BEV [12]. Besides, electric vehicles' charging time could be much higher than gasoline vehicles' refueling time, even with direct current fast charging (DCFC). One solution is battery swapping stations, which are commonly used in the public transportation system. It could

save time but with a higher cost to buy extra batteries [13]. Another solution is dynamic wireless recharging lanes, which can charge the vehicles while driving [14].

The last issue of BEV is the potential overload of the electricity grid. The existing electricity grid and system may not have enough capacity to supply the additional power of BEVs in certain areas where they are concentrated. During charging a BEV at home, the electricity consumption is three times compared to a typical home [11]. It could increase the pressure of electricity, especially during summer peak hours.

This study solves two main limitations of BEVs: the availability of charging infrastructures and the potential overload of the power grid. We build an optimization work to decide the charging infrastructure locations considering the constraints of the electricity grid.

1.1.2 *Charging Infrastructures*

This study considered two types of charging infrastructures: stationary charging stations and dynamic charging lanes. Much literature has investigated the deployment of charging stations. However, because the charging lane is still under experiment and mainly used by public transportation, much less literature has researched it. Nevertheless, If the charging lanes are utilized in the future, there could be a tradeoff between the two charging methods. Charging lanes have a higher cost, but they can charge the vehicles while driving. Whereas charging stations have a relatively low charging cost, but the drivers must wait while charging.

Currently, public BEV charging facilities have a relatively low charging speed than fueling facilities, and most of the BEV drivers charge their vehicles at home. There are three levels of charging stations. A Level 1 charging provides a standard 120V household outlet, and it only provides about 5 miles of driving range per hour. The Level 2 charger supplies over 200

volts and can charge a typical EV with a rate of 12 to 60 miles of driving range per hour, depending on the power the charger supplied. Level 3 charging, mostly called “Direct Current Fast Charging” (DCFC), is different from the above two alternating current (AC) charging levels. This type of charger can supply some BEVs with as high as about 800 volts, and it can charge the BEVs to 80% state-of-charge (SOC) within 30 minutes [15].

The dynamic wireless charging lanes, which are still under experiments, have some applications in America and Asia. There are two types of charging lanes: conductive and inductive charging. Conductive charging transfers electricity by physical devices, and inductive charging transfers the power by wireless techniques. Now the wireless dynamic charging lanes are mainly used in public transportation and trucks. Some promising experiments of dynamic charging lanes are Wireless Advanced Electric Vehicles (WAEV) and Online Electric Vehicle (OLEV). Utah State University develops WAEV technology, and this technology is used to charge the electric buses on the campus [16]. OLEV is conducted by the Korea Advanced Institute of Science and Technology (KAIST) in Korea. They used dynamic wireless charging lanes to supply electricity to their OLEV, which is also a type of public transportation [17].

However, most charging stations' deployment methods in the literature use the simplest traffic assignment model on the road network or treat electric vehicles traveling as gasoline vehicles. The research of charging lanes focuses on the technology, cost, and experiment of this emerging charging technology. Still, few of them investigated the deployment model of charging lanes. Moreover, most deployment models assume that there is just one charging method on the road network. The only paper that combines charging lanes and charging stations as two recharging strategies are conducted in a corridor. Therefore, this paper, as far as we know, represents the first attempts to combine the two charging methods on the road network.

1.2 Problem Statement and Dissertation Objective

1.2.1 *Charing Behavior of BEV Drivers*

Because the charging lanes are still under experiment, the literature is sparse. They focus more on developing technology and investment, and very few of the works analyze the charging choice behaviors between charging lanes and charging stations. Therefore, this study's first objective is that, given the traffic conditions, including travel distance and cost of charging facilities, which charging method the drivers choose to use based on their situation.

To answer the first research question, we use DCFC as a substitute for charging lanes and design a stated-preference survey to seek the most significant attributes for drivers to choose charging lanes and DCFC. The survey includes socio-demographic information and a travel scenario. Then we dispatched it to the BEV drivers. After collecting the results, we use some classification methods to determine under which condition BEV drivers would like to use charging lanes instead of charging stations.

1.2.2 *Location Problem of Charing Facilities*

In addition to the attributes affecting charging lanes' usage, this study also addresses the location problem of charging lanes and DCFC stations together, considering the traffic network and the power grid. To the best of our knowledge, there is no current work covering the system of wireless charging lanes and DCFC stations together, considering both the transportation demand and the power network structure. This paper intends to fill this research gap. We envision a future in which high-efficiency wireless charging technology is mature and offers another charging choice to BEV drivers in addition to DCFC. This paper represents one of the first attempts to build the wireless charging lane system from the power supply level to the traffic

assignment level. We design an integrated network of charging facilities, including charging lanes and charging stations considering social welfare and the construction cost. Besides, this study also gives BEV drivers an optimal strategy given the charging facilities' locations to make a tradeoff between their energy needs and travel time. Therefore, we provide an entire design system from the planning level to the operation level.

1.3 Dissertation Outline

This dissertation proposal is organized as follows: Chapter 2 reviews the related existing literature about charging stations and charging lanes. It also includes the development of charging lane technology and DCFC charging station technology. We also reviewed some literature about the power grid and its connection with the charging facilities. Chapter 3 provides the overall structure of this study. Chapter 4 proposes the stated preference survey to investigate the charging choices of PEV drivers. Chapter 5 builds the traffic assignment model given the locations of charging facilities. Chapter 6 makes the location problem of charging lanes and charging stations. At last, Chapter 7 provides conclusions and discussion of future research.

Chapter 2. LITERATURE REVIEW

Because DCFC charging stations and charging lanes have appeared recently, there is relatively little research to investigate them, especially analyzing BEV drivers' charging behavior and the deployment of these charging facilities. This chapter reviews the existing technology and applications about charging lanes to understand this new charging method better. Next, we review the research about the cost and benefit analysis of charging lanes. Then, the deployment of both charging facilities is reviewed. Since locating charging stations for BEVs and placing refueling stations for conventional vehicles are similar, the literature about refueling stations' deployment is also included. Finally, the literature about the supporting system of the charging facilities is reviewed, such as the literature on the relationship of transportation network and electricity network.

2.1 Wireless Charing Lane Technology and Applications

There are two types of charging lanes technology: conductive method and inductive method. The conductive process is very similar to how modern trolleys or streetcars are powered in the cities. They use overhead electric wires or metal bars on the pavement to transmit electric powers to the vehicles. The inductive method uses technologies (such as Laser, photoelectric, radio waves, microwaves, and magnetic resonance coupling) to send electricity to vehicles without physical connections.

The earliest concept of wireless charging BEVs was proposed by Bolger in 1978 [18]. After that, significant technological accomplishments have been achieved in developing conductive charging technology. Herron introduced an eHighway concept of electrification of trucks to reduce their pollution [19]. They build some electric wires overhead to charge the

trucks on selected highways. Thus, trucks could be powered by these wires on highways and use a diesel engine or battery pack without charging wires. Scania's group is currently testing the conductive method and inductive method [20]. The group tested electric trucks receiving powers from overhead wires in a two-kilometer-long track in Gross Dölln outside Berlin. The group also test the electric buses receiving electricity from the inductive technology. The buses are refilled with enough power at each bus stop to complete the entire journey in just six-seven minutes. In Sweden, Volvo uses the technology of trams and trains: use two metal bars on the road to charge the electric trucks and cars [21]. They built a 400-meter track near Gothenburg to transfer electricity. The author claimed that the technology is safe for passengers because it only transmits electric powers when vehicles pass at a certain speed. However, this technology could only supply powers for cities. For highways, it needs more infrastructures.

The inductive method of electric charging vehicles, also called Wireless Power Transfer (WPT), has many advantages compared with wired charging lanes. WPT technology could also be used in stationary charging stations and dynamic charging lanes. Lukic and Pantic reviewed the development of WPT technology [22]. WPT could be used during stationary charging (at stationary charging stations), during opportunity charging (when the vehicle is parked for a short time, for instance, at the bus stop), and during dynamic charging (when the vehicle is driven at charging lanes). The authors claimed that for stationary charging and opportunity charging, the technology is mature under pertinent standardizations. However, dynamic charging technology is still under development. With the infrastructures installed on the road, this technology can extend BEVs' driving range because they could be recharged while driving. Besides, the battery size could be decreased with this technology: it only needs to support the vehicles when the charging lanes are not available.

The dynamic wireless charging could be used in two scenarios [23]. The first scenario is in urban areas, and the wireless charging infrastructures are installed at traffic signals. The second scenario is installing the infrastructures on highways with a specific distance interval. There have been some promising developments in operation. The first implementation is Wireless Advanced Electric Vehicles (WAEV) technology at Utah State University [16]. It is a new type of electric public transit vehicle that could reduce the battery's size and emission. The bus could recharge when it enters a bus stop or returns to the base station by stopping above a magnetic pad. The charging time at each bus stop is five minutes after a 15-minute operation. The bus could be operated for 12 hours a day with about 40 times of recharging. The second implementation is conducted by the Korea Advanced Institute of Science and Technology (KAIST) [17]. The KAIST developed the Online Electric Vehicle (OLEV) platform for electric buses in Gumi, South Korea, with a short passenger route. The route's current length is about fifteen miles using Shaped Magnetic Field in Resonance Transfer (SMFIR) technology. The electricity is generated by underground cables and transferred to the bus via a magnetic field under the vehicle. The size of the battery in the electric bus is just one-third of that in electric cars. Bisides, the length of charging lanes is only about 5% to 15% of the total road length, so just a few sections needs to be rebuilt [24].

The most crucial advantage of dynamic wireless charging is that it could enlarge the driving range of electric vehicles. It could eliminate the charging anxiety of electric vehicle drivers. Besides, after the technology is applied, it could reduce the congestion of charging stations [25]. Some disadvantages of dynamic wireless charging are still being researched. One paper claimed that induction charging infrastructures would harm health. When using induction facilities, electric vehicles could induce an Electro-Motive Force (EMF) in the human body [26].

2.2 Cost and Benefit Analysis

One of the biggest challenges to promoting the wireless charging lane is the high construction cost at the installation stage [22].

Jang et al. proved this claim by analyzing the initial investment cost of these three types of WPT charging (stationary charging, opportunity charging, and dynamic charging) [27]. The paper mainly focused on energy logistics costs in transportation, including transferring and storing energy. For each type of WPT charging, an optimization function is built considering the tradeoffs between EV batteries and infrastructures. The results pointed out that the dynamic charging might not be as competitive as the other two because of its high cost.

Ko et al. investigated the optimal wireless charging bus system design, especially for OLEV in South Korea [28]. Their paper aims to minimize the total system cost, and the decision variable is the location of charging lanes in a single bus route and the battery size in each bus. Based on their results, the total route distance is 2.85 km, and the optimal total length of the charging lane is 367.2 m (13%) along the route. Therefore, the charging lanes can expand the driving range of electric buses once the construction cost decreases in the future.

Both above papers claimed that the initial investment of wireless charging lane bus system is high at the installation stage. However, some researchers conclude that the wireless charging lane has its benefits in the long term and has similar costs with the stationary charging system.

Jeong et al. proved that the Wireless Dynamic charging could reduce the battery size due to the frequent charging using the charging lanes [29]. Their study also shows that dynamic charging lanes can be beneficial to battery life. As the paper of Ko et al. [28], the authors also

use the data of OLEV to build an optimization model to minimize the total costs of battery and power tracks. Based on their results, if we only consider the costs of battery and power tracks, the total costs of dynamic charging lanes are lower than those of charging stations. Besides, the authors state that due to the frequent charging, the battery life of charging lane electric vehicles could be improved compared to the stationary charging method.

Suomalainen and Colet compared the infrastructure costs of dynamic charging lanes and DCFC charging stations in the long term [30]. Their study's infrastructure costs include the installation size and related costs based on the demand, material, maintenance, and replacement costs in 25 years (from 2020 to 2045). They built a scenario with a 200 km highway in their article. They assumed a charging station every 30 km, and the charging lane length is 30 km, which could ensure all the vehicles finish their trip. Based on their model, the total costs of charging stations are $127.12M ($19.07M per station) in 25 years, and the total costs of charging lanes are $202.18M ($1.63M per mile) in 25 years. Based on their results, the charging lane costs are 60% higher than DCFC charging stations' costs. However, considering the charging lane could save BEVs' charging time, it is crucial to promote electric vehicles in the future.

Based on the literature, the dynamic charging lane's infrastructure costs are about 60% higher than the DCFC charging stations in the long term. However, we notice that since the charging lanes could charge the BEVs while driving, they could save charging time. Besides, the battery life of electric vehicles could be improved by using dynamic charging lanes. Therefore, charging lanes have the potential to expand the driving range of BEVs and promote the usage of them.

2.3 Deployment Methods of Charging Facilities

2.3.1 *Deployment of Charging Stations*

There are several methods to decide the optimal locations of charging stations. Some of them are based on the models to determine the locations of refueling stations. The models include:

- Travel data-based approach.
- Flow-capturing location model.
- Flow refueling location model.
- Clustering model.
- Traffic assignment-based approach.

The travel data-based approach is used to develop charging station models, such as simulation or theoretical methods, based on travel survey data from conventional gasoline vehicles. Therefore, this approach treats the travel behavior of BEVs as traditional vehicles.

Dong et al. proposed an activity-based assessment method to evaluate the BEV feasibility based on the real driving content. They use the travel survey data from the Puget Sound Regional Council (PSRC) [31]. This article first defined missed trips, which means the trips' distances are longer than the maximum driving range of BEV. The goal of the model in this article is to build the charging stations in the candidate places in the road network to minimize the number of missed trips, subject to a budget constraint.

In their model, the input variables include:

$s_{jd(k)}$: The travel distance of driver j's k-th trip on the day d (miles).

$t_{jd(k)}$: The dwell time after driver j's k-th trip on the day d (h).

$l_{jd(k)}$: The destination of driver j's k-th trip on the day d.

R_j: The maximum travel distance for driver j's BEV (miles).

r_j: The electric consumption rate of driver j's BEV (kWh/mile).

If there is a charging station at the driver's destination, the available charging power is $P_{l_{jd(k)}}$. If there is no charging station, then $P_{l_{jd(k)}} = 0$. Then the charging energy at the destination, measured in miles, could be determined by the battery's current state. The charging power of the station and dwelling time after the trip could be represented in the following equation.

$$R_{jd(k)} = min\left(R_j - R_{SOC,jd(k)}, \frac{P_{l_{jd(k)}} \times t_{jd(k)}}{r_j}\right) \quad (2.1)$$

Where, $R_{jd(k)}$ means the energy should be charged at the destination of driver j's k-th trip on the day d (miles).

$R_{SOC,jd(k)}$ means the battery's state of charge (SOC) at the destination of driver j's k-th trip on the day d (miles). This could be determined by the previous trip: $R_{SOC,jd(k)} = R_{SOC,jd(k-1)} + R_{jd(k-1)} - s_{jd(k)}$. A negative $R_{SOC,jd(k)}$ value indicates the range of BEV could not support the daily trip of the driver. Then the author counts it as a missed trip. Let y_{jd} represent the number of missed trips for driver j on the day d, the optimization problem could be written as:

$$Min \sum_{j} \sum_{d} y_{jd} \tag{2.2}$$

s.t.

$$\sum_{i} C_i \leq B \tag{2.3}$$

Where B is the total budget to install the charging infrastructures ($).

After building the optimization function, the authors used a genetic algorithm to find the charging stations' optimal locations. A numerical study is then conducted with PSRC travel survey data. The results show that within the PSRC region, a small budget and level-1 chargers are sufficient to support all the travel demands.

Xi et al. developed a simulation-based optimization model to determine electric vehicle chargers' location to maximize the private electric vehicles' service levels [32]. They also considered the charging time of electric vehicles and the condition that the drivers may not fully charge their vehicles. This paper separates the study region into sub-regions so that the OD demand could be calculated. Their approach includes three steps. The first step is to determine the EV flows between each sub-region. The author assumed a BEV adoption proportion based on demographic data. The authors developed a simulation model in the second step to determine the expected number of BEVs successfully charged at a candidate location based on the number of chargers in the location. The simulation model follows a simple rule: a BEV charges if and only if there is an unoccupied charger and occupied the charger for the whole parking duration. If there is no charger, the vehicle will park without charge for the entire parking duration. In the final step, the authors used a linear integer programming model to identify the location and number of chargers of charging stations in the study area. Finally, a sensitivity analysis is conducted. The results show that although the "optimal location is sensitive to the specific

optimization criterion considered, overall service levels are less sensitive to the optimization strategy."

Andrews et al. proposed an optimization model to determine charging stations' optimal location to support EV usage. They use the Metropolitan Travel Survey Archive (MTSA) data in Chicago and Seattle [33]. The authors first identified the vehicle tours in the data. They then used them as input to develop a "user charging model" to determine where to charge the vehicle and choose which level to charge. The model defined the failed vehicle, which means the tour could not be completed with the input information and the user's charging behavior. Then the public charging stations should be built to help eliminate the failed vehicles. A Mixed-Integer programming is built to assign the charging stations to each failed vehicle to minimize the vehicles' total distance to travel to the charging stations.

Hodgson firstly progressed the flow-capturing location-allocation model (FCLM) in 1990 [34]. The FCLM model's goal is to put the charging stations on the links with most flows subject to a certain number of charging facilities. Therefore, the objective function is:

$$Max\ Z = \sum_{q \in Q} f_q y_q, \tag{2.4}$$

Where, q denotes a particular OD pair; Q is the OD pair set; f_q is the flow of OD pair q; and y_q is a binary variable: if $y_q = 1$, the OD pair q is captured. The objective function is to maximize the flows captured.

After determining which OD pair is captured, the paper defined the location of charging stations. Let K denotes a set of all potential locations of charging stations. Then k denotes a potential facility location in set K, x_k is a binary variable, and if $x_k = 1$, there is a charging

station at location k. N_q is the number of nodes in OD pair q. They define the number of charging stations the system should build, p. Then the constraints for this problem are:

$$\sum_{k \in N_q} x_k \geq y_q \tag{2.5}$$

$$\sum_{k \in K} x_k = p, \tag{2.6}$$

The first constraint means flow on path q is captured only if there is at least one charging station on the path. The second constraint limits the number of facilities on the road network. Berman et al. found that if the facilities are built on the junctions instead of mid-on the link, they could also capture most of the flows, limiting the potential positions of the charging infrastructures [35].

Kim et al. expand the FCLM to consider the necessary deviations of drivers to refuel or recharge their vehicles [36]. The authors developed a mixed-integer linear programming model to decide the locations and refueling stations. The model includes the fuel those stations can capture, and the deviation distance vehicles need to travel to the stations. The test results show that the travel distance from the recharging station's path will affect the refueling stations' attraction.

The FCLM could capture most traffic flows so that the charging stations' utilization could be maximized. However, this method is mostly used when deciding the refueling stations for conventional gasoline. It could not guarantee that all the electric vehicles' trip could be satisfied. Furthermore, in FCLM, if there is one facility on the path, the whole path is considered covered. However, one charging station on the path may not be sufficient in the electric vehicle scenario

because of its location. Therefore, FCLM may not be the best method to solve the optimization of the recharging location problem.

Kuby and Lim progressed the Flow Refueling Location Model (FRLM) by extending the FCLM to find the optimal charging stations for alternative-fuel vehicles [37]. In the FCLM, if there is one refueling facility alone the path, the whole path is treated as covered. However, alternative-fuel vehicles may need more than one stop to refuel to complete the entire path. The FRLM optimizes the locations of p refueling stations on the network to maximize the flows to refuel. The authors built a mixed-integer programming formulation to model the problem. They analyzed the relationship between the number of refueling stations and the flow they captured.

In FRLM, most variables are the same as FCLM, and some new variables are introduced in the model. The first variable is the combination of facilities k that can refuel path q. Note that one facility combination may serve more than one path. H is the set of all the possible facility combinations. The optimization problem could be formulated as follows.

$$Max\ Z = \sum_{q \in Q} f_q y_q \tag{2.7}$$

s.t.

$$\sum_{h \in H} b_{qh} v_h \geq y_q \ , \forall q \in Q \tag{2.8}$$

$$a_{hk} x_k \geq v_h \tag{2.9}$$

$$\sum_{k \in K} x_k = p \tag{2.10}$$

$$x_k, v_h, y_q \in \{0,1\}, \forall q, k, h \tag{2.11}$$

The objective function is the same as FCLM, which needs to capture most of the road network flows. a_{hk} is a binary variable, and if facility k is in the combination h, $a_{hk} = 1$. v_h is another binary variable, and if all facilities in the combination h is open, $v_h = 1$. b_{qh} is another binary variable, and if the combination h could support the OD pair q, $b_{qh} = 1$.

The objective function is to maximize the flows that the charging stations can refuel. The first constraint is like FCLM. FCLM puts at least one facility in each captured path, but in FRLM, if one path is captured, at least one combination of facilities is needed to build. The second constraint controls v_h to be 0 unless the combination h is opened. The third constraint contains the number of total facilities.

However, the FRLM assumes that all the charging stations have enough chargers to support all the vehicles passing through them. Upchurch relaxed this assumption by introducing a Capacitated Flow Refueling Location Model (CLRLM) to limit the number of vehicles refueling in each charging station [38]. The first difference is that instead of using a binary variable y_q to indicate whether a path is captured, in CLRLM, the author used y_{qh} to indicate that the facilities in a combination would not exceed their capacity and to show exactly which combination could support a flow. Moreover, one facility combination may not be sufficient to support a whole path. So, y_{qh} is no more a binary variable but a continuous variable between 0 and 1. The second difference is that instead of using a binary variable x_k to indicate whether a facility in location k, in CLRLM, x_k should be an integer variable to suggest that there could be more than one facility in each candidate site. Because in a statewide road network, a site could be a town or a city. There likely has more than one charging facility. The third difference is that CLRLM adds a constraint to the capacity in each station. The model could be written as follows.

$$Max\ Z = \sum_{q \in Q} \sum_{h|b_{qh}=1} f_q y_{qh} \tag{2.12}$$

s.t. $$\sum_{q \in Q} \sum_{h|b_{qh}=1} e_q g_{qhk} f_q y_{qh} \leq c x_k \qquad \forall k \in K \tag{2.13}$$

$$\sum_{k \in K} x_k = p \qquad \forall q \in Q \tag{2.14}$$

$$\sum_{h|b_{qh}=1} y_{qh} \leq 1 \tag{2.15}$$

$$y_{qh} \geq 0 \qquad \forall q \in Q, h \in H \tag{2.16}$$

$$x_k \in \{nonnegative\ integer\}$$

Where y_{qh} is the proportion of flows in path q that can be refueled by combination h. x_k is the number of chargers located in site k. p is the total number of chargers that could be built. c is the number of vehicle stops that could be refueled at each charger, which could indicate the capacity of refueling chargers. e_q is the proportion of vehicles requiring refueling. g_{qhk} is the number of recharging times at node k for travelers of OD q stopping at facility combination h.

The objective function is like before, and it maximizes the flow that could be captured in the network. The first constraint limits the capacity of each charging facility in the system. The second constraint is the same as FRLM, and it specifies the total number of facilities needed to build. The rest constraints limit the value of y_{qh} and x_k.

However, these flow-captured related methods have the same defect. Although those charging stations based on these methods could have the highest utilization, they could not guarantee to meet all the OD demand conducted by electric vehicles.

Ip et al. proposed a Hierarchical Clustering method to location the BEV charging stations in urbanized areas, considering the traffic condition, street space, and power grids [39]. This paper introduced a two-step method to find the optimal location of charging stations. The first step is to determine the demand cluster or regions where at least one station is built by using the hierarchical clustering algorithm. The second step is to apply optimization technologies to meet the supplies and demand. To find each cluster's demand, the paper first measures the traffic occupancy in a city area by "road pressure sensors, road-side video surveillance cameras, and other traffic monitoring devices." Then the authors turned the traffic information data into data points over a control grid. The grid size is fixed, so the data point's value is proportional to the traffic occupancy rate. At last, the hierarchical clustering method is applied to group similar data points into clusters. After clusters were identified, the planner should decide the location of the charging stations. This paper showed three types of optimization: 1. Assign stations to clusters to reduce the operation cost. 2. the same as the first one but considering each station's capacity. 3. deciding the new stations in new cities based on the current traffic information and constraints.

All the above methods have some defects. First, they could not guarantee all the OD demand could be completed by electric vehicles. Second, they all assume that electric vehicles will choose the shortest path but not an equilibrium traffic assignment on the road network. It may not be realistic in the real driving scenario He et al. defined network equilibrium to consider electric vehicles' dynamic traffic assignment to decide the charging stations' optimal locations on the road network [40].

In this paper, at first, the authors assume that energy consumption does not depend on the traffic flow and travel time but only depends on the travel distance on the path. Therefore, whether the path could support an OD pair could be predetermined before the traffic assignment.

Then, in the traffic assignment process, the authors follow the user equilibrium. The user equilibrium means drivers will have the same travel time in all the usable paths with the same OD pair. No driver could reduce their total travel cost by switching paths.

To represent the model in mathematics, the author first built a graph $G\ (N, A)$ where N and A are set of nodes and links in the graph, respectively. $a \in A$ is a specific link in the network. Let W to be a set of OD pairs in the graph; g^w and P^w are the travel demand and the set of paths between OD pair $w \in W$. Then the path-link incidence could be dictated as $\delta_{a,p}$. In the matrix, if link a is in the path p, the value equals to 1, otherwise 0. f_p^w means the traffic flow on path $p \in P^w$ of OD pair $w \in W$. v_a is the traffic flow on link a in total and d_a is the distance of the link a. Then the travel time on link a depends on the traffic flow on this link, i.e., $t_a(v_a)$.

Note that P^w could not be used by all the electric vehicles because not all the paths have charging stations to support all the vehicles. Let $\hat{P}^w$ to denote all the available paths of OD pair $w \in W$. Then the formulation for network equilibrium is:

$$\min_f \sum_{a \in A} \int_0^{\sum_{w \in W} \sum_{p \in \hat{P}^w} f_p^w \delta_{a,p}} t_a(z)dz \tag{2.17}$$

s.t.
$$\sum_{p \in \hat{P}^w} f_p^w = g^w \qquad \forall w \in W \tag{2.18}$$

$$f_p^w \geq 0 \qquad \forall w \in W, p \in \hat{P}^w \tag{2.19}$$

The base model ignores the energy consumption due to the traffic condition. It also ignores the recharging time in the refueling station. Therefore, the author added the recharging time to the base model in the objective function. Let s_p^w denote the minimal time that an electric vehicle of OD pair $w \in W$ need to recharge in the path $p \in \hat{P}^w$, then the objective function turns to be:

$$\min_{f} \sum_{a \in A} \int_{0}^{\sum_{w \in W} \sum_{p \in \hat{P}^w} f_p^w \delta_{a,p}} t_a(z)dz + \sum_{w \in W} \sum_{p \in \hat{P}^w} s_p^w f_p^w \tag{2.20}$$

The constraints are the same.

Furthermore, the authors consider the flow-dependent energy consumption in the system. In other words, the energy consumption now depends on not only the distance the vehicle traveled but also the travel time through the link, which is more realistic. This time, the travel time in each path is not the same.

The authors divided each path p into n_p sub-paths to model the new scenario, denoted as $p_q, q = 1,2,\cdots,n_p$, based on the charging stations on the path. The sub-paths origin and destination are charging stations or origin or destination of the path p. There is no charging station in the middle of the sub-path. The energy consumption is denoted by $e_a(d_a, t_a)$, and the consumption will increase when the distance d_a and the travel time increase t_a. The author ignores the recharging time in this model. The author first introduced the concept of the charge-depleting path, which means that in a sub-path, the energy consumption of a BEV is precisely the size of its battery. In other words, if $e_{p_q} = \sum_{a \in A} \delta_{a,p}\, e(d_a, t_a) = L_{max}$, the whole path is called the charge-depleting path. The authors claimed that the travel time of all usable non-charge-depleting paths is the same under network equilibrium (denoted by u^w). The travel time of all usable charge-depleting paths is less than or equal to u^w. Then the model is a nonlinear complementarity problem (NCP) as follows:

$$\sum_{p \in P^w} f_p^w = g^w \qquad \forall w \in W \tag{2.21}$$

$$f_p^w \geq 0 \qquad \forall w \in W, p \in P^w \tag{2.22}$$

$$f_p^w \left(L_{max} - e_{p_q}\right) \geq 0 \qquad w \in W, p \in P^w, q = 1,2,\cdots,n_p \qquad (2.23)$$

$$\gamma_{p_q}^w \geq 0 \qquad \forall w \in W, p \in P^w, q = 1,2,\cdots,n_p \qquad (2.24)$$

$$\gamma_{p_q}^w f_p^w \left(L_{max} - e_{p_q}\right) = 0 \qquad \forall w \in W, p \in P^w, q = 1,2,\cdots,n_p \qquad (2.25)$$

$$\sum_{a \in A} \delta_{a,p} t_a + \sum_{q=1}^{n_p} \gamma_{p_q}^w \left(f_p^w - L_{max} + e_{p_q}\right) - \mu^w \geq 0 \qquad \forall w \in W, p \in P^w \qquad (2.26)$$

$$f_p^w \left[\sum_{a \in A} \delta_{a,p} t_a + \sum_{q=1}^{n_p} \gamma_{p_q}^w \left(f_p^w - L_{max} + e_{p_q}\right) - \mu^w\right] = 0 \qquad \forall w \in W, p \in P^w \qquad (2.27)$$

Note that this is just an equilibrium condition given the locations of charging stations. We still need to build a model to decide the optimal location of charging facilities. He et al. developed an optimization deployment model of the charging locations based on the network equilibrium condition. [41] Unlike the other paper considering the total travel time or cost from the drivers' perspective, this paper considers the social welfare includes driving and recharging time cost on the road network, and the penalty of the missed trip. The optimization problem of network equilibrium is now a constraint of the whole optimization problem.

2.3.2 *Deployment of Dynamic Charing Lanes*

In contrast to a large body of literature on charging stations' deployment, the literature focuses on charging lanes' deployment is sparser.

Because the construction cost of dynamic wireless charging lanes is higher than public charging stations, the technology is now mainly used for public transportation and freight transportation. Jang and his colleagues in KAIST did many works to optimize the location of charging lanes and battery sizes of electric buses. They optimized them in a closed environment in which vehicles are operated at regular speed with less traffic. [42] They turned the

optimization problem into a Mixed Integer Programming model and solved it accordingly. Besides, their another paper also progressed the model to make the electric buses operated in the open environment, [43] which means they manage their system in normal traffic condition considering the energy logistics.

Fuller examined the probability and cost of building dynamic wireless charging technologies in California for private electric vehicles [44]. The candidate destinations of EV travel are some popular regions in California. The paper test different combinations of wireless charging power (20-120 kW) and vehicle driving range (100-300 miles). The results show that a 200-mile driving range EV and a 40-kW wireless charging system could satisfy the travel demand between popular destinations in California. The cost of the whole system is about $2.5 billion. The author also claimed that a system combined with dynamic charging facilities and statistic charging stations could be more cost-effective over ten years than gasoline refueling. Moreover, the dynamic wireless charging system is more cost-effective than increasing the battery's size for electric vehicles.

Like the deployment of charging stations, the flow-capturing model could still be applied to optimize charging lanes' location. Riemann et al. progressed a model to locate a given number of wireless charging facilities for BEVs out of some candidate locations to capture most of the network's vehicles [45]. Moreover, FCLMs and FRLMs approach just assigned the traffic based on the shortest path. Riemann's paper uses the User Equilibrium to assign the BEV traffic on the road network. This model formulated the problem into a mixed-integer nonlinear program to capture most flows on the road network. The model could be formulated as follows:

$$Max\ Z = \sum_{w \in W} \sum_{r \in R^w} f_r^w y_r^w \tag{2.28}$$

s.t.
$$\sum_{k \in \Psi_{i,j,k}^w} x_k \geq y_r^w \qquad \forall a_{i,j} \in A_{i,j,k}^w, w \in W, r \in R^w \tag{2.29}$$

$$\sum_{k \in K} x_k = p \tag{2.30}$$

$$h_a = \sum_{w \in W} \sum_{r \in R^w} f_r^w \delta_{a,r}^w \qquad \forall a \in A \tag{2.31}$$

$$P_r^w = \frac{\exp\left(\alpha t_r^w + \beta y_r^w\right)}{\sum_{s \in R^w} \exp\left(\alpha t_s^w + \beta y_s^w\right)} \qquad \forall w \in W, r \in R^w \tag{2.32}$$

$$t_r^w = \sum_{a \in A} \delta_{a,r}^w t_a \qquad \forall w \in W, r \in R^w \tag{2.33}$$

$$t_a = t_a^0 \left[1 + 0.15 \left(\frac{h_a}{c_a}\right)^4\right] \qquad \forall a \in A \tag{2.34}$$

$$f_r^w = q^w P_r^w \qquad \forall w \in W, r \in R^w \tag{2.35}$$

The objective function also aims to capture as many as possible. In it, W is the set of OD pairs, and $w \in W$. R^w is the set of all feasible paths r of OD pair w. f_r^w is the flow in path r of OD pair w. Unlike the FRLM and the FCLM, the flow is not given but determined by a multinomial logit model. y_r^w is a binary variable, and if the route is captured, $y_r^w = 1$. In the first constraint, x_k is a binary variable that is the same in the FCLM. If there is a charging facility at site k, $x_k = 1$. Thus, the first two constraints are very similar to the FCLM. The first one guarantees that if there is one facility on the path, the path is captured. The second constraint limits the number of facilities in the road network. The third constraint determines the flows on the link a, h_a. t_r^w is the travel time of the whole path, which is determined by the fifth constraint, and the sixth constraint specifies the travel time of a particular link. The fourth constraint is a multinomial logit model to assess the probability of drivers choosing path r of OD pair w, P_r^w.

Then the flow of path r of OD pair w could be gained by the total flow demand q^w and the probability to choose the path r, P_r^w, in the last constraint. This paper assumed that if one vehicle passed a recharging lane, it could be fully charged. Thus, it could be treated as a modified FCLM.

However, Riemann's paper just treated the dynamic charging lanes as stationary charging stations without waiting time. It ignored the attributes of charging lanes. Some other articles improved the equilibrium conditions and improved the deployment algorithm based on network equilibrium. Chen et al. firstly modeled the travel behavior of drivers to select routes when the wireless charging lanes are available [14]. So, a network equilibrium is built that all the EV drivers could decide their charging plans to finish the trip with minimum travel time. Compared with the above article, the recharging plans are more detailed: it includes how long to charge and at what speed to charge. Then an optimization problem is built to determine the deployment and length of charging lanes with complementarity constraints.

Most of the deployment of charging lanes papers are only deploying the charging lanes. There is just one paper combined with the stationary stations and charging lanes together in a corridor [46]. The input variables include the number of charging stations, the chargers at each station, the length of charging lanes, and the charging price in each facility type. The authors first modeled the equilibrium condition of charging behavior along the corridor. The charging facilities are then assumed to be built by government agencies to minimize social cost and by private companies to maximize their profits to decide the number of charging stations, the number of chargers in each station, and the length of charging lanes in the corridor.

One assumption the author made in the paper is that the charging stations are uniformly distributed along the corridor to simplify the problem. The author also assumed that all the

vehicles on the corridor are EVs. They need to use either charging stations or charging lanes to finish the corridor. Assume the length of the corridor is l and the travel length of one battery unit is β. Let θ denotes the range anxiety factor of an EV with battery size E. In other words, when the battery of one vehicle is θE, the driver will choose to charge. Then the minimum charging amount to finish the trip is $\frac{l}{\beta} - \theta E$. The travel speed for all vehicles is v, and the value of time (VOT) is γ. Then the cost charging at stationary facilities are:

$$\gamma \cdot \frac{\frac{l}{\beta} - \theta E}{\alpha P_s} + q_s \left(\frac{l}{\beta} - \theta E\right) + \gamma \cdot \frac{l}{v} \tag{2.36}$$

Where α represents the recharging efficiency and P_s is the charging power. q_s is the charging price at charging stations. Similarly, the charging cost for dynamic charging facilities are:

$$c_e \left(\frac{l}{\beta} - \theta E\right) + q_l \left(\frac{l}{\beta} - \theta E\right) + \gamma \cdot \frac{l}{v} \tag{2.37}$$

Where c_e is the equipment cost per charging unit (about \$0.4/kWh with 10-year usage) and q_l is the charging price at charging lanes. When the above costs are equal, the VOT equals to

$$\gamma^* = (q_l + c_e - q_s) \cdot \alpha P_s \tag{2.38}$$

Based on this value, the traffic flows to use charging stations (f_s) and charging lanes (f_l) could be determined:

$$f_s = f \cdot \int_{\gamma_{min}}^{\gamma^*} h(x)dx \tag{2.39}$$

$$f_l = f \cdot \int_{\gamma^*}^{\gamma_{max}} h(x)dx \tag{2.40}$$

Then the deployment model could be progressed. m is the number of charging stations, and n_c is the number of chargers, d denotes the length of charging lanes. ξ represents the recharging efficiency and P_l is the charging power of charging lanes. Then:

$$\beta\theta E \geq \frac{l}{m+1} \tag{2.41}$$

$$mn_c \geq \frac{\left(\frac{l}{\beta} - \theta E\right) f_s}{\alpha P_s} \tag{2.42}$$

$$d \geq \left(\frac{l}{\beta} - \theta E\right) \cdot \frac{v}{\xi P_l} \tag{2.43}$$

$$d \leq l \tag{2.44}$$

These four equations could be four constraints in the optimization problem. The first constraint guarantees that all the vehicles could complete the corridor without running out of charge. The second constraint satisfies all the power needs of BEV at charging stations. The third constraint shows that the length of charging lanes should fulfill the power demand of BEVs. Then the cost of building one charging station with n_c chargers and the cost of building the one-mile charging lane used by f_l are given as follows:

$$C_s(n_c) = A_s + B_s^0 n_c + B_s^1 P_s n_c \tag{2.45}$$

$$C_l(f_l) = A_l + B_l P_l \cdot \frac{f_l}{v} \tag{2.46}$$

Where A_s is construction cost to build on charging station, B_s^0 is the construction cost to build one charger, B_s^1 is construction cost for one unit of electric power [47]. For charging lanes, A_l is construction cost and B_l is the cost of one-unit charging power.

In the optimization model, the public provision considered the total cost of construction and management of charging stations and dynamic charging lanes, charging time cost at charging stations, the cost of producing and transmitting electricity for charging facilities, the equipment cost of installing and enabling of BEVs in charging lanes, and the cost while driving for all the vehicles. On the other hand, the private provision just considered the total income of charging, the cost of construction, and the cost of transmission of the electricity to charging lanes and charging stations.

2.4 Supporting System of Charing Facilities

Besides the research focus on transportation, some researchers considered the supporting system of the dynamic charging lanes and DCFC charging stations, including the power supply, pricing, and the relationship between the electricity network and transportation network. It is crucial to have a business model in commercialization for charging lanes considering the supporting system. Still, the research investigating this aspect is sparse.

He et al. creates a mathematical model to determine the price of charging lanes and electricity [48]. Because the cost of electricity at the charging lanes could affect the route choice of BEV drivers, and the usage of charging lanes could also affect the operation of the power network and thus the electricity price. The study built two optimization models to decide the optimal first- and second-best price of charging lanes. The first price means when the government can manage both power network and transportation network. The second price means the government agency, e.g., traffic authority, can only manage the transportation network. Their results suggest that promoting BEVs and charging lanes could reduce the cost of energy consumption. It could also help government regulate traffic flow by applying the integrated pricing strategy.

Manshadi et al. built an optimization model considering both the transportation network and power grid [49]. The objective function of their optimization model is to minimize the electricity generation cost and transportation cost. In their model, the positions of dynamic charging lanes are fixed. All the BEVs follow the rules of User Equilibrium. The decision variables include BEV drivers' route choice and the electricity they charge at each charging lane to finish their trips. Their study also analyzed the battery size on the total travel cost of BEVs using a charging lane.

The above two studies have their focus. He's paper considered the charging price of the transportation network and power grid. Manshadi's analysis assigns the BEVs on the transportation network following User Equilibrium. However, the positions of the charging lanes in both articles are fixed. So, in our study, we try to include the charging lane positions to be a decision variable.

2.5 SUMMARY

The literature review shows that there are a lot of deployment models of charging stations. The FCLM and FRLM try to capture most of the flow on the network so that charging stations could be maximum. The clustering method tries to simplify the extensive road network into a simple network. The network equilibrium model improved the choice behavior of drivers. On the other hand, dynamic wireless charging technology is still under development. The current experiments are mostly utilized by public transit and trucks. The literature modeling deployment of dynamic charging lanes is sparser compared with charging stations. Most of their models are modified methods of charging stations. Besides, there is very little literature considering both transportation networks and the power grid. From the literature, we could also conclude that a system combined with dynamic charging facilities and statistic charging stations could be more cost-effective [44].

However, to our best knowledge, very little literature investigated the deployment of different infrastructure types and consider drivers' choice, especially considering transportation network and power network [46]. There may be various charging facilities, and drivers choose the infrastructures to charge their electric vehicles based on their demand. Thus, it is critical to understand the choice behavior of drivers of these two types of facilities. We need to build an optimal deployment model for charging stations and charging lanes on the road network.

This paper addresses the location problem of charging lanes and DCFC charging stations together. To the best of our knowledge, there is no current work covering the system of wireless charging lanes and DCFC charging stations together and considering both the transportation demand and the power network structure. This paper intends to fill this research gap. We envision a future in which high-efficiency wireless charging technology is mature and offers

another charging choice to BEV drivers in addition to DCFC. This paper represents one of the first attempts to build the wireless charging lane system from the power supply level to the traffic assignment level. We design an integrated network of charging facilities, including charging lanes and charging stations considering social welfare and the construction cost. Besides, this study also gives BEV drivers an optimal strategy given the charging facilities' locations to make a tradeoff between their energy needs and travel time. Therefore, we provide an entire design system from the planning level to the operation level.

Chapter 3. STUDY STRUCTURE

In this study, we first design a stated-preference survey to investigate which type of BEV drivers under what condition will choose to use charging lanes. Then we use a mixed logit model to make predictions. Next, this study builds a predicted traffic equilibrium model to consider the charging lanes and the charging stations on one road network based on the prediction model from the prediction model. We design an integrated two-step framework to combine the two processes. The first step is to determine the proportion of different charging methods users. The second step is to assign the traffic on the road network. Then we go back to the first step to recalculate the proportion until the two steps' results converge.

However, the objective of this study is to determine the optimal locations of charging facilities. To design the charging lane system, we characterize the entire design into a bi-level optimization problem. We regard the locations of building charging lanes, the DCFC stations along with the network, and the electricity generated by each bus in the power grid as decision variables in the upper level. The objective is to minimize the electricity generation cost and total traffic cost for all the BEV drivers. The decision variables in the lower level include the charging time on charging lanes, charging time on charging stations, and the State-of-Charge (SOC) at each node, given a path from the origin to the destination of each driver. It is to minimize the user costs of BEV drivers.

In this study, we use Karush–Kuhn–Tucker conditions (KKT) conditions to convert the bi-level optimization problem into a single-level optimization problem. We use binary variables to turn the non-linear optimization problem into mixed-integer linear optimization work and solve it accordingly. The structure of this study could be seen in the following figure.

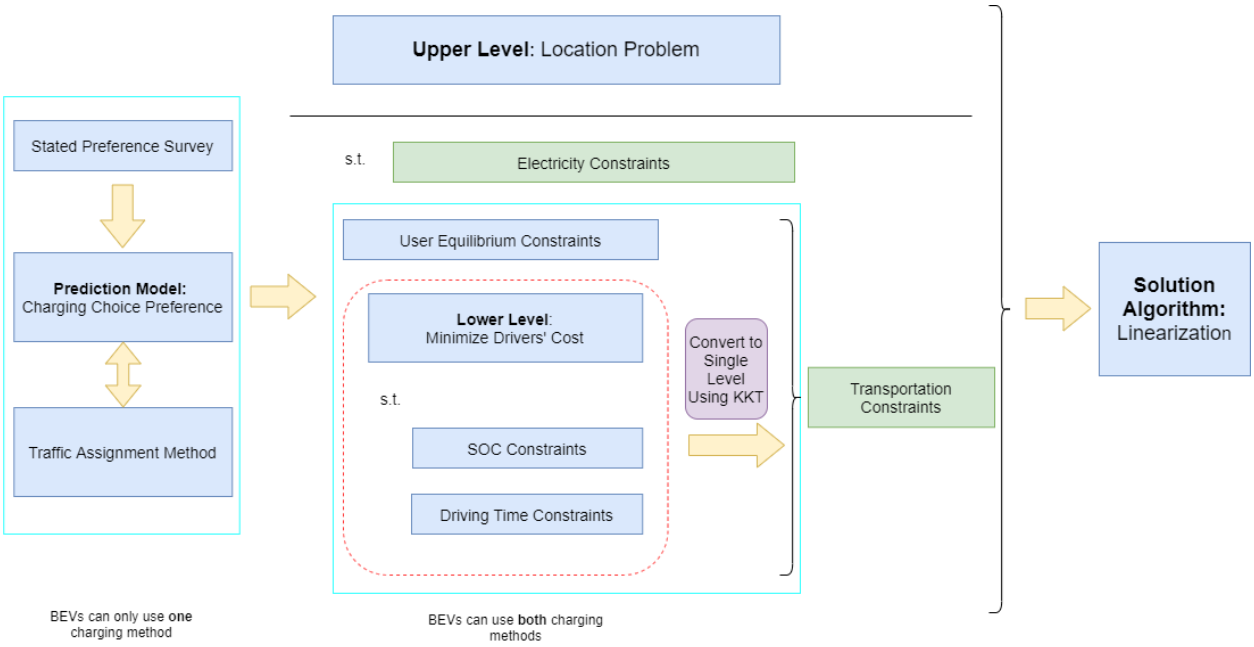

Figure 3.1 Study Structure Flow Chart.

Chapter 4. STATED PREFERENCE SURVEY

4.1 SURVEY DESIGN

We intend to seek the most important features to attract BEVs to use charging lanes in the first step. We also need to develop an appropriate model to predict BEV drivers' proportions using the two charging methods. So, the first research question could be answered. Since the charging lane is still under experiment, most BEV drivers do not have the experience to use it. We design a stated preference (SP) survey and dispatch it to 161 BEV drivers in China. Next, we try to find a prediction model, so we test three classification methods' accuracy.

Since dynamic charging lanes are still under experiment, we used an SP survey in this study. This SP survey includes two parts:

- A questionnaire of socio-demographic information (BEV ownership, gender, age, education level, monthly income, year of buying a BEV, days of driving a BEV per week); and
- A travel scenario includes six designed attributes shown in Table 3.1. Three designed attributes (travel purpose, travel distance, and SOC left) are shown to the respondents. The rest of the designed attributes (charging power of DC fast charging station, unit electricity cost of charging station and charging lane) are not given directly. Instead, we compute the total charging time, total cost of charging lanes and charging stations to make the scenario clearer to drivers to make the scenario more intuitive. The unit cost is based on the research of Jang et al [27]. The scenario given to the respondents is shown in Fig. 3.1.

We assume the driving range and battery size of BEV in the survey are the same, and the length of the charging lane is long enough to ensure the drivers complete the trip.

In our survey, each respondent who has experience of driving BEV is given 2 or 3 scenarios. Besides, having the experience of driving BEV does not mean the driver owns a BEV. Hence, BEV ownership is a variable in our prediction model. We sent the survey to China because China is one of the largest BEV markets worldwide. In 2017, there were 2.24 million BEVs in China, but the number of private chargers was just 0.23 million. It indicates most BEVs owners do not have personal chargers, and the public charging facilities are in high demand.

Table 4.1 Attributes and Their Levels of the Experiments.

Attributes	**Description**	**Attributes Levels**
Travel Purpose	The travel purpose of a one-way trip	Tourism, Commuting, Appointment
Travel Distance (km)	The total travel distance of the one-way trip	150 km, 180 km, 210 km, 250 km, 300 km
SOC left	The state-of-charge left when arriving the destination	10%, 25%, 50%, 75%, 100%
DC Charging Power (kW)	The charging power of DC fast charging stations	50kW, 100kW, 120kW
DC Charging Price (¥/kWh)	The unit electricity cost of DC fast charging stations	0.9, 1.2, 1.5, 1.8, 2, 2.4
Charging Lane Price (¥/kWh)	The unit electricity cost of DC charging lanes	2, 2.5, 3, 3.5

The scenario given to the respondents are shown in Figure 4.1.

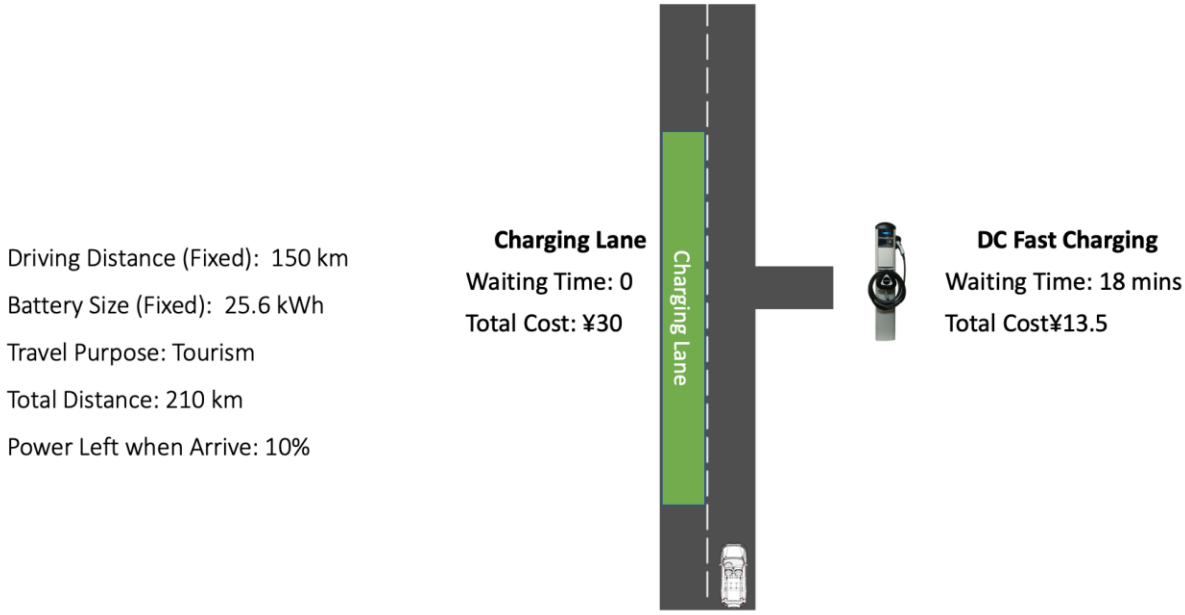

Figure 4.1 Screenshot of the Survey Tool: Charging Decision of a One-way Trip.

The full factorial design requires all factor combinations, and the number is huge (3 * 5 * 5 * 3 * 6 * 4 = 5400). Since we have 161 respondents, it is impossible to distribute all the combinations. This study chose to use a D-optimal experiment design, which is a computer-aided design containing the best subset of all possible experiments. [50] By using D-optimal, we reduced the total combinations from 5400 to 200. In our survey, each respondent has 2 or 3 scenarios. At last, we have 403 results.

4.2 Data Collection

The survey was dispatched to a Chinese BEV drivers forum from February 2018 to March 2018. We dispatch our survey during the two months and give some rewards to the participants who respond to it. There are 161 BEV drivers among 341 respondents (47%), and we only show the choice scenarios to the BEV drivers. BEV drives include BEV owners and the people who could drive BEV, such as car sharing.

Among all the results, 147 of the 341 respondents own a BEV (43%), and only 65 of them own a private charging facility. (20% out of all the respondents, 40% out of all the BEV

owners). Among all the BEV drivers, 60% of them are male, and 79% are under age 40. Most of them (66%) own the BEV for less than two years, and most of the BEV drivers' monthly income is less than 10,000 RMB ($1553.23). This indicates most BEV drivers must use public charging facilities to charge their vehicles. They are probably hard to afford a private charging position for their BEV. It is essential to build enough public charging methods to meet these BEV drivers' demands if we promote BEV usage.

Since we give each BEV driver 2 or 3 scenarios to choose between charging lanes and charging stations, we collect 403 travel scenarios. In all the 403 travel scenarios, 235 (58%) prefer to using charging lanes. We also included an intentional question in the survey for all the 341 respondents, which is whether they accept charging lanes or not in the future. If they choose to decline the technology, we also ask for the reason. The results show that only 25 (7%) of them reject using dynamic charging lanes, and the most concern is the safety to health.

4.3 Charging Choice Model

After getting the survey results, we intend to seek a classification method with the highest prediction accuracy. We can give us enough information about the choice decision of the drivers. The statistical classification method can demonstrate the value of coefficients and the significant level of each variable. On the other hand, the machine learning methods may have higher accuracy when we have sufficient data to train the model. This paper uses one statistical classification model (mixed logit model) and two machine learning models (random forest and support vector machine) to analyze our survey results data. Then we find the most accurate method to get the result.

4.3.1 *Mixed Logit Model*

We use the mixed logit model because the standard logit model has three limitations: random taste variation, restricted substitution patterns, and unobserved factors over time [51]. The Mixed logit model can prevent the limits because it utilizes some distributions for random coefficients. Our model makes the sociodemographic parameter. Some trip information parameters include travel distance and cost difference (the cost difference of charging lane method and charging station method) to be random. So different people can have different coefficients to predict the probability of choosing charging lanes and charging stations.

The probabilities of mixed logit choices are integrals of the standard logit function and a density of coefficients. A mixed logit model whose choice probabilities can be expressed in the following form:

$$P_{ni} = \int \left(\frac{e^{\boldsymbol{\beta} \cdot \boldsymbol{x_{ni}}}}{\sum_{j \in I} e^{\boldsymbol{\beta} \cdot \boldsymbol{x_{nj}}}} \right) f(\boldsymbol{\beta}) d\boldsymbol{\beta} \tag{4.1}$$

Where, P_{ni} means the probability of individual n having choice i ($i \in I$ with I denoting all possible choices for individual n).

$\boldsymbol{\beta}$ is a coefficients vector and $\boldsymbol{x}$ is a characteristic vector.

$f(\boldsymbol{\beta})$ is density function of $\boldsymbol{\beta}$.

However, there is no closed-form to solve the integral to get the choice probabilities. "Rchoice" package in R provides a simulation method to gain the value of the probabilities [52].

4.3.2 *Support Vector Machines*

The next classification method we use is support vector machines (SVM). Unlike the logit model obtaining choice probabilities, SVM uses classifiers to build a non-probability supervised classification model. Given a set of training data labeled as belonging to one or the other

category, SVM can create an algorithm based on the training data set to assign a new example [53].

The SVM classification algorithm is building a hyperplane in a p-dimensional space, where p is the number of variables in the model. Then all the training datasets are drawn in it. The algorithm's task is to build some gaps called decision boundaries between different categories as broad as possible. New data points are mapped on the hyperplane and decided to belong to a class based on which side they lay.

The core problem of SVM is how to define the decision boundaries between categories. Unlike linear classification models with linear boundaries in the space, SVM uses a much higher dimensional space, making separation easier to map data. We build a map function, $\phi(x_i)$, to project the data point, x_i. Given the decision boundaries and two categories $+$ and $-$, the decision rule is:

$$w \cdot \phi(x_i) + b \geq 1, then + \tag{4.2}$$

$$w \cdot \phi(x_i) + b \leq -1, then - \tag{4.3}$$

In the two formulas, w denotes a vector to represent boundaries.

$\phi(x_i)$ means the projection in the higher dimensional space of data point x_i.

b is a constant vector to represent the intercept of decision boundaries.

1 and -1 represent the width of decision boundaries. The equations hold if the data point in the gutter of the boundaries.

We need to find the vector w to represent the decision boundaries. Because the boundaries should be as wide as possible, they can be obtained by an optimization process. Literature proved that it could be represented as a linear combination of all the data points [53]:

$$\boldsymbol{w} = \sum_j \alpha_j \cdot y_j \cdot \phi(x_j) \tag{4.4}$$

Where α_j are constants getting from the optimization process.

y_j are true labels (+1 or -1) of data points x_j.

Then the decision rules turn to be:

$$\sum_j \alpha_j \cdot y_j \cdot \phi(x_j) \cdot \phi(x_i) + \boldsymbol{b} \geq 1, then + \tag{4.5}$$

$$\sum_j \alpha_j \cdot y_j \cdot \phi(x_j) \cdot \phi(x_i) + \boldsymbol{b} \leq -1, then - \tag{4.6}$$

Now the problem is how to get the dot product of two data points $\phi(x_j) \cdot \phi(x_i)$. We define a function called kernel function $k(x_i, x_j)$. It just obtains the dot product of two points on the higher dimensional space. The exact form of map function $\phi(x_i)$ is not included [50]. Some examples of kernel functions include Linear kernel ($k(x_i, x_j) = x_i^T x_j$) and Gaussian kernel ($k(x_i, x_j) = e^{-\frac{\|x_i - x_j\|^2}{2\sigma^2}}$).

4.3.3 *Decision Tree*

The third classification method we use in the study is the random forest. To better understand the random forest, we first present the concept of the decision tree. The decision tree builds a tree-like structure to decide, in which each node is a test of an attribute [54]. Each branch connected to the node means the outcome of the trial. The path from the root to the leaf means the classification rule.

However, this algorithm's disadvantage is obvious. In each node of the tree, we need to consider all the features, and the tree can be so deep that the decision rule is not meaningful. Besides, suppose the tree structure is too complicated. In that case, it might be overfitting for the training data (it only fits the data used to build the model).

An advanced method to reduce the calculation time is tree bagging. [55] It builds multiple decision trees, and the outcome is the mode of results from these trees. Given a training data set, the tree bagging algorithm repeatedly (B times) selects a random subset from it with replacement and trains B decision trees. The tree bagging method decreases the variance without increasing the bias. However, each tree still must include all the features.

The random forest model is very similar to tree bagging. The only difference is that in addition to randomly select train data, this model also randomly selects features in the splitting learning process. So, it is sometimes called “feature bagging.” Typically, if a model has p features, each tree uses $\sqrt{p}$ features to split data [55].

4.3.4 *Evaluation of the Three Models*

To evaluate the three models, we compare the prediction accuracy of their results. For the two machine learning models, we use 80% of all data to be the train data and the rest to be the test data. The same train data set is also used to build a mixed logit model. Because the mixed logit model's prediction outcome is probabilities, to get the classification, we define if the probability is higher than or equal to 0.5, the output is 1 (choosing to use charging lanes). In contrast, if the probability is less than 0.5, the outcome is 0. (The threshold of 0.5 is calibrated by cross-validation method) The results are presented in Table 4.2.

Table 4.2 Classification Results of Three Models.

	Mixed Logit Model	**SVM**	**Random Forest**	**Actual Data**
True Positive	363	416	362	458
False Positive	129	268	184	
True Negative	213	74	158	342
False Negative	95	42	96	
Accuracy	72%	61.25%	65%	

In Table 4.2, the term “Positive” means drivers utilize charging lanes, and “Negative” indicates drivers use charging stations. “True Positive” implies the predicted and original data are positive, and “False Positive” means the prediction is positive, but the actual data is negative. Similarly, “True negative” implies the predicted and original data are negative, and “False Negative” means the prediction is negative, but the original data is positive. The summation of the “True Positive” and the “True Negative” is the number of successful predictions. The accuracy is the quotient of the number of successful predictions and the total data number.

Table 4.2 demonstrates that the mixed logit model has the highest prediction accuracy compared to the two machine learning classification models. It may be because our dataset is not large enough to train a suitable machine learning method. The accuracy of the random forest model is slightly lower. The numbers of True Positive and False Negative are close. Still, the number of False Positive is higher than the mixed logit model. It implies that the random forest model is more likely to predict users using charging stations to use charging lanes. SVM model has the lowest prediction accuracy, but it has the highest number of True positive. So, given any input, the SVM model tends to predict it as a charging lane trip.

Another advantage of the mixed logit model is that it could tell us the noteworthy features to affect the drivers' charging choice. Table 4.3 displays the coefficients of the mixed

logit model. The reference level uses the charging station, which means if the results are close to zero, the BEV drivers prefer to use the charging station. In contrast, if the results are close to one, the BEV drivers prefer to use the charging lane.

From the result, for sociodemographic attributes, income significantly influences the charging choice of BEV drivers. People with higher income would like to use charging lanes instead of charging stations. The preference may because the value of time of people with the higher income is high, so these people choose to use the charging lane to save their charging time.

We could see the cost difference, travel distance, and SOC left for travel attributes significantly affect the charging method choice in our survey. With power left increases, people would like to choose dynamic charging lanes. Because when the energy left at the destination is high, people need more electricity. Using a charging lane could save a lot of charging time compared to charging stations. When the cost difference increases, people prefer to use charging stations; drivers prefer to use charging lanes when the travel distance increases. Besides, the standard deviation of cost difference also significantly affects the charging choice. This indicates substantial variations across individuals in their choices based on the cost difference, and the effects of different levels of cost are not the same. Even if it is not statistically significant, we notice that the constant term has a significant impact on the choice probabilities. The constant value is about -1.3, which indicates the respondents have a high probability of using charging stations if other parameters are not given.

Because the mixed logit model has the highest accuracy, we decide to choose it to classify the data in our numerical example.

Table 4.3 Mixed Logit Model Result.

	Estimate	Std. Error	z-value	Pr(>|z|)
constant	-1.31	1.31	-0.998	0.31819
Own PEV	-0.0424	0.253	-0.168	0.86673
Trip purpose (ref = Shopping)				
Commuting	0.157	0.263	0.596	0.55125
Appointment	0.272	0.267	1.019	0.30835
Mean of Travel Distance	0.0125	0.00615	2.028	0.04259*
Std of Travel Distance	0.285	0.0891	3.202	0.13639
Mean of Cost Difference	-0.0304	0.00899	-3.382	0.00072**
Std of Cost Difference	0.165	0.0166	9.973	<2e-16***
Power Left	0.0229	0.00914	2.508	0.01214*
Waiting Time	-0.000767	0.0121	-0.063	0.94943
Gender: Male	0.221	0.245	0.903	0.3667
Mean of Age	0.00605	0.0141	0.43	0.6672
Std of Age	-0.144	0.0283	-5.088	0.7842
Education (ref = less than high school)				
High School	0.047	0.312	0.151	0.8803
Undergraduate	-0.387	0.335	-1.155	0.24809
Graduate	-1.22	0.529	-2.299	0.0215*
Higher	-0.415	0.898	-0.462	0.64394
Mean of Income	1.49	0.671	-2.214	0.02684*
Std of Income	0.28	0.0918	3.046	0.1299
Mean of Year of Buying BEV	0.0161	0.0099	1.624	0.10429
Std of Year of Buying BEV	0.0114	0.00737	1.540	0.12362
Signif. codes: 0 ‘***’ 0.001 ‘**’ 0.01 ‘*’ 0.05 ‘.’ 0.1 ‘ ’ 1				
Log Likelihood: -263.3				
Number of observations: 403				
Number of iterations: 3				
Exit of MLE: successive function values within tolerance limit				

4.4 SUMMARY

This section designed a stated-preference survey and disputed to BEV drivers to see under which condition the BEV drivers will choose to use charging lanes. Besides, we choose some classification models to predict the results. Finally, we decide to use the mixed-logit model as

SVM, random forest, and mixed logit model as our prediction model and compare their prediction accuracy. At last, we choose to use the mixed logit model because it has the highest prediction accuracy.

Based on the mixed logit model result, we found that the mean cost difference, travel distance, income, and SOC left significantly affect the charging method choice. People with higher income our they need more power to charge prefer to use the charging lane. However, if the charging lane's electricity price is too high, drivers choose to use the charging station.

Chapter 5. TRAFFIC ASSIGNMENT MODEL ASSUMING ONLY USE ONE CHARGING METHOD

This section discusses the lower-level optimization: given the locations of dynamic charging lanes and charging stations, what the BEV drivers' choice of charging facilities. This section assumes that each BEV can only use one charging method and solve the traffic assignment. The volume of each origin-destination (OD) pair is decided by the mixed logit model above.

5.1 NETWORK EQUILIBRIUM MODEL

Before we build the traffic assignment model, some assumptions and considerations are listed as follows:

- All vehicles are electric vehicles with the same battery pack.
- All electric vehicles need only one charging method to carry out their travel.
- The energy consumption only depends on the travel distance, i.e., the consumption is flow-independent, as suggested by [1], [2].
- We disregard the queuing time at charging stations.
- When in dynamic charging lanes, drivers could choose to charge or not, and they do not need to change their speed to charge.
- All vehicles travel at the same speed in one link, but their travel speed might differ in different links built on the traffic flow.

The notations in the model are listed below:

- $G(N, A)$ denotes the network; N is the set of nodes and A is the set of links.

- a denotes a link with starting node i and ending node j, and $a = (i, j) \in A$. (The links on the graph are directed.)
- W means the set of O-D pairs and w is one O-D pair on the road network, $w \in W$.
- g_s^w denotes the demand of charging station and g_l^w denotes the demand of charging lane for the O-D pair w
- P^w means the set of paths between O-D pair w. p denotes one path.
- $\delta_{a,p}$ means path-link incidence, where the value equals to 1 if path p passes the link a and 0 otherwise.
- E denotes the initial SOC of the BEVs.
- E_{max} means the maximum battery size.
- β denotes the distance of one-unit electricity can travel (we assumed that the energy consumption is only related to the travel distance, so β is a constant).
- γ is the electricity the charging lanes could provide per mile.

However, in our problem, not all the paths in P^w could support electric vehicles to finish the trip for O-D pair w. He et al [6] defined the concept of the **usable path**, which means electric vehicles could complete the path with or without recharging. In our problem, there are two charging methods: charging lanes and charging stations. We defined two concepts: the **station-based usable path**, which means the BEV can finish the trip by using charging stations only, and the **lane-based usable path**, which means the BEV can finish the trip by using charging lanes only. The following node network shows an example of the two types of usable paths.

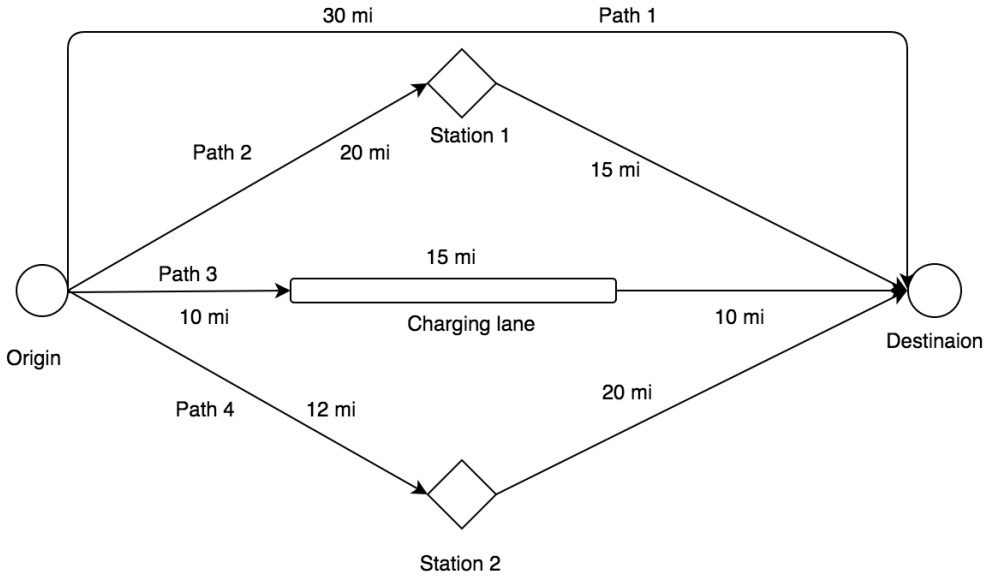

Figure 5.1 Illustration Network

The above network shows an O-D pair connected by four paths. Path 2 and Path 4 have one charging station in the middle, and Path 3 has a charging lane. Suppose the initial SOC of BEV is 8 kWh, and the distance of one-unit electricity can travel is three mi/kWh. The maximum battery size of BEV is 30 kWh. For charging lanes, the power it could provide per mile is 2 kWh/mi. We could easily find that Path 1 is not a usable path; Path 2 and Path 4 are station-based usable paths; Path 3 is a lane-based usable path.

Now we can define variables related to usable paths:

- $\widehat{P_s^w}$ and $\widehat{P_l^w}$ denote the set of station-based usable paths and the set of lane-based usable paths of O-D pairs w respectively. s denotes one station-based usable path and l denotes one lane-based usable path. ($s \in \widehat{P_s^w}$, $l \in \widehat{P_l^w}$)
- L_s denotes the length of path $s \in \widehat{P_s^w}$ and L_l denotes the length of path $l \in \widehat{P_l^w}$.

- f_s^w and f_l^w denote the flow on the path $s \in \widehat{P_s^w}$ and $l \in \widehat{P_l^w}$ for electric vehicles using charging stations and charging lanes, respectively.
- L_a denotes the length of link a.

With the length of the path and the initial SOC, the minimum electricity needs to be recharged could be represented as $\frac{L}{\beta} - E$. The flow on a link a contains both flows using charging stations and charging lanes for all the O-D pairs. It could be represented in (5.1):

$$v_a = \sum_{w \in W} \left(\sum_{s \in \widehat{P_s^w}} f_s^w \delta_{a,s} + \sum_{l \in \widehat{P_l^w}} f_l^w \delta_{a,l} \right) \tag{5.1}$$

Where v_a is the flow on the link a.

The travel time of one link is related to the free flow speed and the flow. We use the Bureau of Public Roads (BPR) function [56].

$$t_a = t_a^0 \left[1 + 0.15 \left(\frac{v_a}{c_a} \right)^4 \right] \tag{5.2}$$

Where t_a^0 is the free-flow travel time and c_a is the capacity of link a.

Beginning with the cost in model formulation, the cost of both charging lane users and charging station users are similar. They both contain the travel time cost and electricity cost. The only difference lies in that for drivers using charging stations, the waiting time cost while recharging should be counted inside travel time. Because energy consumption is flow-independent, the usability of a path could be pre-determined.

For one vehicle using charging stations, the cost on the path $s \in \widehat{P_s^w}$ is shown as follows:

$$c_s^w = \sum_{a \in A} \delta_{a,s} \cdot t_a \cdot VOT + \frac{\frac{L_s}{\beta} - E}{P_s} \cdot VOT + \left[\frac{L_s}{\beta} - E\right] \cdot q_s \quad (5.3)$$

Where, c_s^w is the cost of path $s \in \widehat{P_s^w}$;

VOT means the value of travel time. We assume that VOT is the same for all the drivers, both using charging stations and charging lanes while driving and recharging.

P_s denotes the charging power at charging station.

q_s denotes the power cost per unit of electricity on charging stations.

The first term on the above equation is the travel time cost, the second term is the waiting time cost while recharging, and the third term represents the charging cost at the station.

Besides, the cost of one vehicle on one lane-based usable path $l \in \widehat{P_l^w}$ is shown as follows:

$$c_l^w = \sum_{a \in A} \delta_{a,l} \cdot t_a \cdot VOT + \left[\frac{L_l}{\beta} - E\right] \cdot q_l \quad (5.4)$$

Where c_l^w is the cost of path $l \in \widehat{P_l^w}$

q_l is the power cost per unit of electricity on charging lanes (typically, it is greater than q_s).

In the equation, the first term represents the travel time cost, and the second term describes the charging cost on the charging lanes.

Given the road network and locations of charging lanes and charging stations, drivers choose the path with the minimum cost. It follows the character of user equilibrium, which

means the costs of all the routes with the same O-D pair are equal. However, in our model, there are two types of charging ways. We allow the cost of different charging methods to be different, but the cost of each O-D's same charging type path should be the same. Therefore, with an O-D pair $w \in W$, at user equilibrium, the cost of one charging station and charging lanes path could be shown as follows:

- If $f_s^w > 0$, $c_s^w = \mu_1^w$
- If $f_s^w = 0$, $c_s^w \geq \mu_1^w$
- If $f_l^w > 0$, $c_l^w = \mu_2^w$
- If $f_l^w = 0$, $c_l^w \geq \mu_2^w$

Where μ_1^w and μ_2^w denote the cost of charging station paths and charging lane paths at user equilibrium, respectively.

The four conditions show that at equilibrium, the costs of all the unutilized **lane-based usable paths** or **station-based usable paths** (the flow is equal to zero) are no less than the utilized paths (the flow is greater than zero). Because of the four conditions above, the model could be formulated as a non-linear complementary problem (NCP) as follows:

$$\sum_{s \in \widehat{P_s^w}} f_s^w = g_s^w, \qquad \forall w \in W \tag{5.5}$$

$$\sum_{l \in \widehat{P_l^w}} f_l^w = g_l^w, \qquad \forall w \in W \tag{5.6}$$

$$0 \leq f_s^w \perp (c_s^w - \mu_1^w) \geq 0, \qquad \forall w \in W, \forall s \in \widehat{P_s^w} \tag{5.7}$$

$$0 \leq f_l^w \perp (c_l^w - \mu_2^w) \geq 0, \qquad \forall w \in W, \forall l \in \widehat{P_l^w} \tag{5.8}$$

In the above equations, c_s^w and c_l^w could be obtained from (5.3) and (5.4). The travel time on a link t_a is determined by both the flows using the charging lane and the charging station on this link ((5.1) and (5.2)). The first two equations ensure the flow satisfies the demand for one O-D pair. The last two equations build the framework of a nonlinear complementary problem. For any utilized lane-based usable path and station-based usable path, we have the flows that are greater than zero ($f_s^w > 0$ and $f_l^w > 0$). Still, the costs are equal to the equilibrium costs ($c_s^w - \mu_s^w = 0$ and $c_l^w - \mu_l^w = 0$). For any unutilized paths, the flows are equal to zero ($f_s^w = 0$ and $f_l^w = 0$), and the costs are higher than the equilibrium costs. So, we get (5.7) and (5.8).

The solution algorithms of NCP in other works of literature can be used in this paper. One approach is converting the NCP equations into a nonlinear optimization problem by using a gap function [57]. Another simplified method changes the NCP to linear equations [58]. The development of solution algorithms is shown in Facchinei et al.'s work [59].

5.2 Combination of Charing Choice and Network Equilibrium Model

The mixed logit model is used to predict the proportion of different types of users. It requires the traffic information include the cost difference and the total travel time. These attributes could be gained from the traffic assignment model. The traffic assignment formulations should also know the proportion of different charging preferences from the traffic assignment formulations. Therefore, we need to combine the two stages and solve them simultaneously.

Charging choices getting from mixed logit model:

$$g_s^w + g_l^w = g^w, \qquad \forall w \in W \tag{5.9}$$

$$g_s^w = logit(c_s^w, L_s, Powerleft), \qquad \forall w \in W \tag{5.10}$$

$$g_l^w = logit(c_l^w, L_l, Powerleft), \qquad \forall w \in W \tag{5.11}$$

Nonlinear Complementary problem of deterministic traffic assignment model:

$$v_a = \sum_{w \in W} \left(\sum_{s \in \widehat{P_s^w}} f_s^w \delta_{a,s} + \sum_{l \in \widehat{P_l^w}} f_l^w \delta_{a,l} \right) \tag{5.12}$$

$$t_a = t_a^0 \left[1 + 0.15 \left(\frac{v_a}{c_a} \right)^4 \right] \tag{5.13}$$

$$c_s^w = \sum_{a \in A} \delta_{a,s} \cdot t_a \cdot VOT + \frac{\frac{L_s}{\beta} - E}{P_s} \cdot VOT + \left[\frac{L_s}{\beta} - E \right] \cdot q_s \tag{5.14}$$

$$c_l^w = \sum_{a \in A} \delta_{a,l} \cdot t_a \cdot VOT + \left[\frac{L_l}{\beta} - E \right] \cdot q_l \tag{5.15}$$

$$0 \le f_s^w \perp (c_s^w - \mu_1^w) \ge 0, \qquad \forall w \in W, \forall s \in \widehat{P_s^w} \tag{5.16}$$

$$0 \le f_l^w \perp (c_l^w - \mu_2^w) \ge 0, \qquad \forall w \in W, \forall l \in \widehat{P_l^w} \tag{5.17}$$

5.3 Solution Algorithm

5.3.1 *A Two-stage Algorithm to Solve the Entire Problem*

The above model has many non-linear terms, including the logit model to get the demand ((5.10) and (5.11)), the travel time function (5.13), and the NCP ((5.16) and (5.17)). It is hard to solve it directly. In this study, we build a two-stage algorithm to solve the whole problem:

Step 0: Initialize the social demographic variables by some certain distributions. (The income and the age follow normal distributions, and the year of buying BEV follows a uniform distribution) and using the free-flow travel time and cost as the trip parameters of each OD.

Step 1: For each OD, build a mixed logit model to predict the proportion of charging lane users and charging station users.

Step 2: Conduct traffic assignment and get the traffic information for each OD.

Step 3: Go back to step 1 and recompute the proportion of charging preferences. Compared it with the previous result with equation (5.18).

$$E = \sum_{j}^{N_{cl}} \frac{\left|D_{j,i} - D_{j,i-1}\right|}{D_{j,i-1}} + \sum_{k}^{N_{cs}} \frac{\left|D_{k,i} - D_{k,i-1}\right|}{D_{k,i-1}} \tag{5.18}$$

Where i is the number of iterations. j represents the index of charging lane and k represents the index of charging station. Then N_{cl} and N_{cs} represent the total number of charging lane OD and charging station OD respectively. $D_{j,i}$ and $D_{k,i}$ mean the demand of charging lane j and charging station k at iteration i.

Equation (5.18) represents the total relative error by summating the absolute value of two iterations for both the charging lane and charging station. If this value is less than tolerant, we terminate our algorithm; otherwise, go back to step 2 to reconduct the traffic assignment.

5.3.2 *Solution Algorithm of Traffic Assignment*

Next, we need a method to solve the traffic assignment with the proportion of charging preference from the mixed logit model. We use the solution algorithm to turn our problem into a mixed-integer linear program (MILP) by utilizing some binary variables. In this study, the two non-linear parts are the NCP constraints ((5.16) and (5.17)) and the travel time in (5.13), so the solution algorithm includes two linearization sections.

1) Linearization of the NCP

For charging lane users, NCP constraints are expressed as follows:

$$\begin{cases} \sum_{s\in\widehat{P_s^w}} f_s^w = g_s^w, & \forall w \in W \\ f_s^w \geq 0, & \forall w \in W, \forall s \in \widehat{P_s^w} \\ c_s^w - \mu_1^w \geq 0, & \forall w \in W, \forall s \in \widehat{P_s^w} \\ f_s^w (\, c_s^w - \mu_1^w) = 0, & \forall w \in W, \forall s \in \widehat{P_s^w} \end{cases} \tag{5.19}$$

The first two constraints represent the demand. The fourth equation is non-convex. Our objective is to modify the equations into a set of mixed-integer constraints. The last two constraints could also be expressed as an "if-then" condition:

$$\begin{cases} c_s^w - \mu_1^w = 0, \quad if \;\; f_s^w > 0 \\ c_s^w - \mu_1^w \geq 0 \end{cases}, \quad \forall w \in W, \forall s \in \widehat{P_s^w} \tag{5.20}$$

We could use a set of binary variables to transform the "if-then" condition into equivalent mixed-integer linear constraints:

$$\begin{cases} 0 \leq f_s^w \leq M \cdot (1 - \sigma_s^w) \\ 0 \leq c_s^w - \mu_1^w \leq M \cdot \sigma_s^w \,, \\ \sigma_s^w \in \{0,1\} \end{cases} \quad \forall w \in W, \forall s \in \widehat{P_s^w} \tag{5.21}$$

In (5.21), M is a very large positive constant. $\sigma_s^w = 1$ if $f_s^w = 0$ and $\sigma_s^w = 0$ if $f_s^w > 0$. This could be verified by using the two possible values of σ_s^w into the first equation above:

$$\begin{cases} \sigma_s^w = 0 \Leftrightarrow \; 0 \leq f_s^w \leq M \Leftrightarrow f_s^w \geq 0 \\ \sigma_s^w = 1 \Leftrightarrow 0 \leq f_s^w \leq 0 \Leftrightarrow f_s^w = 0 \end{cases} \tag{5.22}$$

Then σ_s^w could determine $c_s^w - \mu_1^w$ according to the value of f_s^w in the second and the third inequation in (5.21):

$$\begin{cases} \sigma_s^w = 0 \Leftrightarrow \; 0 \leq c_s^w - \mu_1^w \leq 0 \Leftrightarrow c_s^w - \mu_1^w = 0 \\ \sigma_s^w = 1 \Leftrightarrow 0 \leq c_s^w - \mu_1^w \leq M \Leftrightarrow c_s^w - \mu_1^w \geq 0 \end{cases} \tag{5.23}$$

For charging lane users, similarly, we could get (5.24):

$$\begin{cases} 0 \le f_l^w \le M \cdot (1 - \sigma_l^w) \\ 0 \le c_l^w - \mu_2^w \le M \cdot \sigma_l^w \,, \quad \forall w \in W, \forall l \in \widehat{P_l^w} \\ \sigma_l^w \in \{0,1\} \end{cases} \tag{5.24}$$

Where, if $f_l^w = 0$, then $\sigma_l^w = 1$ and if $f_l^w > 0$, then $\sigma_l^w = 0$.

2) Linearization of the Travel Time

We could use a piecewise linear function to represent the travel time (in (5.2)) to turn it into a linear equation. In each link, we use a set of values $K_{a,n}$ to partition v_a and a set of binary variables ξ_a^n to indicate whether v_a falls in the section $[K_{a,n}, K_{a,n+1})$, i.e., $K_{a,n} \le v_a < K_{a,n+1}$ if $\xi_a^n = 1$. In each segment, we build an approximately linear function to represent the travel time t_a:

$$t_a = A_n^a \cdot v_a + B_n^a \tag{5.25}$$

Where A_n^a and B_n^a are two coefficients to be determined. We can use the first-order Taylor series to estimate the travel time as follows:

$$\begin{aligned} A_n^a &= \left.\frac{dt_a}{dv_a}\right|_{K_{a,n}} = 0.6 * \frac{t_a^0}{c_a^4} * {K_{a,n}}^3 \\ B_n^a &= t_a^0 \left[1 + 0.15 \left(\frac{K_{a,n}}{c_a}\right)^4\right] - A_n^a * K_{a,n} \end{aligned} \tag{5.26}$$

The piecewise function can be transformed into mixed-integer linear constraints:

$$\begin{cases} K_{a,n} \cdot \xi_{a,n} \le v_a < M \cdot \left(1 - \xi_{a,n}\right) + K_{a,n+1} \\ (-M) \cdot \left(1 - \xi_{a,n}\right) \le t_a - (A_n^a \cdot v_a + B_n^a) \le M \cdot \left(1 - \xi_{a,n}\right) \\ \xi_{a,n} \in \{0,1\} \\ \sum_n \xi_{a,n} = 1 \end{cases} \tag{5.27}$$

In equations (5.27), M are still very a very large negative constant and a very large positive constant, respectively. The binary variable $\xi_{a,n}$ means that $\xi_{a,n} = 0$ if $v_a \ge K_{a,n}$ and

$v_a < K_{a,n+1}$; $\xi_{a,n} = 1$ otherwise. This can be verified by using the two possible values of $\xi_{a,n}$ in the first constraint above:

$$\begin{cases} \xi_{a,n} = 0 \Leftrightarrow 0 \le v_a < M + K_{a,n+1} \Leftrightarrow v_a \ge 0 \\ \xi_{a,n} = 1 \Leftrightarrow K_{a,n} \le v_a \le K_{a,n+1} \end{cases} \tag{5.28}$$

The binary variable $\xi_{a,n}$ could also indicates the relationship of t_a and $A_n^a \cdot v_a + B_n^a$. This can be verified by using the two possible values of $\xi_{a,n}$ in the second constraint in (5.27):

$$\begin{cases} \xi_{a,n} = 0 \Leftrightarrow -M \le t_a - (A_n^a \cdot v_a + B_n^a) \le M \\ \xi_{a,n} = 1 \Leftrightarrow 0 \le t_a - (A_n^a \cdot v_a + B_n^a) \le 0 \Leftrightarrow t_a = (A_n^a \cdot v_a + B_n^a) \end{cases} \tag{5.29}$$

Now all the equations are turned to be mixed-integer constraints, and the whole problem is transformed into:

(i) Demand constraints:

$$\begin{cases} \sum_{s \in \widehat{P_s^w}} f_s^w = g_s^w, \quad \forall w \in W \\ f_s^w \ge 0, \quad \forall w \in W, \forall s \in \widehat{P_s^w} \\ c_s^w - \mu_1^w \ge 0, \quad \forall w \in W, \forall s \in \widehat{P_s^w} \\ f_s^w (\, c_s^w - \mu_1^w) = 0, \quad \forall w \in W, \forall s \in \widehat{P_s^w} \end{cases} \tag{5.30}$$

(ii) User equilibrium constraints:

For charging station users:

$$\begin{cases} 0 \le f_s^w \le M \cdot (1 - \sigma_s^w) \\ 0 \le c_s^w - \mu_1^w \le M \cdot \sigma_s^w \,, \quad \forall w \in W, \forall s \in \widehat{P_s^w} \\ \sigma_s^w \in \{0,1\} \end{cases} \tag{5.31}$$

For charging lane users:

$$\begin{cases} 0 \le f_l^w \le M \cdot (1 - \sigma_l^w) \\ 0 \le c_l^w - \mu_2^w \le M \cdot \sigma_l^w \,, \quad \forall w \in W, \forall l \in \widehat{P_l^w} \\ \sigma_l^w \in \{0,1\} \end{cases} \tag{5.32}$$

(iii) Linearization of the travel time function of each link:

$$\begin{cases} K_{a,n} \cdot \xi_{a,n} \le v_a < M \cdot \left(1 - \xi_{a,n}\right) + K_{a,n+1} \\ (-M) \cdot \left(1 - \xi_{a,n}\right) \le t_a - (A_n^a \cdot v_a + B_n^a) \le M \cdot \left(1 - \xi_{a,n}\right) \\ \xi_{a,n} \in \{0,1\} \\ \sum_n \xi_{a,n} = 1 \end{cases} \tag{5.33}$$

Where

$$\begin{aligned} A_n^a &= \left.\frac{dt_a}{dv_a}\right|_{K_{a,n}} = 0.6 * \frac{t_a^0}{c_a^4} * {K_{a,n}}^3 \\ B_n^a &= t_a^0 \left[1 + 0.15 \left(\frac{K_{a,n}}{c_a}\right)^4\right] - A_n^a * K_{a,n} \end{aligned} \tag{5.34}$$

(iv) Defined constraints

$$\begin{aligned} v_a &= \sum_{w \in W} \left(\sum_{s \in \widehat{P_s^w}} f_s^w \delta_{a,s} + \sum_{l \in \widehat{P_l^w}} f_l^w \delta_{a,l} \right) \\ c_s^w &= \sum_{a \in A} \delta_{a,s} \cdot t_a \cdot VOT + \frac{\frac{L_s}{\beta} - E}{P_s} \cdot VOT + \left[\frac{L_s}{\beta} - E\right] \cdot q_s \\ c_l^w &= \sum_{a \in A} \delta_{a,l} \cdot t_a \cdot VOT + \left[\frac{L_l}{\beta} - E\right] \cdot q_l \end{aligned} \tag{5.35}$$

The book *Urban Transportation Networks* proved that the constraints hold and unique at the user equilibrium point [56]. We could use the methods of solving MILP to solve the NCP in our paper.

5.4 Numerical Analysis

5.4.1 *Transportation Network Builds*

In this section, we build a numerical example to demonstrate the traffic assignment model. BEVs can only use one charging method. We first create a road network in Figure 5.2, which consists of 9 nodes and 24 links. The orange links represent charging lanes, and the blue nodes are charging stations. The charging station nodes cannot generate trips, i.e., they are intermediate points. The number of OD pairs is 30. The length, free-flow travel time, and capacity of each link are given in Table 5.1.

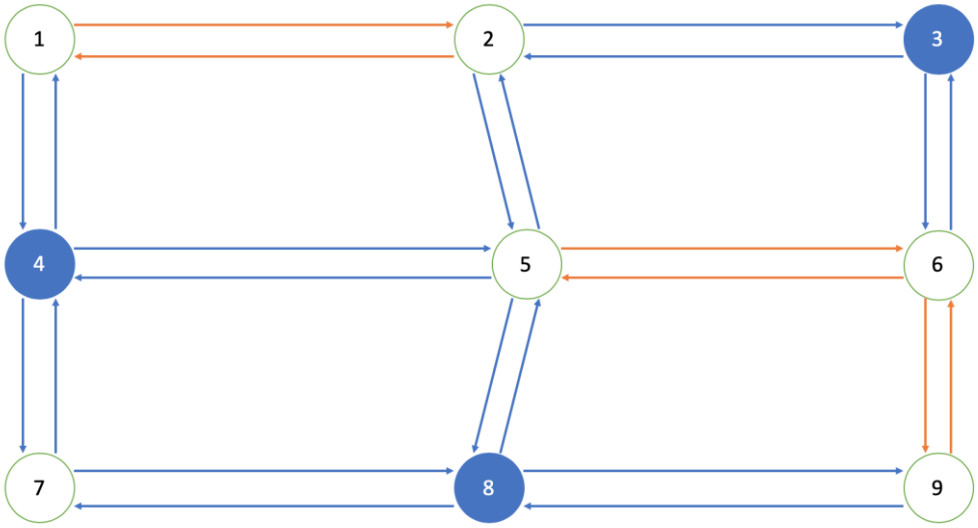

Figure 5.2 Numerical Analysis Road Network

We use Beijing's average income in 2018, ¥10,310 per month (¥14 per hour), as the value of travel time (VOT). The max size of battery E_{max} is 30 kWh, and the driving range is 210 km (from a Chinese EV, 2016 BYD E5). The energy consumption rate, β, is 210/30 = 7 km/kWh (4.35 mi/kWh). We set the initial SOC, E, to be 20 kWh. Then in our road network, a BEV could travel between two adjacent points without charging. Besides, if any of the two methods fully charge the vehicle, it can travel at most two links. The power outlet of charging stations, P_s, is

100 kW, one type of DCFC, and the unit cost of charging station, q_s, is ¥1.8 per kWh. At last, the unit cost of charging lane, q_l, is ¥3 per kWh, which is derived from Jang, Y et al.'s initial investment report of charging lanes [27].

Table 5.1 Link Length (km), Free-flow Travel Time (min), and Capacity (10^3 veh/h).

Link	Length	Free-flow Travel Time	Capacity	Link	Length	Free-flow Travel Time	Capacity
1-2	90	90	11	5-6	75	75	18
2-1	90	90	11	6-5	75	75	18
2-3	85	85	21	4-7	80	80	25
3-2	85	85	21	7-4	80	80	25
1-4	75	75	16	5-8	90	90	38
4-1	75	75	16	8-5	90	90	38
2-5	85	85	10	6-9	80	80	13
5-2	85	85	10	9-6	80	80	13
3-6	75	75	25	7-8	95	95	35
6-3	75	75	25	8-7	95	95	35
4-5	100	100	34	8-9	80	80	25
5-4	100	100	34	9-8	80	80	25

5.4.2 *Model Results*

After building the network and assigning values to the parameters, we could use the two-stage algorithm to solve it.

Figure 5.3 shows the iteration process. We could see that after about two hundred iterations, the demand of charging lane users and charging station users remain stable.

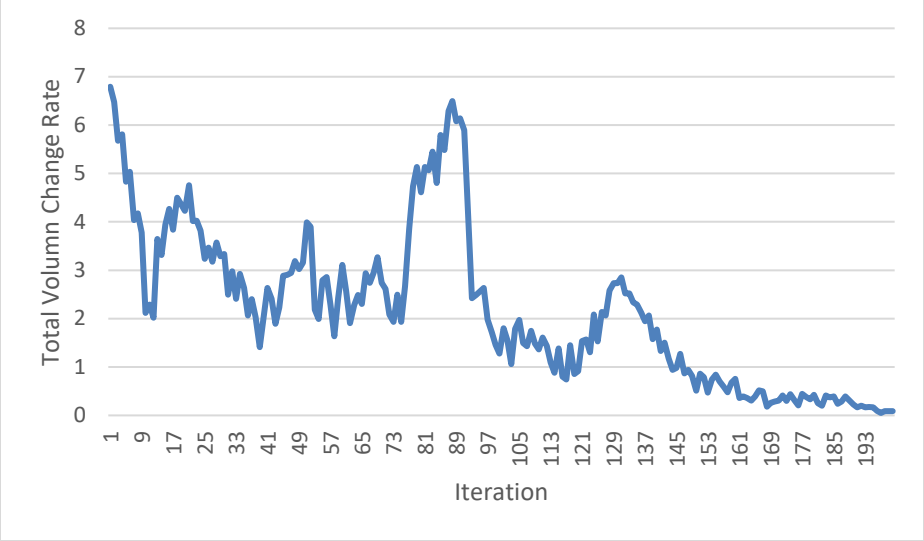

Figure 5.3 Tolerance vs Iteration Times

Table 5.2 shows the demand for different charging methods after 200 iterations. Table 5.3 shows the traffic flow on each link at equilibrium. It shows that the total influx and outflux are equal for the charging station nodes because they do not generate trips. Hence, as the charging lane flows and charging station flows.

Table 5.2 Travel Demand for each OD.

O-D	Total demand	Charing Lane demand	Charing Station demand	O-D	Total demand	Charing Lane demand	Charing Station demand
1-2	3000	NA	NA	7-2	2650	1408	1242
2-1	2800	NA	NA	2-9	2300	1362	939
1-5	2500	1480	1021	9-2	2700	1738	962
5-1	2650	1543	1107	5-6	2900	NA	NA
1-6	2880	1775	1106	6-5	3100	NA	NA
6-1	2700	1582	1118	5-7	2400	1275	1125
1-7	3100	0	3100	7-5	2750	1679	1071
7-1	2890	0	2890	5-9	1800	948	852
1-9	1700	1026	674	9-5	2000	1193	808
9-1	1990	1167	823	6-7	1900	1900	0
2-5	3400	NA	NA	7-6	2100	1147	953
5-2	3200	NA	NA	6-9	3300	NA	NA
2-6	3200	1678	1522	9-6	3000	NA	NA
6-2	2500	1465	1036	7-9	2300	1295	1005
2-7	2400	1529	871	9-7	2400	1412	988

Table 5.3 Equilibrium Link Flow.

Link	No Charging Flow (veh/h)	Charing Station Flow (veh/h)	Charing Lane Flow (veh/h)	Total (veh/h)
1-2	3000	494	4281	7775
2-3		2091	0	2091
1-4		5901	1529	7430
2-5	3400	0	5308	8708
3-6		2091	2013	4104
4-5		3995	0	3995
5-6	2900	1551	5215	9666
4-7		3773	1672	5445
5-8		1978	2605	4583
6-9	3300	939	3763	8002
7-8		2583	6629	9212
8-9		3039	2003	5042
2-1	2800	1118	4403	8321
3-2		2154	1817	3971
4-1		5314	1419	6733
5-2	3200	1710	5668	10578
6-3		2154	1817	3971
5-4		1905	1387	3292
6-5	3100	0	6627	9727
7-4		5276	175	5451
8-5		2791	3087	5878
9-6	3000	508	4445	7953
8-7		2114	4619	6733
9-8		3581	2014	5595

Figure 5.4 shows the proportion of charging lane flow over the charging station flow of each link. In the figure, the wide of each link represents the total link flow. The green arrows represent charging lanes, and the green nodes represent charging stations. It shows that the locations of charging lanes and charging stations affect the traffic assignment significantly. The average proportion of the charging lane flows over the charging station flows is about 60%. However, this proportion is much higher on the charging-lane links (1-2, 2-1, 5-6, 6-5, 6-9, 9-6). On the other hand, this proportion on the links connected to charging station links is relatively low. (1-4, 4-1, 4-7, 7-4, 3-2, 3-6, 6-3). It implies that most of the charging lane users are

concentrated on the charging lanes. It makes the charging station users avoid using those links and choose to use other links to reduce their total travel cost.

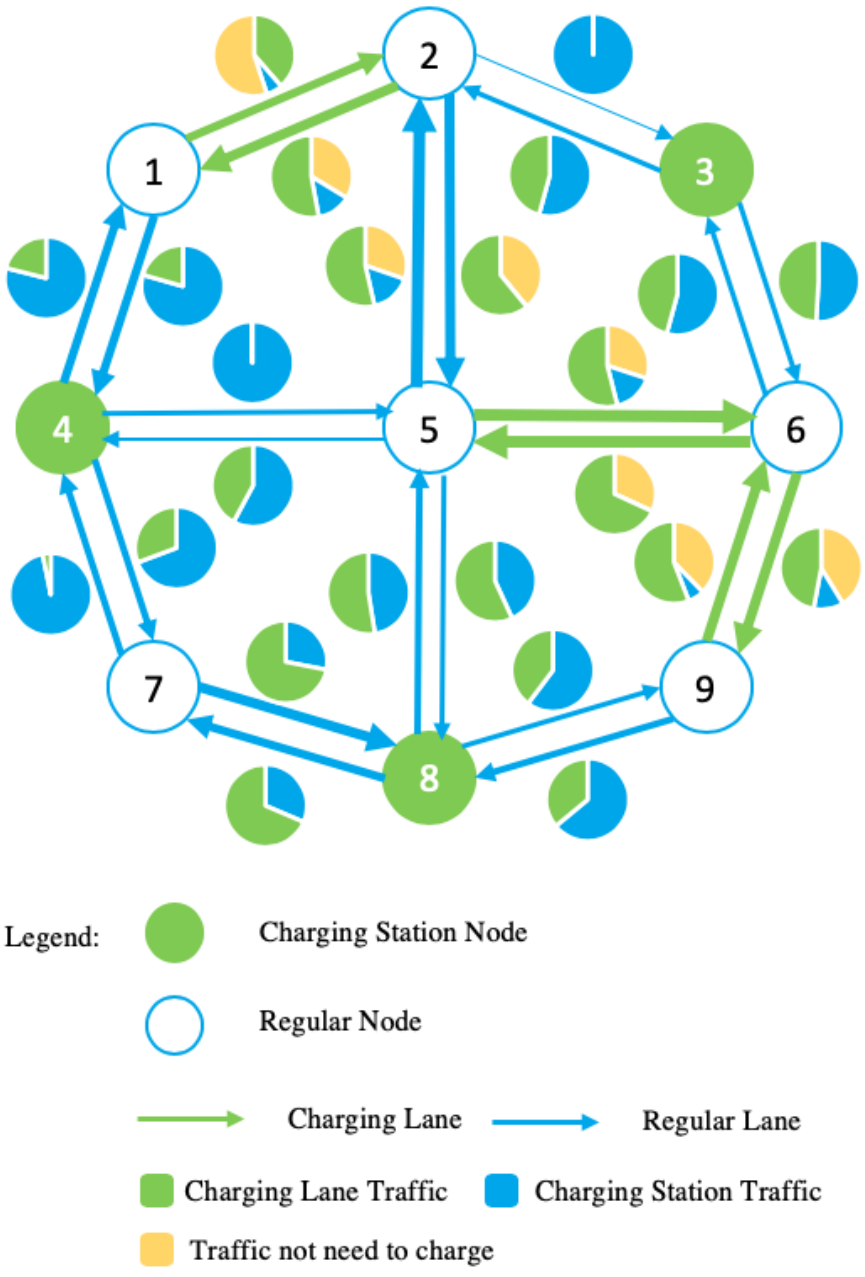

Figure 5.4 Numerical Analysis Results

5.5 Summary and Discussion

In this section, we assume the BEVs can only use one charging method. Based on the significant features affecting BEV drivers' charging choice, we build a two-step algorithm to determine the demand proportion of charging facilities and volume on the road. The traffic assignment results show that charging lane users are more likely to be concentrated on the charging lane links (link 1-2, 2-1, 5-6, 6-5). However, the charging station users avoid charging links and choose to use normal links (link 1-4, 2-3, 3-6).

Hence, the government could rebalance the traffic by making a reasonable deployment plan of charging facilities when income increases or the charging lanes' investment decreases. The charging lanes can be a more economical charging method for drivers.

The demand analysis is necessary because the users could change their charging strategy based on the current traffic condition. It is also reflected in the mixed logit model: the cost power left and cost difference also play a significant role when determining users' choices. The results show that our two-step algorithm converges and is capable of determining the proportion of different types of users and assigning the traffic efficiently.

An issue with the cost analysis process is that the unit cost of charging lanes we use. It is retrieved from the initial investment estimation of Jang, Y et al.'s work [27] and may not be accurate. The value will significantly affect our exact number in the value of time and cost analysis. Still, it will not influence the overall trend and our conclusion.

This section can be a part of a deployment plan of charging stations and changing lanes. It provides a systematic process to analyze the effect of the charging facilities on the current

traffic system. It also provides a prediction method of the demand for the different charging methods.

This whole process can be used to solve the lower level of the optimization problem. However, we designed a two-stage algorithm, which will make our solution time very high when we consider the upper level. So, in our next traffic assignment model, we release this assumption, i.e., each BEV in our network could use charging stations and charging lanes based on their demand.

However, this does not mean the above work is pointless. Some BEVs can only use charging stations, or the BEV drivers predetermine the charging method before the trip. Our traffic assignment model will make contributions to these conditions.

Chapter 6. LOCATION PROBLEM OF CHARGING INFRASTURCTURES

This chapter addresses the location problem of charging lanes and DCFC charging stations together, considering the traffic network and the power grid. In the beginning, we release the assumption that BEVs can only use one charging method. i.e., BEVs could use both charging lanes and charging stations based on their electricity demand and cost strategy. In the lower-level problem, we develop a single-vehicle problem (SVP) to minimize the drivers' user costs given the locations of charging facilities and the path from their origins and destinations. Second, for the upper-level problem, we characterize infrastructure deployment decisions via binary variables. A set of constraints then expresses the mutual impact between the power grid and the traffic network. We also include the user equilibrium constraints to decide the path choice of BEV drivers. In this way, we could build a bi-level, nonlinear, and nonconvex mixed-integer programming problem whose details are given below.

6.1 SINGLE VEHICLE PROBLEM (SVP)

6.1.1 *Notations and Assumptions*

This chapter treats every BEV driver as the same, which means they could use both the charging methods. At User Equilibrium, their costs are also the same regardless of the path they choose. Besides, other assumptions include:

- All vehicles are homogenous and electric vehicles.
- Each link on the transportation network could be built as a charging lane, and each link is connected to a bus (a bus is a facility in power grid to generate electricity). Similarly,

each node could be made into a DCFC charging station, and each node is connected to a bus in the power grid.

- The electricity consumption only depends on the travel distance. This means we can pre-determine the energy consumption on each link.
- The travel time on each link depends on the corresponding total traffic flow.
- When vehicles are on charging lanes, drivers can choose to charge or not based on their travel demand.

The parameters and variables of the transportation network are listed as follows:

Parameters:

- $G(N, A)$ denotes the transportation network. N denotes the set of nodes, and A denotes the set of links. $a = (i, j) \in A$ represents a link connecting nodes from i to j.
- W represents the set of O-D pairs, and w means one O-D pair, $w \in W$.
- P^w represents the set of paths between O-D pair $w \in W$, and $p \in P^w$ represents one path belonging to a path set.
- $A(p)$ represent the set of links belonging to path $p \in P^w$. $N(p)$ represents the set of nodes belonging to path $p \in P^w$.
- Δ_a^p means path-link incidence, where the value equals to 1 if path p passes the link a and 0 otherwise.
- g^w represents the demand of O-D pair $w \in W$.
- $o(w), d(w)$ represent the origin and destination of O-D pair $w \in W$.
- d_a denotes the distance of link $a \in A$.

- E_0 means the initial SOC of BEVs.
- E_1 denotes minimum SOC drivers try to maintain.
- E_2 means the battery size.
- Ω denotes the electricity consumption rate of BEVs per unit distance.
- E_l denotes the charging speed of charging lane per unit time.
- E_s denotes the charging speed of charging station per unit time.
- Γ_l denotes the electricity cost of charging lane.
- Γ_s denotes the electricity cost of charging station.
- V represents the value of travel time for BEV drivers.
- C_l represents the cost to construct one mile of charging lane.
- C_s represents the cost to construct one charging station.
- Ψ represents the total budgets to build all the charging facilities.

Variables:

- t_a means the travel time of BEVs on link $a \in A$.
- f_p denotes the traffic flow on path $p \in P^w$.
- v_a means the traffic flow on the link $a \in A$.
- s_a^p denotes the charging time of BEVs on charging link $a \in A$ of path $p \in P^w$.
- τ_i^p denotes the charging time of BEVs on charging station $i \in N$ along the path $p \in P^w$.
- L_i^p denotes the SOC in leaving the node $i \in N$ along the path $p \in P^w$.
- l_i^p denotes the SOC in entering the node $i \in N$ along the path $p \in P^w$.

- x_a is a binary variable, which means whether to build a charging lane on link $a \in A$.
- y_i is a binary variable, which means whether to build a charging station on node $i \in N$.

6.1.2 *Single Vehicle Problem Formulations*

In this section, we start the problem from the perspective of one BEV driver. Given the locations of charging facilities and a path between the origins and destinations, each driver chooses their optimal charging strategy to reach the destination. The objective function of SVP is to minimize the user cost along the path, which includes two parts: the electricity cost and the time cost. The decision variables include the charging time at charging stations and charging lanes and the SOC at each node. The constraints should guarantee that the driver could arrive at the destination without using up the battery. The SVP optimization is shown as:

$$\text{Min} \quad \sum_{a \epsilon A(p)} s_a^p \, E_l \Gamma_l + \sum_{i \epsilon N(p)} \tau_i^p \, E_s \Gamma_s + V \cdot \left(\sum_{a \epsilon A(p)} t_a + \sum_{i \epsilon N(p)} \tau_i^p \right)$$

s.t.

$$s_a^p \geq 0, \qquad \forall a \epsilon A(p) \qquad (6.1)$$

$$s_a^p \leq t_a \cdot x_a, \qquad \forall a \epsilon A(p) \qquad (6.2)$$

$$\tau_i^p \geq 0, \qquad \forall i \epsilon N(p) \qquad (6.3)$$

$$\tau_i^p \leq M \cdot y_i, \qquad \forall i \epsilon N(p) \qquad (6.4)$$

$$L_i^p \geq E_1, \qquad \forall i \epsilon N(p) \qquad (6.5)$$

$$L_i^p \leq E_2, \qquad \forall i \epsilon N(p) \qquad (6.6)$$

$$L_{O(W)}^p = E_0 \qquad (6.7)$$

$$l_i^p \geq 0 \qquad \forall i \epsilon N(p) \qquad (6.8)$$

$$L_i^p - l_j^p - d_a\omega + s_a^p E_l = 0, \qquad \forall (i,j) = a \epsilon A(p) \tag{6.9}$$

$$L_i^p - l_i^p - \tau_i^p E_s = 0, \qquad \forall i \epsilon N(p) \tag{6.10}$$

The objective function includes three costs: $\sum_{a\epsilon A(p)} s_a^p \, E_l \Gamma_l$ represents the electricity cost using charging lanes (charging time using charging lane s_a^p multiplied by the charging speed using charging lane E_l, then multiplied the unit electricity cost using charging lane Γ_l). Similarly, $\sum_{i\epsilon N(p)} \tau_i^p \, E_s \Gamma_s$ represents the electricity cost using charging stations. $\sum_{a\epsilon A(p)} t_a + \sum_{i\epsilon N(p)} \tau_i^p$ represents the total travel time from the origin to the destination, and it is multiplied by the value of time V to get the total travel time cost.

Constraint (6.1) and (6.2) mean that the charging time at the charging lane is conditional on the upper-level deployment decisions x_a. When the link is a charging lane ($x_a = 1$), the charging time on the charging lanes (s_a^p) should be non-negative and less than the travel time, but it should be zero when there is no charging lane ($x_a = 0$). Similarly, in constraint (6.3) and (6.4), M is a large number, and the charging time at the charging station (τ_i^p) should be non-negative when there is a charging station ($y_i = 1$), but it should be zero when there is no charging station ($y_i = 0$). Constraint (6.5) and (6.6) ensure that the leaving SOC for each node is no less than the minimum SOC and no larger than each vehicle's battery size. Constraint (6.7) means that the SOC equals the initial SOC of each BEV at the origin. Constraint (6.9) and (6.10) means energy conservation law. Constraint (6.9) represents the SOC balance in each link $(i,j) = a$. l_i^p and L_i^p represent the SOC when vehicle enters and leaves the node i, respectively. Then constraint (6.9) means the SOC leaving node i (L_i^p) minuses the SOC entering node j (l_j^p), and minus the electricity consumption at the link ($d_a\omega$), and pluses the electricity charged from the charging lane ($s_a^p E_l$)

equals to zero. Constraint (6.10) represents the SOC balance in each node i. The entering SOC (l_i^p) plus the electricity from charging station ($\tau_i^p E_s$) equals to the leaving SOC (L_i^p).

The travel time t_a in a link is determined by the volume v_a on this link, the and the free flow travel time on the link t_a^0. We use Bureau of Public Roads (BPR) function (5.2).

Next, we will build the upper level and combine it with the lower-level model. Then we create an algorithm to solve it.

6.2 CHARING FACILITY LOCATION PROBLEM

6.2.1 *Path Selection Constraints*

The above optimization is from the perspective of one driver given the path. Next, we try to decide which path the drivers choose to use among all the paths to satisfy the energy constraints. Given a network and each OD's demand, each driver selects the path with the lowest user cost. Finally, all the drivers and traffic will reach an equilibrium called User Equilibrium (UE) [60]. At the UE, no driver could reduce his/her user cost by switching the path for the same OD, i.e., at the UE, all the used paths for the same OD have the same user cost for all the drivers. This cost is no higher than the cost of unused paths for this OD. We could build the following non-linear complementary problem (NCP) to illustrate the UE:

$$\sum_{p\in P^w} f_p = g^w, \qquad \forall w \in W \tag{6.11}$$

$$v_a = \sum_{w\in W}\sum_{p\in P^w} f_p \Delta_a^p, \qquad \forall w \in W \tag{6.12}$$

$$f_p \geq 0, \qquad \forall p \in P^w, \forall w \in W \tag{6.13}$$

$$\sum_{a\epsilon A(p)} s_a^p E_l \Gamma_l + \sum_{i\epsilon N(p)} \tau_i^p E_s \Gamma_s + V \cdot \left(\sum_{a\epsilon A(p)} t_a + \sum_{i\epsilon N(p)} \tau_i^p \right) - \mu^w \geq 0, \qquad \forall p \in P^w, \forall w \in W \tag{6.14}$$

$$\left(\sum_{a\epsilon A(p)} s_a^p E_l \Gamma_l + \sum_{i\epsilon N(p)} \tau_i^p E_s \Gamma_s + V \cdot \left(\sum_{a\epsilon A(p)} t_a + \sum_{i\epsilon N(p)} \tau_i^p\right) - \mu^w\right) \cdot f_p = 0, \qquad \forall p \in P^w, \forall w \in W \qquad (6.15)$$

Here, μ^w means the equilibrium cost of the OD pair w. Constraint (6.11) means the summation of all the path flows equals the total demand of OD pair w. Constraint (6.12) means the flow on the link a equals the summation of all the path flows using this link. Constraint (6.13) ensures the flow of each path is non-negative. Constraint (6.14) and (6.15) formulate an NCP: when the path is used ($f_p > 0$), the cost of this path equals to the equilibrium cost μ^w of the OD pair w, and when the path is not used ($f_p = 0$), the cost of this path is no less than the equilibrium cost μ^w.

6.2.2 *Power Grid Constraints*

To build a location design of charging facilities, we also need to consider the power grid constraints. The notations of the power grid are listed as follows:

Parameters:

- $G_E(L, K)$ denotes the power grid, where K denotes the set of buses in the power grid. L is the set of transmission lines in the system.
- A_k, B_k represent the lower and upper real power limit in a bus k.
- Θ_k represents the regular real power load in a bus k, which is given in our model.
- R_{km} is the thermal limit of real power flow in the transmission n line from bus k to bus m.
- D_{km} means the inverse of the pu reactance.

- $\Lambda_{k,l}$ represents the set of links powered by the bus k, and
- $\Lambda_{k,s}$ represents the set of nodes powered by the bus k.

Variables:

- φ_k denotes the real power in a bus k
- δ_k means the base apparent power and voltage angle (in radians) in bus k
- h_{km} denotes the power flow in transmission line from bus k to bus m
- $Z(\varphi_k)$ denotes the total cost of generating φ_k amount of electricity at bus k

We use K to denote the set of buses in the power grid to serve the charging facilities. We use H to denote the set of transmission line as the pair of its starting and ending buses: $(k,m) \in H$. h_{km} denotes the power flow in the transmission line from bus k to bus m. h_{km} is determined by the inverse of the pu reactance D_{km}, and the multiplication of base apparent power and voltage angle (in radians) δ_k. φ_k represents the real power injection of bus k, and Θ_k is the regular real power load of bus k, which is given.

The constraints of power grid are given as follows:

$$\varphi_k - \Theta_k - \sum_{a\in\Lambda_{k,l}} \sum_{w\in W} \sum_{p\in\bar{P}^w} f_p \cdot \Delta_a^p \cdot s_a^p \cdot E_l - \sum_{i\in\Lambda_{k,s}} \sum_{w\in W} \sum_{p\in\bar{P}^w} f_p \cdot \Delta_a^p \cdot \tau_i^p \cdot E_s - \sum_{(k,m)\in H} h_{km} + \sum_{(n,k)\in H} h_{nk} = 0, \quad \forall k \in K \tag{6.16}$$

$$h_{km} = D_{km}(\delta_k - \delta_m), \quad \forall (k,m)\epsilon H \tag{6.17}$$

$$-R_{km} \le h_{km} \le R_{km}, \quad \forall (k,m)\epsilon H \tag{6.18}$$

$$A_k \le \varphi_k \le B_k \quad \forall k \in K \tag{6.19}$$

$$\delta_1 = 0 \tag{6.20}$$

Constraint (6.16) is the nodal power balance constraint. $\sum_{w\in W}\sum_{p\in\hat{P}^w} f_p \cdot \Delta_a^p \cdot s_a^p \cdot E_l$ means the total energy requirement from the charging lane on link a, and if link a is powered by bus k and it is a charging lane ($s_a^p > 0$), the bus k should supply the electricity of this charging lane. Similarly, $\sum_{w\in W}\sum_{p\in\hat{P}^w} f_p \cdot \Delta_a^p \cdot \tau_i^p \cdot E_s$ means the total energy requirement from the charging station on node i, and if node i is powered by bus k, and it is a charging station ($\tau_i^p > 0$), the bus k should supply the electricity of this charging station. Constraint (6.17) is the linear expression of the real power branch flow equation. Constraint (6.18) and (6.19) ensure the power injection's feasibility and the real power flow. Constraint (6.20) sets the voltage angle at the node 1 to be 0, which considered to be the reference node.

6.2.3 *Upper-level Objective Function*

At last, we build the whole model given the constraints from the traffic and power grid.

Our decision variables include two binary variables:

- x_a means whether the link a is a charging lane.
- y_i means whether the node i is a charging station.

And two continuous variables:

- The real power injection of each bus φ_k
- The multiplication of base apparent power and voltage angle δ_k

The objective function is to minimize the total cost of the whole system, including the cost of generating the electricity and the cost from the transportation.

The full model is written as follows:

$$\text{Min} \quad \sum_{k} Z_k(\varphi_k) + \sum_{w \in W} \mu^w \cdot g^w$$

s.t.

$$\sum_{a \in A} x_a \cdot d_a \cdot C_l + \sum_{i \in N} y_i \cdot C_s \leq \Psi \tag{6.21}$$

$$x_a \in \{0,1\}, \qquad \forall a \epsilon A \tag{6.22}$$

$$y_i \in \{0,1\}, \qquad \forall i \epsilon N \tag{6.23}$$

(6.11) – (6.20)

$$v_a, t_a \in argmin \left(\sum_{a \epsilon A(p)} s_a^p \, E_l \Gamma_l + \sum_{i \epsilon N(p)} \tau_i^p \, E_s \Gamma_s + V \cdot \left(\sum_{a \epsilon A(p)} t_a + \sum_{i \epsilon N(p)} \tau_i^p \right) \right)$$

Where (6.1) – (6.10)

Where $Z_k(\varphi_k)$ means the total cost of generating φ_k amount of electricity at bus k. The function is given as follows [48]:

$$Z_k(\varphi_k) = a_{k,0} \cdot \varphi_k^2 + a_{k,1} \cdot \varphi_k + a_{k,2} \tag{6.24}$$

$\mu^w \cdot g^w$ means the total traffic cost of OD pair $w \in W$. μ^w is the equilibrium cost and g^w is the total traffic demand of OD pair $w \in W$. Constraint (6.21) limits the total budget of construction charging facilities. (6.1) – (6.10) represents the lower-level optimization work, which is the single vehicle problem from the BEV drivers' perspective in section 6.1. (6.11) – (6.20) are constraints from the power grid and traffic assignment.

6.3 Solution Algorithm

The model we build is a bi-level optimization problem, and we need an efficient algorithm to solve it. In this section, we first use KKT conditions to turn the bi-level optimization into a single level

optimization. The single-level optimization still non-linear. We introduced some integer variables to handle nonlinearity. At last, our problem will turn to be a mixed-integer linear optimization problem, which could be solved by commercial solvers such as Gurobi.

6.3.1 *Convert into Single Level Optimization*

To convert the SVP into constraints of the upper level, we could turn the SVP into non-linear complimentary problems (NCP) by using Karush–Kuhn–Tucker (KKT) conditions. Since the UE is also an NCP, we only need to solve both the NCP together to get the traffic volume in each link given the locations of charging lanes and charging stations.

The optimal conditions of SVP by using KKT is shown:

(6.1) - (6.10)

$$s_a^p \cdot \lambda_{1,a}^p = 0, \qquad \forall a \epsilon A(p), p \in P^w, w \epsilon W \tag{6.25}$$

$$\lambda_{1,a}^p \geq 0, \qquad \forall a \epsilon A(p), p \in P^w, w \epsilon W \tag{6.26}$$

$$\left(s_a^p - t_a \cdot x_a\right) \cdot \lambda_{2,a}^p = 0 \qquad \forall a \epsilon A(p), p \in P^w, w \epsilon W \tag{6.27}$$

$$\lambda_{2,a}^p \geq 0 \qquad \forall a \epsilon A(p), p \in P^w, w \epsilon W \tag{6.28}$$

$$\tau_i^p \cdot \lambda_{3,i}^p = 0, \qquad \forall i \epsilon N(p), p \in P^w, w \epsilon W \tag{6.29}$$

$$\lambda_{3,i}^p \geq 0, \qquad \forall i \epsilon N(p), p \in P^w, w \epsilon W \tag{6.30}$$

$$\left(\tau_i^p - M \cdot y_i\right) \cdot \lambda_{4,i}^p = 0, \qquad \forall i \epsilon N(p), p \in P^w, w \epsilon W \tag{6.31}$$

$$\lambda_{4,i}^p \geq 0, \qquad \forall i \epsilon N(p), p \in P^w, w \epsilon W \tag{6.32}$$

$$\left(E_1 - L_i^p\right) \cdot \lambda_{5,i}^p = 0, \qquad \forall i \epsilon N(p), p \in P^w, w \epsilon W \tag{6.33}$$

$$\lambda_{5,i}^p \geq 0, \qquad \forall i \epsilon N(p), p \in P^w, w \epsilon W \tag{6.34}$$

$$\left(L_i^p - E_2\right) \cdot \lambda_{6,i}^p = 0, \qquad \forall i \epsilon N(p), p \in P^w, w \epsilon W \tag{6.35}$$

$$\lambda_{6,i}^p \geq 0, \qquad \forall i \epsilon N(p), p \in P^w, w \epsilon W \tag{6.36}$$

$$-l_i^p \cdot \lambda_{8,i}^p = 0 \qquad \forall i \epsilon N(p), p \in P^w, w \epsilon W \tag{6.37}$$

$$\lambda_{8,i}^p \geq 0, \qquad \forall i \epsilon N(p), p \in P^w, w \epsilon W \tag{6.38}$$

$$E_l \Gamma_l - \lambda_{1,a}^p + E_l \lambda_{9,ij}^p + \lambda_{2,a}^p = 0, \qquad \forall (i,j) = a \epsilon A(p), p \in P^w, w \epsilon W \tag{6.39}$$

$$E_s \Gamma_s + V - \lambda_{3,i}^p + \lambda_{4,i}^p - E_s \lambda_{10,i}^p = 0, \qquad \forall i \epsilon N(p), p \in P^w, w \epsilon W \tag{6.40}$$

$$-\lambda_{5,i}^p + \lambda_{6,i}^p + \lambda_{9,ij}^p + \lambda_{10,i}^p = 0, \qquad \forall (i,j) = a \epsilon A(p), p \in P^w, w \epsilon W \tag{6.41}$$

$$-\lambda_{8,j}^p - \lambda_{9,ij}^p - \lambda_{10,j}^p = 0, \qquad \forall (i,j) = a \epsilon A(p)\,, p \in P^w, w \epsilon W \tag{6.42}$$

Together with (6.11) – (6.15), the above constraints form a traffic assignment model. By solving the traffic assignment model, we could know the volume in each link once given the charging lanes and charging stations' locations.

6.3.2 *Linearization of Non-linear Complimentary Problem*

With the KKT conditions, we could convert the bi-level optimization problem into single level. However, there are still some non-linear constraints. The first type of non-linear constraint is the NCP. The NCP include three components: x and $f(x)$ are two non-negative parts, but their multiplication is zero ($x^T f(x) = 0$). The general formulation is shown as:[61]

$$x \geq 0 \tag{6.43}$$

$$f(x) \geq 0 \tag{6.44}$$

$$x^T f(x) = 0 \tag{6.45}$$

It is non-linear because of the term $x^T f(x)$. However, because of that both terms are non-zero, but their multiplication is zero, we could use a binary variable to linearize it:

$$0 \leq x \leq M \cdot \beta \tag{6.46}$$

$$0 \leq f(x) \leq M \cdot (1 - \beta) \tag{6.47}$$

Where β is a binary variable, and M is a very large positive number.

- If $\beta = 0$, then $0 \leq x \leq 0$, i.e., $x = 0$, and $0 \leq f(x) \leq M$, then $x^T f(x) = 0$ is satisfied.
- If $\beta = 1$, then $0 \leq f(x) \leq 0$, i.e., $f(x) = 0$, and $0 \leq x \leq M$, then $x^T f(x) = 0$ is satisfied.

The binary variable β indicates whether x or $f(x)$ is zero.

By using binary variables, we could linearize almost all the NCP for traffic assignment constraints as follows:

(6.13), (6.14)

$$\sum_{a \epsilon A(p)} s_a^p \, e_1 c_1 + \sum_{i \epsilon N(p)} \tau_i^p \, e_2 c_2 + V \cdot \left(\sum_{a \epsilon A(p)} t_a(v_a) + \sum_{i \epsilon N(p)} \tau_i^p \right) - \mu^w \leq M \cdot \beta_{0,p}^w, \qquad \forall p \in P^w, \forall w \in W \tag{6.48}$$

$$f_p^w \leq M \cdot \left(1 - \beta_{0,p}^w\right), \qquad \forall p \in P^w, \forall w \in W \tag{6.49}$$

$$\beta_{0,p}^w \in \{0,1\} \qquad \forall p \in P^w, \forall w \in W \tag{6.50}$$

(6.1), (6.26)

$$s_a^p \leq M \cdot \beta_{1,a}^p \qquad \forall a \epsilon A(p), p \in P^w, w \epsilon W \tag{6.51}$$

$$\lambda_{1,a}^{p} \leq M \cdot (1 - \beta_{1,a}^{p}), \qquad \forall a \epsilon A(p), p \in P^{w}, w \epsilon W \qquad (6.52)$$

$$\beta_{1,a}^{p} \in \{0,1\} \qquad \forall a \epsilon A(p), p \in P^{w}, w \epsilon W \qquad (6.53)$$

(6.2), (6.28)

$$t_a \cdot x_a - s_a^{p} \leq M \cdot \beta_{2,a}^{p} \qquad \forall a \epsilon A(p), p \in P^{w}, w \epsilon W \qquad (6.54)$$

$$\lambda_{2,a}^{p} \leq M \cdot (1 - \beta_{2,a}^{p}), \qquad \forall a \epsilon A(p), p \in P^{w}, w \epsilon W \qquad (6.55)$$

$$\beta_{2,a}^{p} \in \{0,1\} \qquad \forall a \epsilon A(p), p \in P^{w}, w \epsilon W \qquad (6.56)$$

(6.3), (6.30)

$$\tau_i^{p} \leq M \cdot \beta_{3,i}^{p} \qquad \forall i \epsilon N(p), p \in P^{w}, w \epsilon W \qquad (6.57)$$

$$\lambda_{3,i}^{p} \leq M \cdot (1 - \beta_{3,i}^{p}), \qquad \forall i \epsilon N(p), p \in P^{w}, w \epsilon W \qquad (6.58)$$

$$\beta_{3,i}^{p} \in \{0,1\} \qquad \forall i \epsilon N(p), p \in P^{w}, w \epsilon W \qquad (6.59)$$

(6.4), (6.32)

$$M \cdot y_i - \tau_i^{p} \leq M \cdot \beta_{4,i}^{p} \qquad \forall i \epsilon N(p), p \in P^{w}, w \epsilon W \qquad (6.60)$$

$$\lambda_{4,i}^{p} \leq M \cdot (1 - \beta_{4,i}^{p}), \qquad \forall i \epsilon N(p), p \in P^{w}, w \epsilon W \qquad (6.61)$$

$$\beta_{4,i}^{p} \in \{0,1\} \qquad \forall i \epsilon N(p), p \in P^{w}, w \epsilon W \qquad (6.62)$$

(6.5), (6.34)

$$L_i^{p} - E_1 \leq M \cdot \beta_{5,i}^{p} \qquad \forall i \epsilon N(p), p \in P^{w}, w \epsilon W \qquad (6.63)$$

$$\lambda_{5,i}^{p} \leq M \cdot (1 - \beta_{5,i}^{p}), \qquad \forall i \epsilon N(p), p \in P^{w}, w \epsilon W \qquad (6.64)$$

$$\beta_{5,i}^{p} \in \{0,1\} \qquad \forall i \epsilon N(p), p \in P^{w}, w \epsilon W \qquad (6.65)$$

(6.6), (6.36)

$$E_2 - L_i^p \le M \cdot \beta_{6,i}^p \qquad \forall i \epsilon N(p), p \in P^w, w \epsilon W \qquad (6.66)$$

$$\lambda_{6,i}^p \le M \cdot (1 - \beta_{6,i}^p), \qquad \forall i \epsilon N(p), p \in P^w, w \epsilon W \qquad (6.67)$$

$$\beta_{6,i}^p \in \{0,1\} \qquad \forall i \epsilon N(p), p \in P^w, w \epsilon W \qquad (6.68)$$

(6.8), (6.38)

$$l_i^p \le M \cdot \beta_{8,i}^p \qquad \forall i \epsilon N(p), p \in P^w, w \epsilon W \qquad (6.69)$$

$$\lambda_{8,i}^p \le M \cdot (1 - \beta_{8,i}^p), \qquad \forall i \epsilon N(p), p \in P^w, w \epsilon W \qquad (6.70)$$

$$\beta_{8,i}^p \in \{0,1\} \qquad \forall i \epsilon N(p), p \in P^w, w \epsilon W \qquad (6.71)$$

The constraints we use previous constraints indicate that $x \ge 0$ and $f(x) \ge 0$ for each NCP. With the binary variables $\beta_{0,p}^w, \beta_{1,a}^p, \beta_{2,a}^p, \beta_{3,i}^p, \beta_{4,i}^p, \beta_{5,i}^p, \beta_{6,i}^p, \beta_{8,i}^p$, we could linearize all the NCP constraints, except the $t_a \cdot x_a$ term in (6.54) and (6.2). We will linearize it in the next part.

6.3.3 *Linearization of Variables' Multiplication*

There are still some non-linear terms, include $t_a \cdot x_a$ in (6.2) and (6.54), $f_p \cdot s_a^p$ and $f_p \cdot \tau_i^p$ in (6.16).

$t_a \cdot x_a$ is a product of a continuous variable (t_a) and a binary variable (x_a). Suppose $Q_a = t_a \cdot x_a$, the product can be linearized as follow: [62]

$$Q_a \le M \cdot x_a, \qquad \forall a \epsilon A(p), p \in P^w, w \epsilon W \qquad (6.72)$$

$$Q_a \le t_a, \qquad \forall a \epsilon A(p), p \in P^w, w \epsilon W \qquad (6.73)$$

$$Q_a \ge t_a - (1 - x_a) \cdot M \qquad \forall a \epsilon A(p), p \in P^w, w \epsilon W \qquad (6.74)$$

$$Q_a \ge 0 \qquad \forall a \epsilon A(p), p \in P^w, w \epsilon W \qquad (6.75)$$

We only need to replace $t_a \cdot x_a$ by Q_a in (6.2) and (6.54), then add (6.72) - (6.75) in our model. The term $t_a \cdot x_a$ is linearized. The replacement of $t_a \cdot x_a$ in (6.2) and (6.54) is written as follows:

$$s_a^p \le Q_a, \qquad \forall a \epsilon A(p), p \in P^w, w \epsilon W \qquad (6.2b)$$

$$Q_a - s_a^p \le M \cdot \beta_{2,a}^p \qquad \forall a \epsilon A(p), p \in P^w, w \epsilon W \qquad (6.54b)$$

$f_p \cdot s_a^p$ and $f_p \cdot \tau_i^p$ are products of two continuous variable. We can use a piecewise linear function to represent f_p. The flow of the path f_p could be partitioned into N segments (when N is large enough, we could estimate flow to any accuracy degree). In each path, we use a set of values $K_{p,n}$ to partition f_p, and a set of binary variables η_p^n to indicate whether f_p falls in each section, i.e., $K_{p,n} \le f_p < K_{p,n+1}$ if $\eta_p^n = 1$:

$$K_{p,n} \cdot \eta_p^n \le f_p < M \cdot \left(1 - \eta_p^n\right) + K_{p,n+1}, \qquad \forall p \in P^w, w \epsilon W \qquad (6.76)$$

$$\eta_p^n \in \{0,1\} \qquad \forall p \in P^w, w \epsilon W \qquad (6.77)$$

$$\sum_n \eta_p^n = 1 \qquad \forall p \in P^w, w \epsilon W \qquad (6.78)$$

The above constraints mean that if $\eta_p^n = 1$, $K_{p,n} \le f_p < K_{p,n+1}$; otherwise, $0 \le f_p < M$. Here M is also the very large positive number. Therefore, f_p in (6.16) could be represented as $\sum_n K_{p,n} \cdot \eta_p^n$. Then the two non-linear terms become two products of one continuous variable and one binary variable. We use the same method above to linearize two products, then constraint (6.16) can be linearized as follows:

$$\begin{aligned} \varphi_k - \Theta_k - \sum_{a \in \Lambda_{k,l}} \sum_{w \in W} \sum_{p \in \hat{P}^w} \sum_n K_{p,n} \cdot \Delta_a^p \cdot E_l \cdot Q_{1,n}^{p,a} \\ - \sum_{i \in \Lambda_{k,s}} \sum_{w \in W} \sum_{p \in \hat{P}^w} \sum_n K_{p,n} \cdot \Delta_a^p \cdot \tau_i^p \cdot Q_{2,n}^{p,i} - \sum_{(k,m) \in H} h_{km} \\ + \sum_{(n,k) \in H} h_{nk} = 0, \qquad \forall k \in K \end{aligned} \qquad (6.16b)$$

And we should add constraint (6.76) - (6.78) in our optimization problem, as well as the constraints of the products by one continuous variable and one binary variable:

$$Q_{1,n}^{p,a} \leq M \cdot \eta_p^n, \qquad \forall a \epsilon A(p), p \in P^w, w \epsilon W, n \in N \qquad (6.79)$$

$$Q_{1,n}^{p,a} \leq s_a^p, \qquad \forall a \epsilon A(p), p \in P^w, w \epsilon W, n \in N \qquad (6.80)$$

$$Q_{1,n}^{p,a} \geq s_a^p - (1 - \eta_p^n) \cdot M \qquad \forall a \epsilon A(p), p \in P^w, w \epsilon W, n \in N \qquad (6.81)$$

$$Q_{1,n}^{p,a} \geq 0 \qquad \forall a \epsilon A(p), p \in P^w, w \epsilon W, n \in N \qquad (6.82)$$

$$Q_{2,n}^{p,i} \leq M \cdot \eta_p^n, \qquad \forall a \epsilon A(p), p \in P^w, w \epsilon W, n \in N \qquad (6.83)$$

$$Q_{2,n}^{p,i} \leq \tau_i^p, \qquad \forall a \epsilon A(p), p \in P^w, w \epsilon W, n \in N \qquad (6.84)$$

$$Q_{2,n}^{p,i} \geq \tau_i^p - (1 - \eta_p^n) \cdot M \qquad \forall a \epsilon A(p), p \in P^w, w \epsilon W, n \in N \qquad (6.85)$$

$$Q_{2,n}^{p,i} \geq 0 \qquad \forall a \epsilon A(p), p \in P^w, w \epsilon W, n \in N \qquad (6.86)$$

After change constraints (6.2), (6.54), and (6.16) to (6.2b), (6.54b), and (6.16b). And add constraints (6.72) – (6.82) to the model, the non-linear multiplication terms are linearized.

6.3.4 *Linearization of Travel Time and Electricity Generation Cost Function*

There remain two non-linear constraints in our optimization: the travel time function (5.2) and the electricity generation cost function (6.24). We use the same method in Chapter 5.1, which uses a piece wise linear function to represent the two functions by partition the flow on the link v_a and the injection flow on each bus φ_k into N segments, respectively.

In each link, we use a set of values $K_{a,n}$ to partition v_a and a set of binary variables ξ_a^n to indicate whether v_a is fall in the section $[K_{a,n}, K_{a,n+1})$, i.e., $K_{a,n} \le v_a < K_{a,n+1}$ if $\xi_a^n = 1$. In each segment, we build an approximately linear function to represent the travel time t_a:

$$t_a = A_n^a \cdot v_a + B_n^a \tag{6.87}$$

Where A_n^a and B_n^a are two coefficients to be determined. We use the first-order Taylor series to determine them as follows:

$$A_n^a = \left.\frac{dt_a}{dv_a}\right|_{K_{a,n}} = 0.6 * \frac{t_a^0}{c_a^4} * {K_{a,n}}^3 \tag{6.88}$$

$$B_n^a = t_a^0 \left[1 + 0.15\left(\frac{K_{a,n}}{c_a}\right)^4\right] - A_n^a * K_{a,n} \tag{6.89}$$

So, the travel time function into mixed-integer linear constraints:

$$K_{a,n} \cdot \xi_{a,n} \le v_a < M \cdot \left(1 - \xi_{a,n}\right) + K_{a,n+1} \qquad \forall a \epsilon A(p), p \in P^w, w \epsilon W, n \in N \tag{6.90}$$

$$\begin{aligned}(-M) \cdot \left(1 - \xi_{a,n}\right) \le t_a - (A_n^a \cdot v_a + B_n^a) \\ \le M \cdot \left(1 - \xi_{a,n}\right)\end{aligned} \qquad \forall a \epsilon A(p), p \in P^w, w \epsilon W, n \in N \tag{6.91}$$

$$\xi_{a,n} \in \{0,1\} \qquad \forall a \epsilon A(p), p \in P^w, w \epsilon W, n \in N \tag{6.92}$$

$$\sum_{n} \xi_{a,n} = 1 \qquad \forall a \epsilon A(p), p \in P^w, w \epsilon W, n \in N \qquad (6.93)$$

Where M is still a very large positive constant. Binary variable $\xi_{a,n}$ indicates that whether v_a is no less than $K_{a,n}$. From (6.90), if $\xi_{a,n} = 0$, then $0 \leq v_a < M$; if $\xi_{a,n} = 1$, then $K_{a,n} \leq v_a < K_{a,n+1}$. And in constraint (6.91), we have if $\xi_{a,n} = 0$ (which indicates v_a not falls into $[K_{a,n}, K_{a,n+1})$), then $-M \leq t_a - (A_n^a \cdot v_a + B_n^a) < M$, and if $\xi_{a,n} = 1$ (which indicates v_a falls into $[K_{a,n}, K_{a,n+1})$), then $0 \leq t_a - (A_n^a \cdot v_a + B_n^a) < 0$, i.e., $t_a = (A_n^a \cdot v_a + B_n^a)$.

Similarly, we could linearize the electricity generation cost function (6.24) as follows:

$$C_n^k = \frac{dZ_k}{d\varphi_k}\Big|_{K_{k,n}} = 2 * a_{k,0} * K_{k,n} + a_{k,1} \qquad \forall k \epsilon K, n \in N \qquad (6.94)$$

$$D_n^k = a_{k,0} \cdot K_{k,n}^2 + a_{k,1} \cdot K_{k,n} + a_{k,2} - C_n^k * K_{k,n} \qquad \forall k \epsilon K, n \in N \qquad (6.95)$$

$$K_{k,n} \cdot \theta_{k,n} \leq \varphi_k < M \cdot (1 - \theta_{k,n}) + K_{k,n+1} \qquad \forall k \epsilon K, n \in N \qquad (6.96)$$

$$(-M) \cdot (1 - \theta_{k,n}) \leq Z_k - (C_n^k \cdot \varphi_k + D_n^k) \leq M \cdot (1 - \theta_{k,n}) \qquad \forall k \epsilon K, n \in N \qquad (6.97)$$

$$\theta_{k,n} \in \{0,1\} \qquad \forall k \epsilon K, n \in N \qquad (6.98)$$

$$\sum_{n} \theta_{k,n} = 1 \qquad \forall k \epsilon K, n \in N \qquad (6.99)$$

With all the transformations in this section, we could have a mixed-integer linear optimization problem, which can be solved by some commercial solvers such as Gurobi.

6.4 NUMERICAL ANALYSIS

This section gives a numerical example to demonstrate the effectiveness of our model and the solution algorithm. Further, we also conduct a sensitivity analysis that varies the traffic demand, the electricity generation of each bus, and the construction cost of charging lanes. So, we can systematically check their effect on our results.

6.4.1 *Transportation and Power Network Build*

We define a nine-node road network and a subset of the IEEE 118-bus system in Figure 6.1.

The transportation network consists of 32 links, and the number of OD pairs is 32. We set the free-flow travel speed to be 60 mile/hour. The length, free-flow travel time, and the capacity of each link are given in Table 6.1. Table 6.2 provides the traffic demand for each OD pair.

For the power grid, we build twelve buses, and each bus numbering from 10 to 22. Each bus serves a road (two directions) or a node or both on the transportation network. The transmission lines are undirected and connect buses in the power network. The input data for each generator are given in Table 6.3. The attributes of each transmission line are given in Table 6.4.

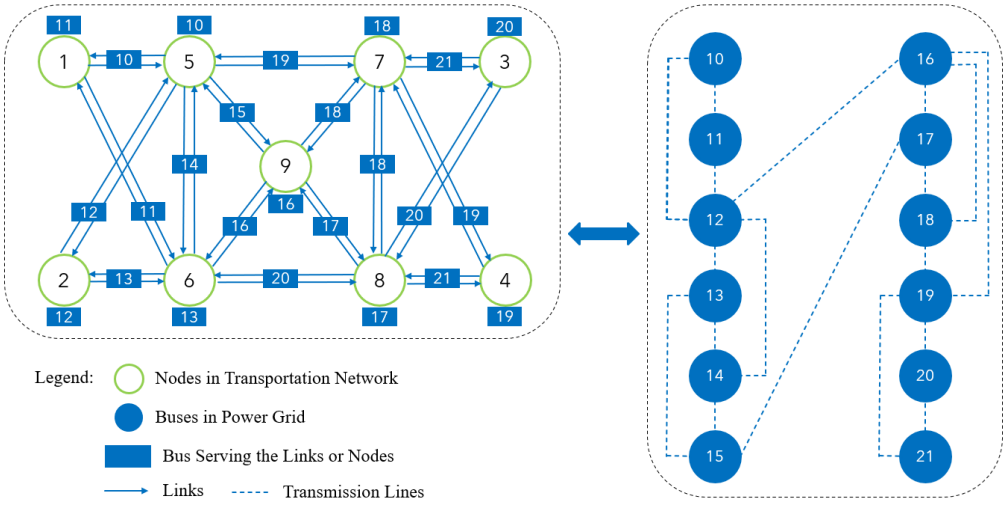

Figure 6.1 Numerical Analysis Transportation and Electricity Network

Table 6.1 Link Length (mile), Free-flow Travel Time (min), and Capacity (10^3 veh/h).

Link	Length	Free-flow Travel Time	Capacity	Link	Length	Free-flow Travel Time	Capacity
1-5	62	62	15	5-1	62	62	15
1-6	102	102	24	6-1	102	102	24
2-5	104	104	26	5-2	104	104	26
2-6	64	64	17	6-2	64	64	17
3-7	59	59	14	7-3	59	59	14
3-8	99	99	23	8-3	99	99	23
4-7	101	101	26	7-4	101	101	26
4-8	64	64	18	8-4	64	64	18
5-6	81	81	29	6-5	81	81	29
5-7	79	79	31	7-5	79	79	31
5-9	56	56	36	9-5	56	56	36
6-8	78	78	29	8-6	78	78	29
6-9	55	55	39	9-6	55	55	39
7-8	84	84	31	8-7	84	84	31
7-9	55	55	36	9-7	55	55	36
8-9	57	57	37	9-8	57	57	37

Table 6.2 Travel Demand of each OD.

O-D	**Traffic Demand**	**O-D**	**Traffic Demand**	**O-D**	**Traffic Demand**	**O-D**	**Traffic Demand**
1-2	500	2-6	520	4-7	600	6-8	500
2-1	550	6-2	500	7-4	650	8-6	480
1-5	600	3-4	500	4-8	550	6-9	512
5-1	650	4-3	550	8-4	530	9-6	520
1-6	700	3-7	600	5-7	590	7-9	420
6-1	750	7-3	650	7-5	600	9-7	470
2-5	535	3-8	700	5-9	630	8-9	490
5-2	530	8-3	750	9-5	625	9-8	481

Table 6.3 Input Data of Generators

Bus	Regular Load (MW)	Lower Limit (MW)	Upper Limit (MW)	$a_{k,0}$(\$/MW^2h)	$a_{k,1}$(\$/MWh)	$a_{k,2}$(\$/h)
10	63	25	110	0.0128	17.82	10.15
11	84	25	110	0.0128	17.82	10.15
12	150	50	210	0.0139	13.29	39
13	78	0	0	0	0	0
14	0	50	210	0.0139	13.29	39
15	77	25	110	0.0128	17.82	10.15
16	0	0	0	0	0	0
17	0	0	0	0	0	0
18	39	100	420	0.0136	8.34	64.16
19	28	0	0	0	0	0
20	0	0	0	0	0	0
21	0	80	300	0.0109	12.89	6.78

Table 6.4 Input Data of Transmission Lines

Line	Capacity	Inverse of the pu reactance (D)	Line	Capacity	Inverse of the pu reactance (D)
10-11	175	66.23	12-16	500	25.91
11-12	175	3.98	16-17	500	50
10-12	175	4.63	14-17	500	37.31
12-13	175	6.90	15-18	175	4.59
12-14	175	6.67	15-19	175	8.55
13-14	500	74.07	18-19	175	9.85
12-15	175	17.83	19-21	175	3.6
14-15	175	26.60	20-21	500	27.03

We use the average income in the U.S. in 2019, $26.5 per hour per capita, as the value of travel time [63]. The battery capacity, E_0, is 40 kWh, a type of Nissan Leaf BEV [64]. The energy consumption rate, ω, is 0.29 kWh/mi. The charging speed of charging lane is 6 kW [49], and the charging power of DCFC charging we use is 100 kW, which is one of the version of Tesla Supercharger [65]. The charging price of charging lanes we use is $0.5 per kWh [49], and that of charging station is $0.3 per kWh [66] .We set the initial SOC, E_0, to be 20 kWh. In addition, we set the minimum SOC drivers try to maintain is 2 kWh.

To estimate the infrastructure cost, we can use the results from the paper of Suomalainen and Colet. [30] Given a 200 km (124 miles) highway in their article, they provide two types of charging facilities: charging lanes and DCFC charging stations to supply electricity to the BEVs. Then they compute the infrastructure costs of the two charging methods. The infrastructure costs include initial installation, material, maintenance, and replacement costs of 25 years (from 2020 to 2045). On the 200 km highway, they build a charging station every 30 km, and the charging lane length is 30 km, which could ensure all the vehicles finish their trip. The total costs of

charging stations are $127.12M ($19.07M per station) in 25 years, and the total costs of charging lanes are $202.18M ($1.63M per mile) in 25 years. We use the two infrastructure data from their paper and set the budget limit to be $3.85B.

6.4.2 *Model Results*

We solve the problem under the parameter settings above. In our optimization model, we have 3857 continuous variables and 2051 binary variables. Using Gurobi solver, the total solution time is 2051 seconds. The results of transportation network are shown in Table 6.5.

Table 6.5 Equilibrium Link Conditions

Link	**Volume (veh/h)**	**Travel Time (min)**	**Link**	**Volume (veh/h)**	**Travel Time (min)**
1-5	850	62	5-1	1950	62
1-6	950	102	6-1	0	0
2-5	0	0	5-2	780	104
2-6	1605	64	6-2	750	64
3-7	1100	59	7-3	900	59
3-8	700	99	8-3	1050	99
4-7	850	101	7-4	1150	101
4-8	850	64	8-4	0	0
5-6	0	0	6-5	2972	81
5-7	590	79	7-5	600	79
5-9	1142	56	9-5	0	0
6-8	500	78	8-6	480	78
6-9	0	0	9-6	1145	55
7-8	0	0	8-7	0	0
7-9	420	55	9-7	470	55
8-9	490	57	9-8	481	57

Table 6.5 shows that some of the links have 0 volumes. It indicates some of the drivers only use the path with charging lanes. Besides, since the roads' capacity is much higher than the traffic volume, the travel time is close to the free-flow travel time on each link. Figure 2 shows construction plans of charging facilities.

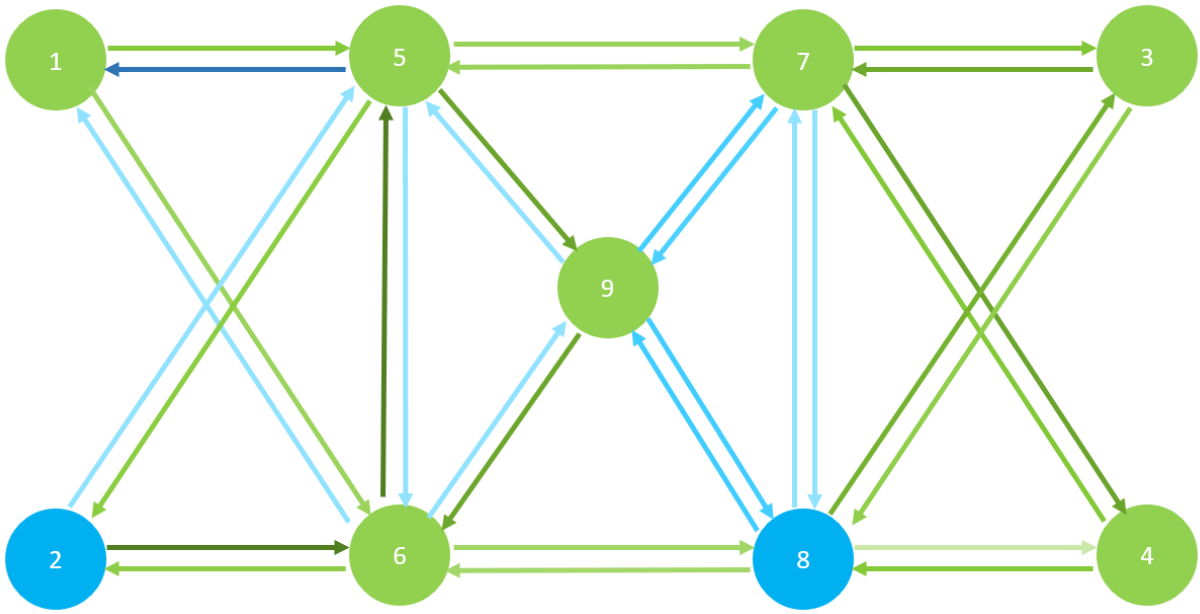

Figure 6.2 Deployment Solution of Charging Facilities

In Figure 6.2, the green nodes mean the nodes constructed as charging stations, and the green links indicate that the links are constructed as charging lanes. The shade of the color represents the volumes on each link: the dark color represents high volume.

The figure and our results show that charging facilities' locations have a high relationship with traffic distribution. Under our traffic condition, more BEV drivers choose to use charging lanes. For example, most of the traffic from OD 2-1 uses path 2-6-5-1, but a minimal volume uses path 2-6-1. Because path 2-6-5-1 has a charging lane on the link 6-5, and path 2-6-1 only has a charging station at node 6. The drivers choose to use the charging lanes on path 2-6-5-1 even if the travel distance is longer than the path 2-6-1.

For the power generation and bus costs, the details are given in Table 6.6.

Table 6.6 Power Generation and Cost of each Bus

Bus	Electricity Generated (MW)	Generation Cost ($/MWh)	Bus	Electricity Generated (MW)	Generation Cost ($/MWh)
10	35	18.56	16	0	0
11	35	18.56	17	0	0
12	70	14.82	18	288.98	12.49
13	0	0	19	0	0
14	70	14.82	20	0	0
15	35	18.56	21	110	14.15

It shows that bus 18 generates the most electricity to minimize the total cost. The objective value (the total electricity generation cost plus the total transportation cost) is $763,951.28 ($9189.96 electricity generation cost plus $754,761.32 transportation cost). We could learn that the transportation cost is much higher than the electricity generation cost in our model. The main contributor to the electricity cost is the regular load in the transportation network. Because the volume on the transportation network is not large in our numerical example. The main contributor to transportation cost is the electricity cost using charging lane and charging station.

Among all the 18,233 BEV traffic on our network, 12,722 of them (69.8%) used the charging lanes, and only 9,415 of them (51%) used the charging stations. This indicates the BEV drivers prefer to using charging lanes. Besides, the average charging time for the vehicles using charging lanes is 41.82 minutes. The average charging time for the vehicles using charging stations is only about 10.34 minutes. The average charging time of using charging lane is much longer because the charging power of charging lane is lower, and the time is not “lost” when the BEV drivers using charging lanes.

6.5 Sensitivity Analysis

In addition to the results based on our numerical results, we also change the demand of BEVs in each OD, the upper bound of bus electricity generation, and the infrastructure costs of charging lanes to see their affects.

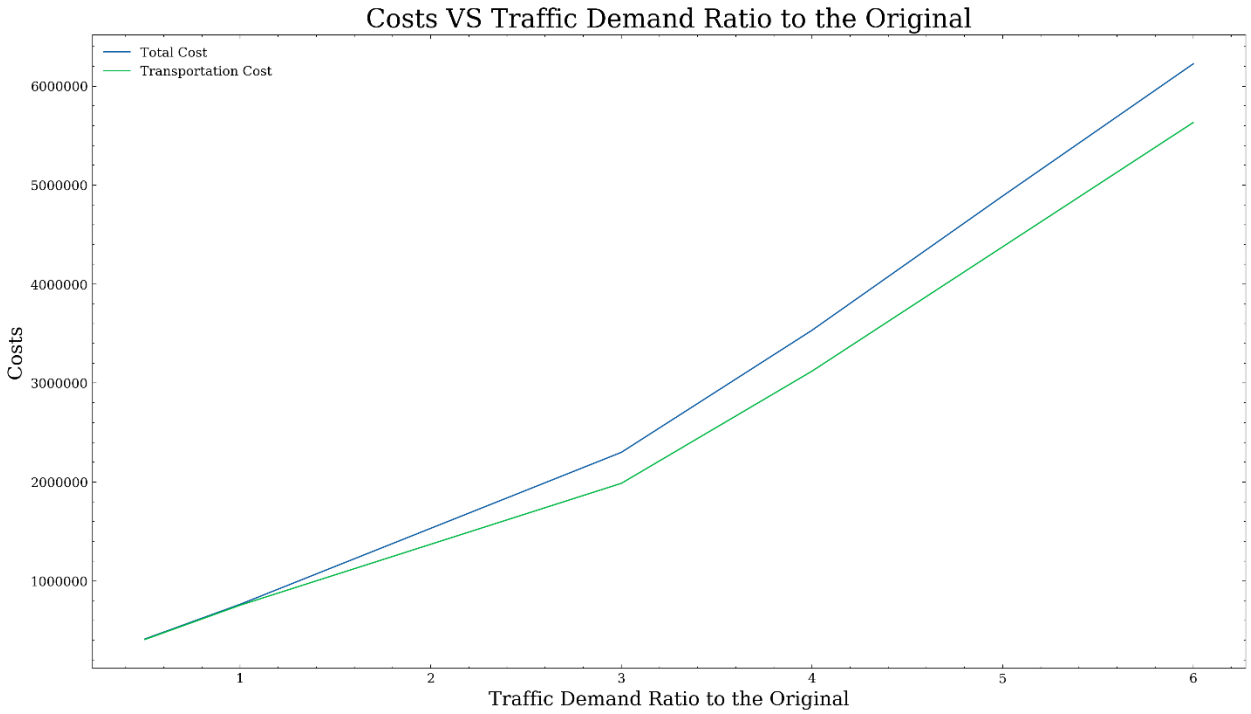

Figure 6.3 Traffic Demand and Costs

The above figure shows when the travel demand of each OD increases, how the total cost (electricity cost and transportation cost) and transportation cost changes. The x-axis, traffic demand ratio to the original, means the current demand ratio and the original demand in Table 6.2. i.e., the value 6 in the x-axis indicates the traffic demand of each OD is six times the original demand. From the figure, we could see that both the total costs and transportation costs increase when the demand ratio rises. When the ratio is high, the increased rates of both costs are high. When the traffic on the road is high, the travel time cost will increase based on the traffic

conditions. From the figure, we also see that most of the costs are from transportation costs. The difference between the total costs and transportation costs (which represent the electricity costs) is steady. This is because we assume that the electricity consumption is only based on the driving distance. The increase of the difference is only from the rise in traffic.

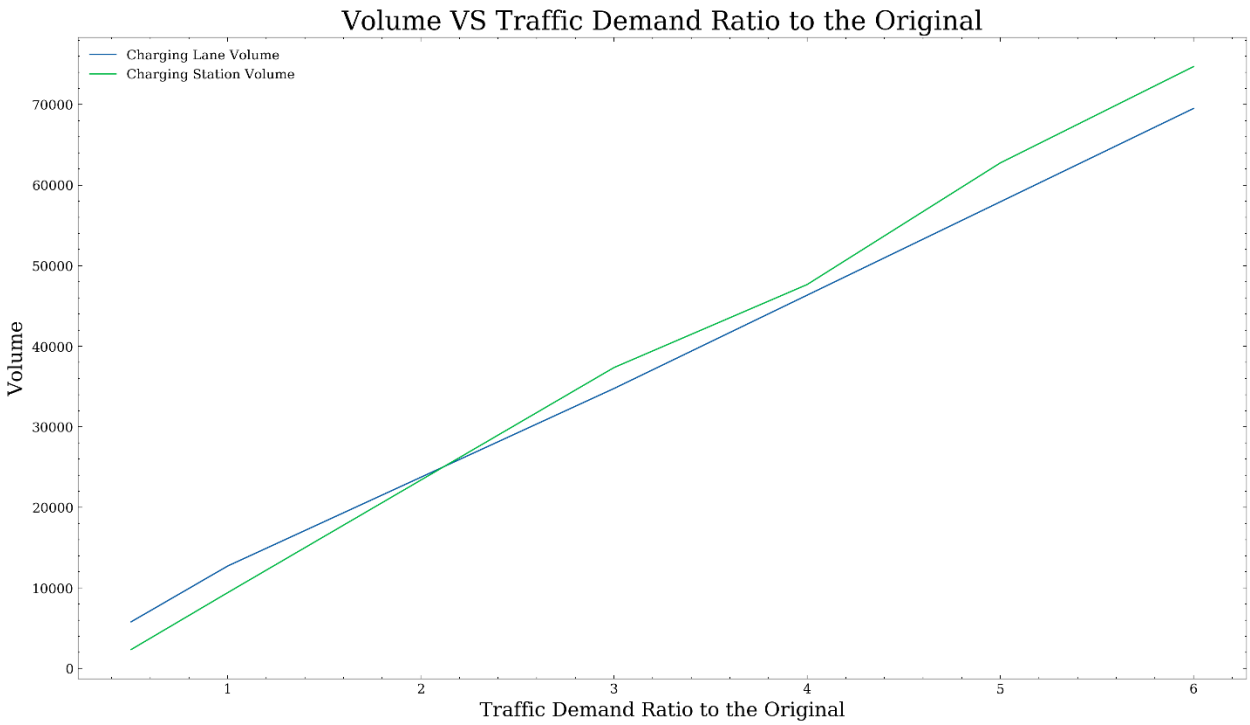

Figure 6.4 Traffic Demand and Volumes Using Each Facility

The above figure shows when the demand changes, how the volumes use in each charging facility change. The x-axis is the same with Figure 6.3. Note that BEVs on our model could use both charging methods. From the figure, we could see that when the ratio is small, the volume using charging lanes is higher than the volume using DCFC charging stations. However, when the demand increases (the ratio is higher than 2), the volume using charging stations exceeds the volume using charging lanes. This is because when the demand increases, the electricity supplied by charging lanes cannot meet all the electricity demand of BEV drivers. So some drivers must

turn to use the charging stations. When the demand increases, more and more vehicles are using the charging lane, which makes the total transportation cost increase. This makes some drivers turn to use charging stations to reduce the total travel cost and finally reach the user equilibrium.

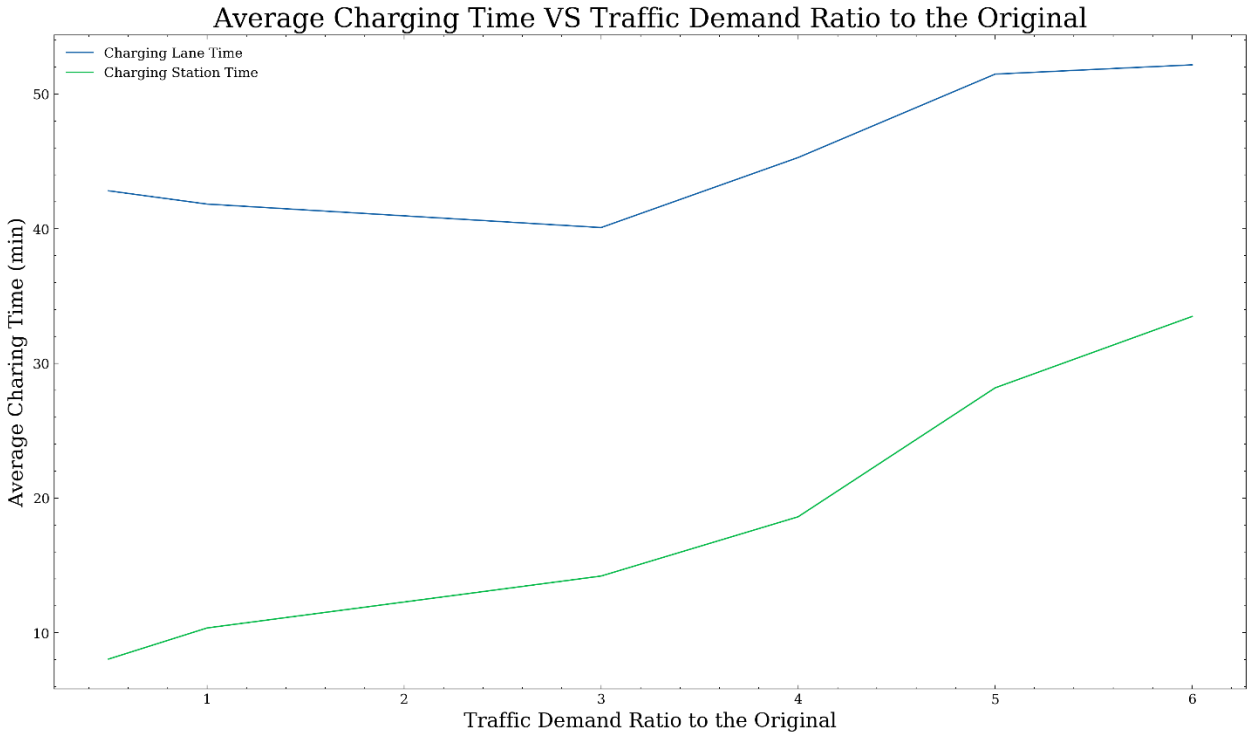

Figure 6.5 Traffic Demand and Average Charging Time Using Each Facility

The above figure shows when traffic demand changes, how the average charging time of charging lanes and charging stations changes. From the figure, we could learn that both the average charging time of the two charging facilities increases when the demand increases. This indicates that when the demand increase, some drivers, who use the charging lane but have a low charging time, would like to use charging stations instead. We think this is because of the electricity generation limit of buses that supply the charging lanes. Therefore, next, we will change the electricity generation upper bound of buses to see how the values change.

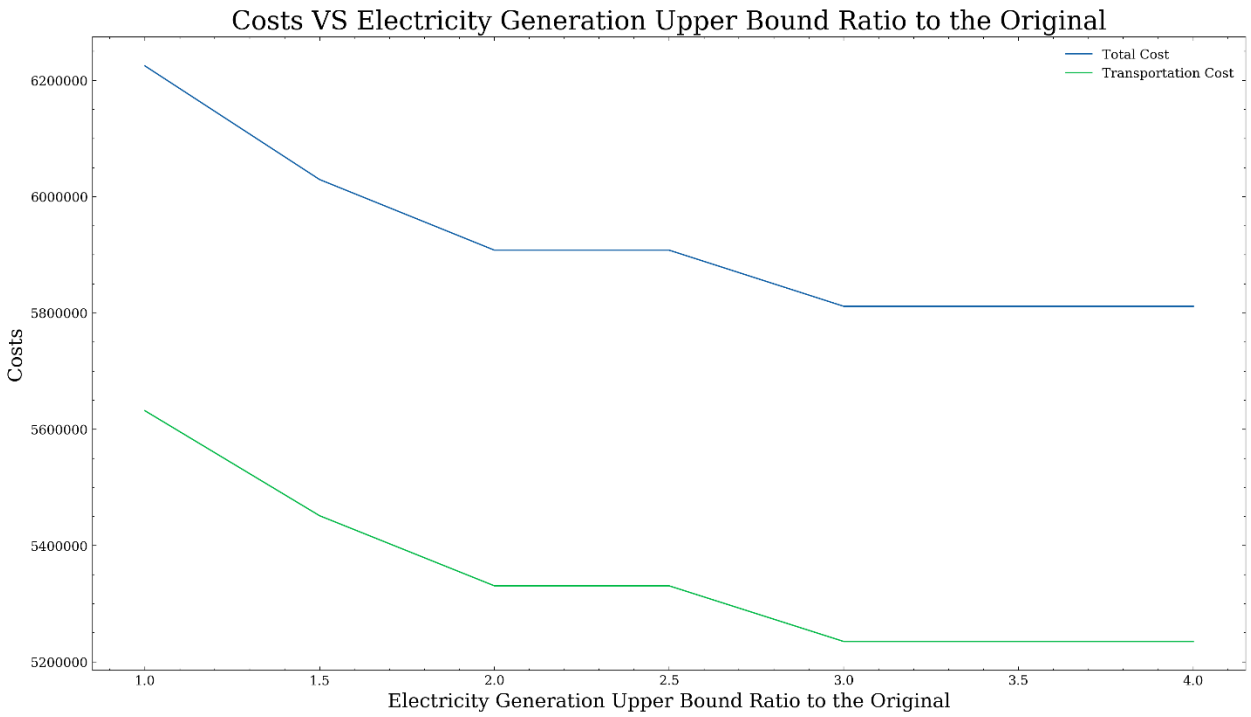

Figure 6.6 Costs and Electricity Generation Upper Bound

Figure 6.6 shows when the upper bound of bus electricity generation changes, how the total costs and transportation costs change. The reason we do this sensitivity analysis is based on the results about the traffic demand. When the demand increases, we could see the volume using charging stations exceed that using charging lanes. We think this is because of the limitation of bus electricity generation. Therefore, in this analysis, we change the upper bound of bus electricity generation upper bound and use the greatest demand in the first sensitive analysis (six times the original demand). From the Figure 6.6. we could see that when the upper bound increases, which means each bus could generate more electricity, both the total cost and the transportation cost decrease. This indicates that the power generation limits the usage of charging lanes. However, both the reductions are not large, which means the limitation is not significant from the current bus electricity generation.

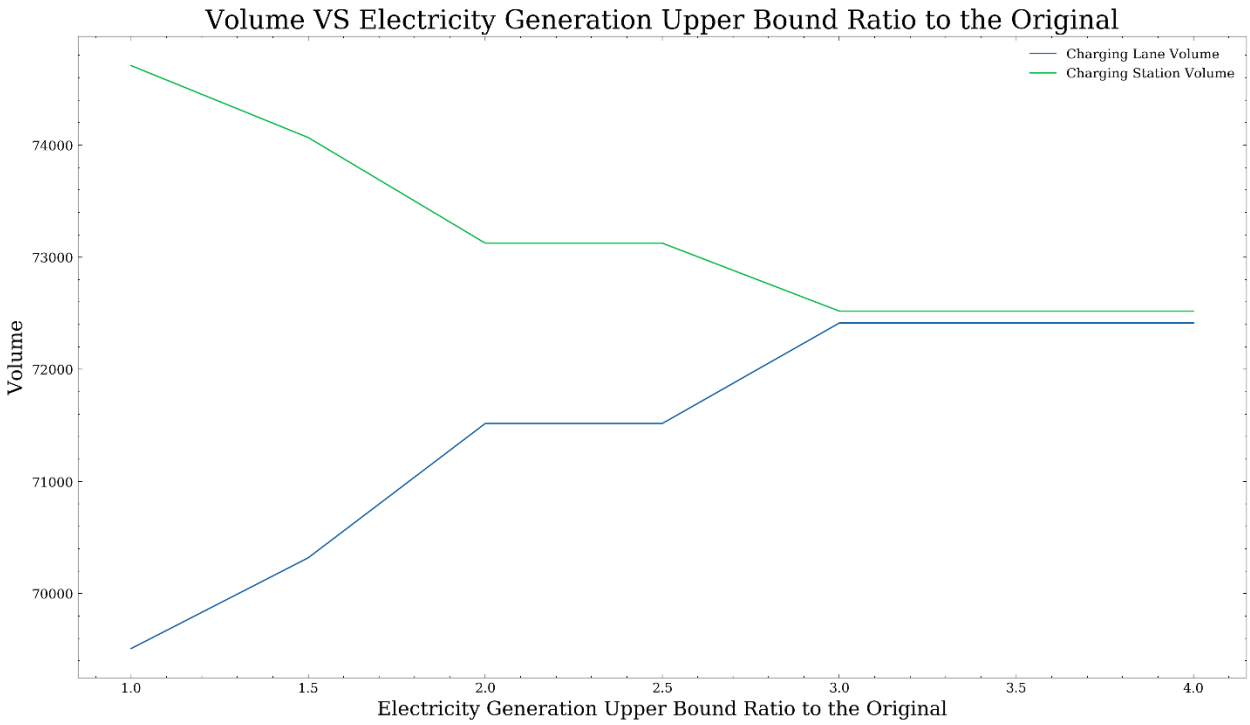

Figure 6.7 Electricity Generation Upper Bound and Volume of Charging Facilities

Similarly, the above figure shows how the volume using each charging facility changes when the electricity generation upper bound changes. We could see that the charging station's volume decreases, and the volume using the charging lane increases. When buses can generate more electricity, more vehicles turn to use charging lanes, leading to the total cost and transportation cost decreasing. This indicates charging lanes is more attractive to BEV drivers, and it is more cost-efficient than DCFC charging stations.

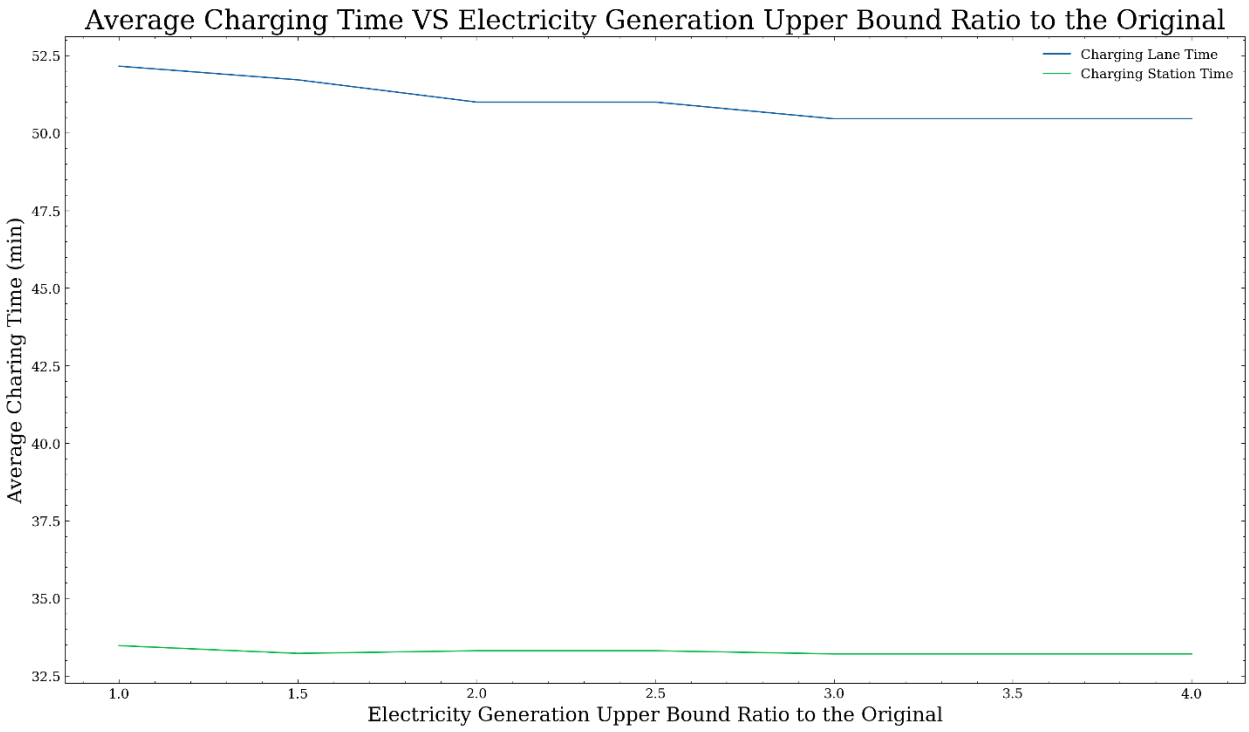

Figure 6.8 Electricity Generation Upper Bound and Average Charging Time

The above figure shows when the electricity generation upper bound changes, how the average charging time changes. It is shown that both the average charging time of using the charging lane and charging station decrease when the upper bound increases. This indicates that when more BEVs choose to use charging lanes, both facilities' charging time decreases, leading to the total cost and transportation cost decrease. This also proves that the charging lanes are more cost-efficient. However, even if the charging lane is cost-efficient, we still need to take the high construction cost of charging lanes into consideration. Next, we will change the infrastructure cost to see how it affects our results.

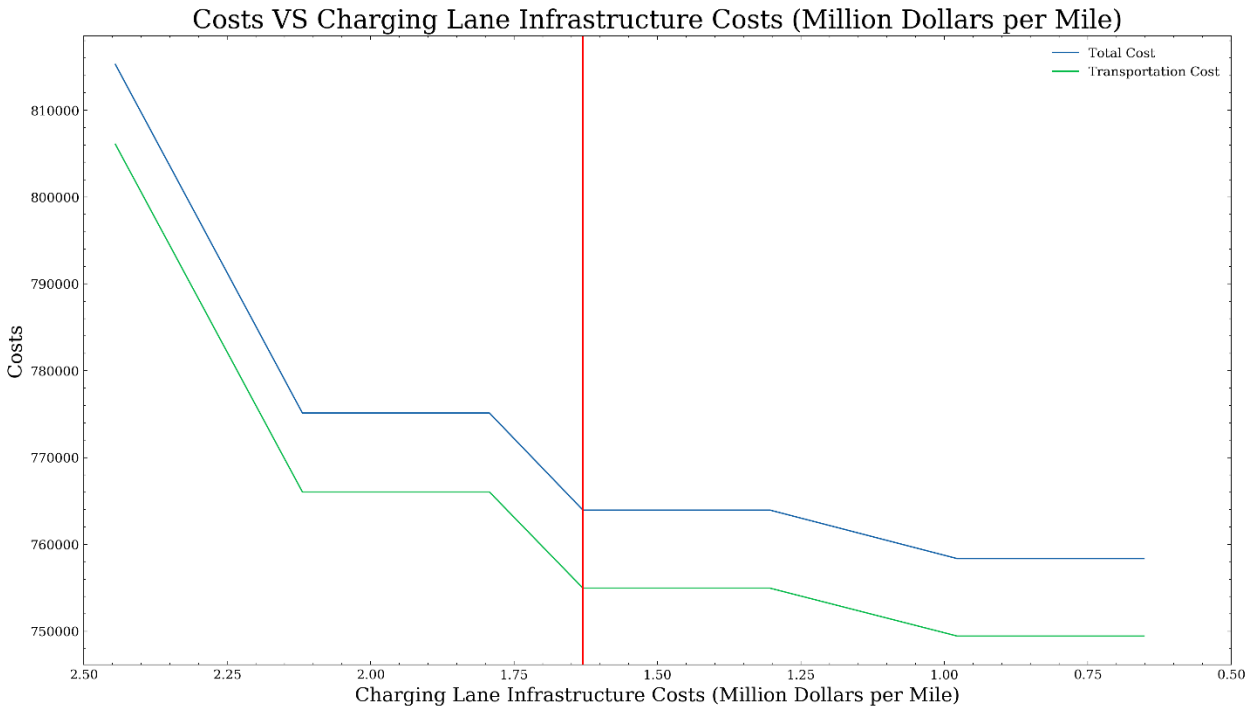

Figure 6.9 Charging Lane Infrastructure Costs and Costs

Figure 6.9 shows when the charging lane infrastructure cost changes, how the total cost and transportation cost change. The red vertical line means the numerical analysis's infrastructure cost ($ 1.63M per mile). The above figure shows that when the infrastructure cost increases (left on the red line), the total cost and transportation cost increase significantly. On the other hand, when the infrastructure cost decreases, both the costs decrease. When the infrastructure cost decreases, more charging lanes will be constructed on the road network. Because the charging lane is more cost-efficient, both the costs decrease.

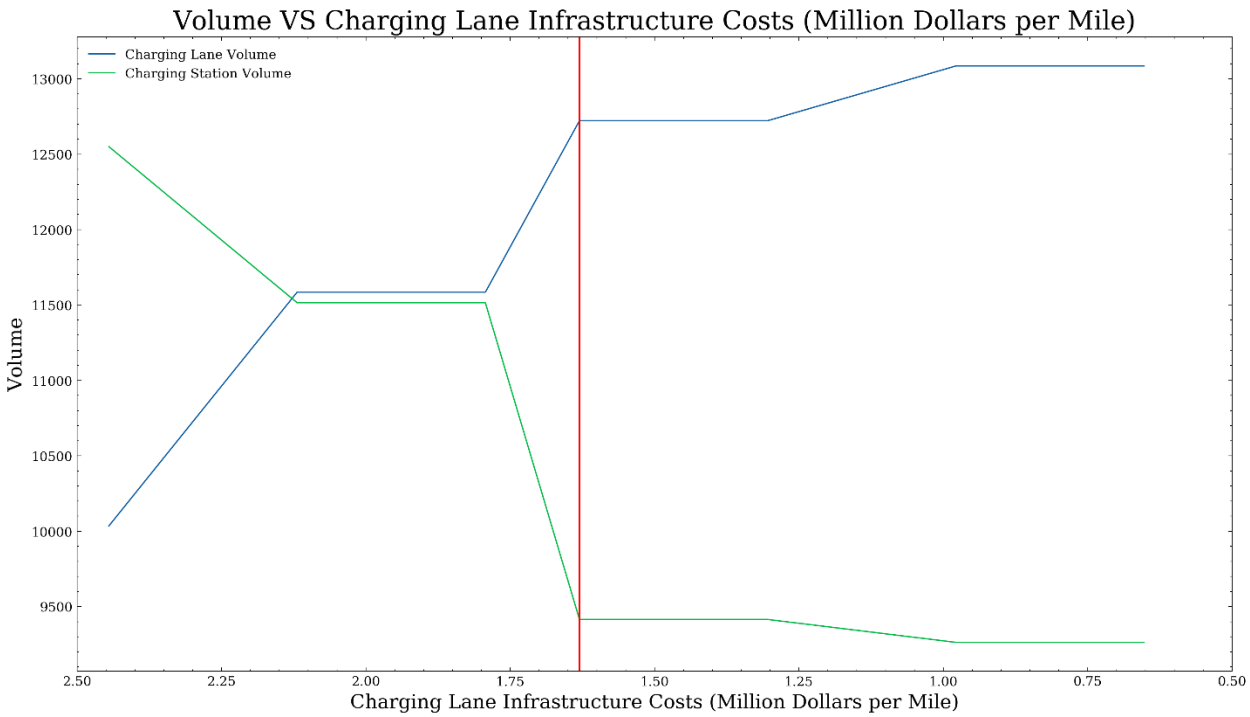

Figure 6.10 Charging Lane Infrastructure Cost and Volumes

The above figure shows how the volumes using charging lanes and charging stations change when the charging lane infrastructure cost changes. The red vertical line means the infrastructure cost in the numerical analysis. It is shown that when the infrastructure cost increases (left on the red line), the volume using the charging lane decreases significantly. More vehicles choose to use charging stations. On the other hand, when the infrastructure cost decreases, more and more BEVs choose to use charging lanes.

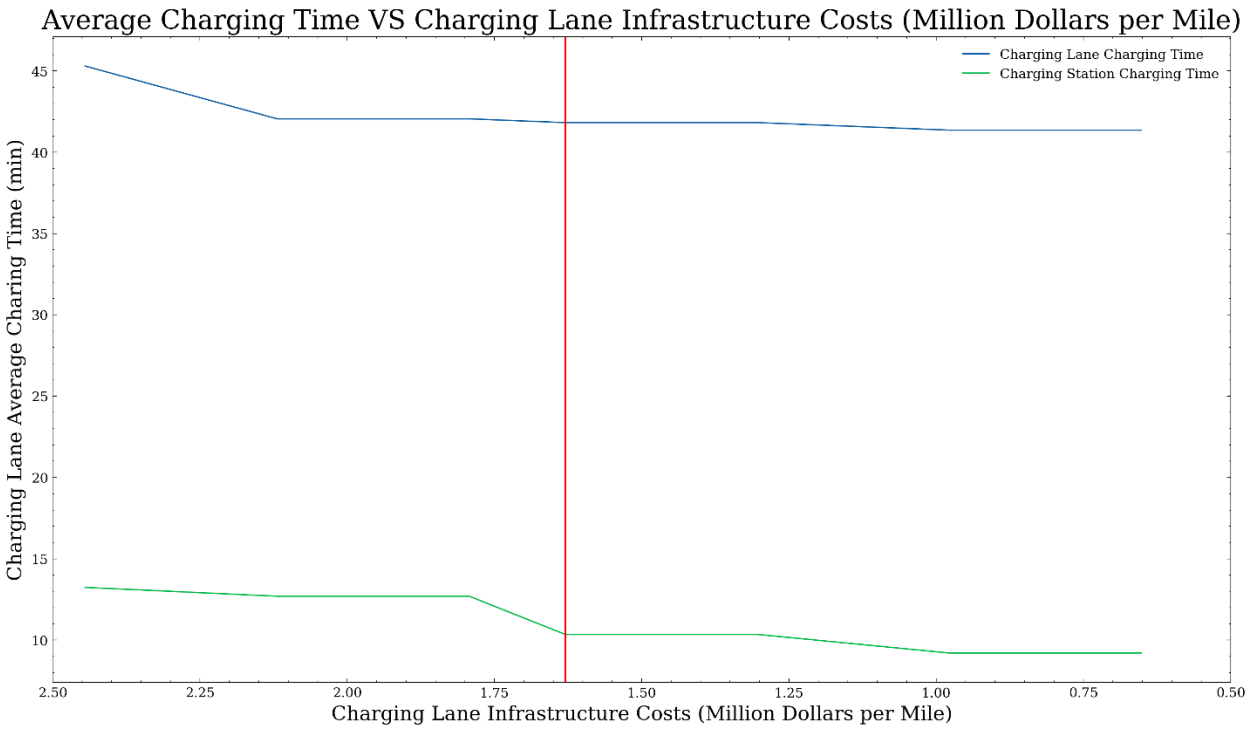

Figure 6.11 Charging Lane Infrastructure Cost and Average Charging Time

The average charging time of the two charging facilities also increases when the charging lane's infrastructure costs increase, and it decreases when this cost decreases. This is the same with the costs when the charging time of both charging methods decreases, the transportation costs of BEV drivers reduce, and the total costs.

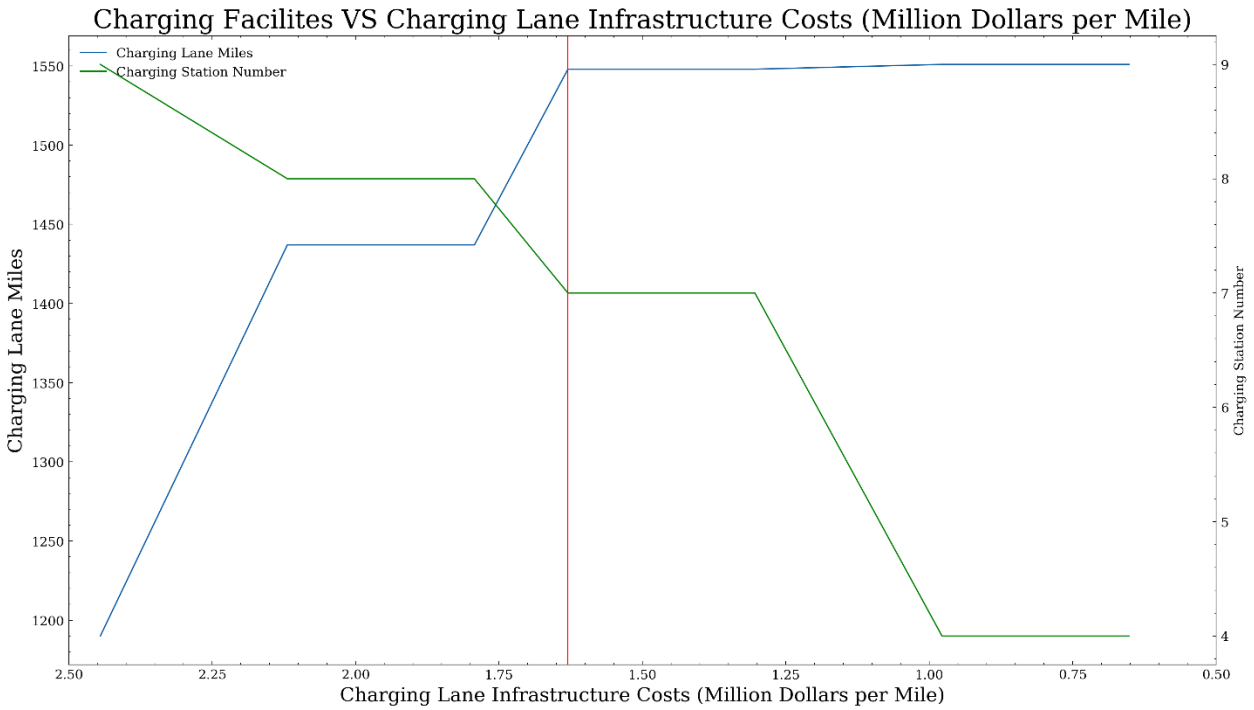

Figure 6.12 Charging Lane Infrastructure Cost and Charging Facilities Construction

The above figure shows when the charging lane infrastructure cost changes, the length of charging lane built, and the number of DCFC charging stations built in our network in Figure 6.2. It is shown that when the cost increases to $2.5 M per mile, there are only 1,200 miles out of 2,400 miles to be constructed as charging lanes (50%), and all the nine nodes are constructed as DCFC charging stations. However, when the cost decreases to $0.75 M per mile, there are 1550 miles out of 2,400 miles to be built as charging lanes (65%), and only four out of nine nodes are constructed as DCFC charging stations. These results indicate that when the charging lane's infrastructure cost decreases, more charging lanes and fewer charging stations are constructed, and the total cost decreases. This also proved charging lanes are more cost coefficient under the current charging speed of charging stations.

6.6 SUMMARY

In this chapter, we design a whole system on a given road network and a power grid. By building an optimization work and solve it using the method, we could decide where to make the charging lanes and fast-charging stations. We could also determine the electricity generated in each bus. All BEV drivers could have an optimal path from origin to destination with minimum cost considering both travel time and charging cost by solving this optimization work. Our numerical analysis results show that charging lanes are more attractive than charging stations, and the charging time of charging lanes is much higher than charging stations. The paths with charging lanes have a higher volume than the paths that only have charging stations. From our sensitivity analysis, we could conclude that the charging lane is more cost-effective than charging stations. Still, the power generation limit of buses may limit the usage of charging lanes.

This chapter shows the new charging method's power, the dynamic charging lane, is attractive to BEV drivers. Charging lanes is more economic effective than charging stations under our numerical analysis and ignore the infrastructure costs of charging lane. However, we still need to consider that the charging lane's construction cost is still very high compared with DCFC charging stations. Yet, it can expand the driving range of BEVs and promote BEVs, especially in the future, the construction cost could be reduced. We can imagine that when the BEVs are broadly adopted, the charging lanes are a useful method to supply electricity with the vehicles. We also consider the traffic assignment based on user equilibrium. So, this study is an entire design from the planning level to the operation level. It gives the government a reasonable deployment plan considering both the traffic network and the power grid.

The next stage of this work includes adding the gasoline vehicles on the network, which will affect the traffic assignment. Besides, we could also release some assumptions such as the

energy consumption only depends on the travel distance. It should be related to the travel time and distance together. Finally, because we turn the optimization problem into a linear mixed-integer problem, it can be used in a larger road and electricity network.

Chapter 7. CONCLUSION AND DISSCUSSION

7.1 CONCLUSION

This study provides a full investigation of the dynamic charging lane, a new charging method of BEV. It uses wireless charging technology to charge the BEVs while driving to save charging time compared to charging stations. In this paper, we first try to find the attributes and conditions that make BEV drivers choose to use the charging lane. To find them, we design a stated preference survey and dispatch them to 161 BEV drivers in China and build a mixed logit model. The model results show that the income, travel distance, cost difference of the two-charging method, and power left at the destination significantly influence BEV drivers' charging choice behavior. When the income is high, or the difference between charging lane cost and charging station cost is low, BEV drivers prefer to use charging lanes. Because they could save charging time. Besides, when the travel distance or power left at the destination is high, BEV drivers also would like to use charging lanes to avoid a long charging time.

Next, we develop a traffic assignment model based on the mixed logit model. We assume that each BEV could only use one charging method, given the transportation network and the charging facility's locations. We design a two-stage algorithm to combine the mixed logit model and the traffic assignment model based on User Equilibrium. The results show that the charging lane users need to concentrate on the links with the charging lane. This leads to the charging stations that users must avoid using these links to reduce congestion. Besides, the equilibrium cost of charging station users is lower than that of charging lane users. Still, charging station users' travel time (including the charging time at DCFC charging stations) is higher than charging lane users.

To build the location models of dynamic charging lanes and DCFC charging stations, we release the assumption that each BEV can only use one charging method. This is because the two-stage algorithm in chapter 5 could be time-consuming when it is the lower-level optimization problem. In the location optimization problem, we first build an SVP from the BEV drivers' point of view as the lower-level optimization problem. Then, we consider the constraints based on User Equilibrium and the power network constraints as the upper-level optimization constraints. The upper-level objective function includes the costs of generating electricity and the costs of all the BEV drivers. We use KKT conditions to turn the lower-level optimization problem into constraints of the upper level. Then we use some binary variables to turn the non-linear optimization work into a mixed-integer linear optimization problem and solve it accordingly. The numerical results suggest that the charging lane is more attractive and cost-coefficient. More BEVs choose to use charging lanes if possible. From the sensitivity analysis result, we could learn that each bus's electricity generation may limit charging lanes, and when more charging lanes are constructed, both the total cost and transportation cost decrease. This also proves the charging lane is more cost-efficient than DCFC charging stations. However, we could not ignore that currently, the charging lane's construction cost is much higher than that of the DCFC charging station. It is not possible to build as many charging lanes as possible to reduce BEV drivers' costs. Hence, if the charging lane's construction cost could be reduced in the future, it has the potential of expanding the driving range of BEVs and promoting the usage of BEVs.

Our study represents the first attempts to investigate the new BEV charging method's fundamental research, dynamic charging lane, from the BEV drivers' viewpoints to the government agency level. We also consider the power grid constraints that may limit the

adoption of charging lanes. The government agency could optimize the locations of both the charging methods based on our study. The BEV drivers could also build their charging strategy if the charging lane is adopted to minimize the total costs. This study is an entire design plan of dynamic charging lanes and DCFC charging stations.

7.2 LIMITATIONS

There are some limitations to the study. The first limitation is that we use a binary variable to indicate whether this link should be built as a charging lane. However, we do not need to build the full link as a charging lane because the construction cost is too high. The literature shows that we only need 5% - 15% of the length to support all the electricity on this link [28]. We could choose about 5% - 15% of the link length to construct the charging lane. But this could not satisfy our model because vehicles need to charge on the charging lane and use the electricity on the links without the charging lane.

The second limitation of our study is the budget constraint. We do not put the construction costs in our objective function. Because the comparing to the electricity generation cost and transportation cost, the construction cost is too high. When we put it in the objective function, the optimization tries to minimize the construction cost of dynamic charging lanes and DCFC charging stations. It ignores the electricity generation costs and transportation costs. Make the construction budget a constraint may not be the best solution. The improvement could be that we choose a tuning parameter of construction costs and add it to the upper-level model's objective function. We could minimize all the three costs from the user's viewpoint and the governor's perspective.

7.3 FUTURE WORK

Besides the two limitations above that could be improved in the future, there are some works we could also investigate of dynamic charging lane.

First, we could improve the solution algorithm of the bi-level optimization work. We solve the bi-level optimization problem using binary variables, which could be time-consuming, especially in an extensive road network. Suppose we could find a more efficient solution algorithm for the bi-level optimization work. In that case, our model could be utilized in an extensive transportation network.

Second, because our model assumes that all the vehicles on the road are BEVs, we could add gasoline vehicles to the transportation network. The gasoline vehicles will affect the traffic assignment of BEVs. Some BEVs may turn to use charging stations because of the traffic conditions on the charging lanes. Besides, the charging lanes may attract more BEVs to use. The gasoline vehicles may need to avoid using these links to reduce the congestion costs, increasing the total cost of the vehicles. The gasoline vehicles on the road could make our traffic assignment model more challenging.

Third, both of our traffic assignment models assume that the electricity consumption only depends on the distance, which is not precise. The electricity consumption of BEVs also related to the driving time, SOC level of BEV, and other attributes. We need to improve the energy consumption model to make it more realistic.

Forth, we could develop a long-term analysis including the revenue and costs of these two types of charging facilities. We could also include these attributes in our optimization model and compare which charging method could be more cost-efficient in the long term.

This study provides a deployment design of dynamic charging lanes and DCFC charging stations, considering the transportation constraints and electricity network constraints. It gives a prediction method of the demand for the different charging methods, a systematic process to analyze the effect of the charging facilities on the current traffic system, and a full analysis of the two charging facilities' varying design conditions.

BIBLIOGRAPHY

[1] M. Duvall, “Advanced batteries for electric-drive vehicles,” *Electr. Power Res. Inst.*, 2004.

[2] A. Maitra, K. S. Kook, J. Taylor, and A. Giumento, “Grid impacts of plug-in electric vehicles on Hydro Quebec’s distribution system,” in *IEEE PES T&D 2010*, 2010, pp. 1–7.

[3] B. Jetin, “Who will control the electric vehicle market?,” *Int. J. Automot. Technol. Manag.*, vol. 20, no. 2, pp. 156–177, 2020.

[4] I. E. A. G. E. V Outlook, “Entering the Decade of Electric Drive.” 2020.

[5] D. Gohlke and Y. Zhou, “Assessment of Light-Duty Plug-in Electric Vehicles in the United States, 2010–2019,” Argonne National Lab.(ANL), Argonne, IL (United States), 2020.

[6] D. Sperling and D. Gordon, *Two billion cars: driving toward sustainability*. Oxford University Press, 2010.

[7] M. Moyer, “The dirty truth about plug-in hybrids.,” *Sci. Am.*, vol. 303, no. 1, pp. 54–55, 2010.

[8] C. Liu, K. T. Chau, D. Wu, and S. Gao, “Opportunities and challenges of vehicle-to-home, vehicle-to-vehicle, and vehicle-to-grid technologies,” *Proc. IEEE*, vol. 101, no. 11, pp. 2409–2427, 2013.

[9] H. Lee and G. Lovellette, “Will electric cars transform the US vehicle market,” *An Anal. key Determ.*, 2011.

[10] M. Suhanek, I. Djurek, and A. Petosic, “A Case Study: The Urban Residents’ Choice for Electric Vehicles Warning Sounds,” *Am. J. Environ. Sci. Eng.*, vol. 3, no. 3, pp. 47–51, 2019.

[11] J. Smart and S. Schey, “Battery electric vehicle driving and charging behavior observed early in the EV project,” *SAE Int. J. Altern. Powertrains*, vol. 1, no. 1, pp. 27–33, 2012.

[12] S. Schey, D. Scoffield, and J. Smart, “A first look at the impact of electric vehicle charging on the electric grid in the EV project,” *World Electr. Veh. J.*, vol. 5, no. 3, pp. 667–678, 2012.

[13] T. Zhang, X. Chen, Z. Yu, X. Zhu, and D. Shi, “A Monte Carlo simulation approach to evaluate service capacities of EV charging and battery swapping stations,” *IEEE Trans. Ind. Informatics*, vol. 14, no. 9, pp. 3914–3923, 2018.

[14] Z. Chen, F. He, and Y. Yin, “Optimal deployment of charging lanes for electric vehicles in transportation networks,” *Transp. Res. Part B Methodol.*, vol. 91, pp. 344–365, 2016.

[15] Z. Liu, W. Zhang, X. Ji, and K. Li, “Optimal planning of charging station for electric vehicle based on particle swarm optimization,” in *IEEE PES Innovative Smart Grid Technologies*, 2012, pp. 1–5.

[16] Z. Bi, T. Kan, C. C. Mi, Y. Zhang, Z. Zhao, and G. A. Keoleian, “A review of wireless power transfer for electric vehicles: Prospects to enhance sustainable mobility,” *Appl. Energy*, vol. 179, pp. 413–425, 2016.

[17] J. Thornton, “Pulling Power from the Road,” *Mech. Eng.*, vol. 136, no. 04, pp. 44–49, 2014.

[18] J. G. Bolger, F. A. Kirsten, and L. S. Ng, “Inductive power coupling for an electric highway system,” in *28th IEEE vehicular technology conference*, 1978, vol. 28, pp. 137–144.

[19] D. Herron, “Siemens eHighway of the future concept.” 2014.

[20] S. Newsroom, “Scania tests next-generation electric vehicles.” 2014.

[21] B. Schiller, “Volvo tests a road that can charge cars and trucks.” 2013.

[22] S. Lukic and Z. Pantic, “Cutting the cord: Static and dynamic inductive wireless charging of electric vehicles,” *IEEE Electrif. Mag.*, vol. 1, no. 1, pp. 57–64, 2013.

[23] S. Chopra and P. Bauer, “Driving range extension of EV with on-road contactless power transfer—A case study,” *IEEE Trans. Ind. Electron.*, vol. 60, no. 1, pp. 329–338, 2011.

[24] I.-S. Suh, “Intelligent Wireless EV Fast Charging with SMFIR. Technology,” *J. Integr. Des. Process Sci.*, vol. 15, no. 3, pp. 3–12, 2011.

[25] P. Bansal, “Charging of electric vehicles: technology and policy implications,” *J. Sci. Policy Gov.*, vol. 6, no. 1, pp. 1–20, 2015.

[26] P. P. Ding, L. Pichon, L. Bernard, and A. Razek, “Electromagnetic Field Computation in Human Body Exposed to Wireless Inductive Charging System,” 2013.

[27] Y. J. Jang, S. Jeong, and M. S. Lee, “Initial energy logistics cost analysis for stationary, quasi-dynamic, and dynamic wireless charging public transportation systems,” *Energies*, vol. 9, no. 7, p. 483, 2016.

[28] Y. D. Ko and Y. J. Jang, “The optimal system design of the online electric vehicle utilizing wireless power transmission technology,” *IEEE Trans. Intell. Transp. Syst.*, vol. 14, no. 3, pp. 1255–1265, 2013.

[29] S. Jeong, Y. J. Jang, and D. Kum, “Economic analysis of the dynamic charging electric vehicle,” *IEEE Trans. Power Electron.*, vol. 30, no. 11, pp. 6368–6377, 2015.

[30] E. Suomalainen and F. Colet, “A corridor-based approach to estimating the costs of electric vehicle charging infrastructure on highways,” *World Electr. Veh. J.*, vol. 10, no. 4, p. 68, 2019.

[31] J. Dong, C. Liu, and Z. Lin, “Charging infrastructure planning for promoting battery

electric vehicles: An activity-based approach using multiday travel data," *Transp. Res. Part C Emerg. Technol.*, vol. 38, pp. 44–55, 2014.

[32] X. Xi, R. Sioshansi, and V. Marano, "Simulation–optimization model for location of a public electric vehicle charging infrastructure," *Transp. Res. Part D Transp. Environ.*, vol. 22, pp. 60–69, 2013.

[33] M. Andrews, M. K. Dogru, J. D. Hobby, Y. Jin, and G. H. Tucci, "Modeling and optimization for electric vehicle charging infrastructure," 2013.

[34] M. J. Hodgson, "A flow-capturing location-allocation model," *Geogr. Anal.*, vol. 22, no. 3, pp. 270–279, 1990.

[35] O. Berman, R. C. Larson, and N. Fouska, "Optimal location of discretionary service facilities," *Transp. Sci.*, vol. 26, no. 3, pp. 201–211, 1992.

[36] J.-G. Kim and M. Kuby, "The deviation-flow refueling location model for optimizing a network of refueling stations," *Int. J. Hydrogen Energy*, vol. 37, no. 6, pp. 5406–5420, 2012.

[37] M. Kuby and S. Lim, "The flow-refueling location problem for alternative-fuel vehicles," *Socioecon. Plann. Sci.*, vol. 39, no. 2, pp. 125–145, 2005.

[38] C. Upchurch, M. Kuby, and S. Lim, "A model for location of capacitated alternative-fuel stations," *Geogr. Anal.*, vol. 41, no. 1, pp. 85–106, 2009.

[39] A. Ip, S. Fong, and E. Liu, "Optimization for allocating BEV recharging stations in urban areas by using hierarchical clustering," in *2010 6th International conference on advanced information management and service (IMS)*, 2010, pp. 460–465.

[40] F. He, Y. Yin, and S. Lawphongpanich, "Network equilibrium models with battery electric vehicles," *Transp. Res. Part B Methodol.*, vol. 67, pp. 306–319, 2014.

[41] F. He, Y. Yin, and J. Zhou, “Deploying public charging stations for electric vehicles on urban road networks,” *Transp. Res. Part C Emerg. Technol.*, vol. 60, pp. 227–240, 2015.

[42] Y. J. Jang, S. Jeong, and Y. D. Ko, “System optimization of the On-Line Electric Vehicle operating in a closed environment,” *Comput. Ind. Eng.*, vol. 80, pp. 222–235, 2015.

[43] Y. J. Jang, E. S. Suh, and J. W. Kim, “System architecture and mathematical models of electric transit bus system utilizing wireless power transfer technology,” *IEEE Syst. J.*, vol. 10, no. 2, pp. 495–506, 2015.

[44] M. Fuller, “Wireless charging in California: Range, recharge, and vehicle electrification,” *Transp. Res. Part C Emerg. Technol.*, vol. 67, pp. 343–356, 2016.

[45] R. Riemann, D. Z. W. Wang, and F. Busch, “Optimal location of wireless charging facilities for electric vehicles: flow-capturing location model with stochastic user equilibrium,” *Transp. Res. Part C Emerg. Technol.*, vol. 58, pp. 1–12, 2015.

[46] Z. Chen, W. Liu, and Y. Yin, “Deployment of stationary and dynamic charging infrastructure for electric vehicles along traffic corridors,” *Transp. Res. Part C Emerg. Technol.*, vol. 77, pp. 185–206, 2017.

[47] Y. M. Nie and M. Ghamami, “A corridor-centric approach to planning electric vehicle charging infrastructure,” *Transp. Res. Part B Methodol.*, vol. 57, pp. 172–190, 2013.

[48] F. He, Y. Yin, and J. Zhou, “Integrated pricing of roads and electricity enabled by wireless power transfer,” *Transp. Res. Part C Emerg. Technol.*, vol. 34, pp. 1–15, 2013.

[49] S. D. Manshadi, M. E. Khodayar, K. Abdelghany, and H. Üster, “Wireless charging of electric vehicles in electricity and transportation networks,” *IEEE Trans. Smart Grid*, vol. 9, no. 5, pp. 4503–4512, 2017.

[50] N. A. Heckert *et al.*, “Handbook 151: NIST/SEMATECH e-Handbook of Statistical

Methods," 2002.

[51] K. E. Train, *Discrete choice methods with simulation*. Cambridge university press, 2009.

[52] M. Sarrias, "Discrete choice models with random parameters in R: The Rchoice Package," *J. Stat. Softw.*, vol. 74, no. 10, pp. 1–31, 2016.

[53] M. A. Hearst, S. T. Dumais, E. Osuna, J. Platt, and B. Scholkopf, "Support vector machines," *IEEE Intell. Syst. their Appl.*, vol. 13, no. 4, pp. 18–28, 1998.

[54] M. A. Friedl and C. E. Brodley, "Decision tree classification of land cover from remotely sensed data," *Remote Sens. Environ.*, vol. 61, no. 3, pp. 399–409, 1997.

[55] A. Liaw and M. Wiener, "Classification and regression by randomForest," *R news*, vol. 2, no. 3, pp. 18–22, 2002.

[56] Y. Sheffi, *Urban transportation networks*, vol. 6. Prentice-Hall, Englewood Cliffs, NJ, 1985.

[57] H. K. Lo and A. Chen, "Traffic equilibrium problem with route-specific costs: formulation and algorithms," *Transp. Res. Part B Methodol.*, vol. 34, no. 6, pp. 493–513, 2000.

[58] D. Wu, Y. Yin, and S. Lawphongpanich, "Pareto-improving congestion pricing on multimodal transportation networks," *Eur. J. Oper. Res.*, vol. 210, no. 3, pp. 660–669, 2011.

[59] D. Z. W. Wang and H. K. Lo, "Global optimum of the linearized network design problem with equilibrium flows," *Transp. Res. Part B Methodol.*, vol. 44, no. 4, pp. 482–492, 2010.

[60] J. G. Wardrop and J. I. Whitehead, "Correspondence. some theoretical aspects of road traffic research.," *Proc. Inst. Civ. Eng.*, vol. 1, no. 5, pp. 767–768, 1952.

[61] L. Yong, "Nonlinear complementarity problem and solution methods," in *International*

Conference on Artificial Intelligence and Computational Intelligence, 2010, pp. 461–469.

[62] P. L. C. Coelho, "Linearization of the product of two variables," *Canada Res. Chair Integr. Logist.*, 2013.

[63] M. Dey and M. A. Loewenstein, "How many workers are employed in sectors directly affected by COVID-19 shutdowns, where do they work, and how much do they earn?," *Mon. Labor Rev.*, pp. 1–19, 2020.

[64] P. Iora and L. Tribioli, "Effect of ambient temperature on electric vehicles' energy consumption and range: Model definition and sensitivity analysis based on nissan leaf data," *World Electr. Veh. J.*, vol. 10, no. 1, p. 2, 2019.

[65] Y. Chen and Y. Perez, "Business model design: lessons learned from Tesla Motors," in *Towards a Sustainable Economy*, Springer, 2018, pp. 53–69.

[66] M. Muratori, E. Kontou, and J. Eichman, "Electricity rates for electric vehicle direct current fast charging in the United States," *Renew. Sustain. Energy Rev.*, vol. 113, p. 109235, 2019.

APPENDIX A

APPENDIX TABLE: VARIABLE TABLE

Parameters	
$G(N, A)$	The network; N is the set of nodes and A is the set of links.
a	A link with starting node i and ending node j, and $a = (i, j) \in A$. (The links on the graph are directed.)
W	The set of O-D pairs and w is one O-D pair on the road network, $w \in W$.
g_s^w	The demand of charging station for the O-D pair w
g_l^w	The demand of charging lane for the O-D pair w
g^w	The total demand for the O-D pair w
P^w	The set of paths between O-D pair w. p denotes one path.
$A(p)$	The set of links belonging to path $p \in P^w$
$N(p)$	The set of nodes belonging to path $p \in P^w$
$\widehat{P_s^w}$	The set of station-based usable paths of O-D pair w.
s	One station-based usable path. $s \in \widehat{P_s^w}$
L_s	The length of path $s \in \widehat{P_s^w}$
$\widehat{P_l^w}$	The set of lane-based usable paths of O-D pair w.
l	One lane-based usable path. $l \in \widehat{P_l^w}$
L_l	The length of path $l \in \widehat{P_l^w}$
L_a	The length of link a.
t_a^0	The free flow travel time.
c_a	The capacity of link a.
$\delta_{a,p}$	Path-link incidence, where the value equals to 1 if path p passes the link a and 0 otherwise.
E_0	The initial SOC of the BEVs.
E_1	The minimum SOC drivers try to maintain.
E_2	The maximum battery size.
Ω	The distance of one-unit electricity can travel (we assumed that the energy consumption is only related to the travel distance, so Ω is a constant).

E_l	The charging speed of charging lane per unit time
E_s	The charging speed of charging station per unit time.
Γ_l	The electricity cost of charging lane
Γ_s	The electricity cost of charging station.
V	The value of travel time
C_l	The cost to construct one mile of charging lane.
C_s	The cost to construct one charging station.
Ψ	The total budgets to build all the charging facilities.
Variables	
v_a	The flow on the link a
t_a	The travel time of one link a
f_s^w	The flow on the path $s \in \widehat{P_s^w}$ for electric vehicles using charging stations
f_l^w	The flow on the path $l \in \widehat{P_l^w}$ for electric vehicles using charging lanes
f_p	the traffic flow on path $p \in P^w$.
c_s^w	The cost of path $s \in \widehat{P_s^w}$ of one vehicle
c_l^w	The cost of path $l \in \widehat{P_l^w}$ of one vehicle
μ_1^w	The cost of charging station paths at user equilibrium for OD pair $w \in W$
μ_2^w	The cost of charging lane paths at user equilibrium for OD pair $w \in W$
s_a^p	The charging time of BEVs on charging link $a \in A$ of path $p \in P^w$
τ_i^p	The charging time of BEVs on charging station $i \in N$ along the path $p \in P^w$.
L_i^p	The SOC in leaving the node $i \in N$ along the path $p \in P^w$
l_i^p	The SOC in entering the node $i \in N$ along the path $p \in P^w$.
x_a	Binary variable, whether to build a charging lane on link $a \in A$.
y_i	Binary variable, whether to build a charging lane on link $i \in N$.
Additional Variables in Solution Algorithm of Deterministic Traffic Assignment Model	
M	A very large positive constant
σ_s^w	A binary variable. $\sigma_s^w = 1$ if $f_s^w = 0$ and $\sigma_s^w = 0$ if $f_s^w > 0$
σ_l^w	A binary variable. $\sigma_l^w = 1$ if $f_l^w = 0$ and $\sigma_l^w = 0$ if $f_l^w > 0$
A_n^a, B_n^a	Coefficients in each segment of separating travel time of link a

$K_{a,n}$	A set of values to partition the flow on each link a
$\xi_{a,n}$	A binary variable, $\xi_{a,n} = 0$ if $v_a \geq K_{a,n}$; $\xi_{a,n} = 1$ otherwise
Power Grid Parameters	
$G_E(L, K)$	The power grid, where K denotes the set of buses in the power grid. L is the set of transmission lines in the system.
A_k, B_k	The lower and upper real power limit in a bus k
Θ_k	The regular real power load in a bus k, which is given in our model.
R_{km}	The thermal limit of real power flow in the transmission n line from bus k to bus m.
D_{km}	The inverse of the pu reactance.
$\Lambda_{k,l}$	The set of links powered by the bus k
$\Lambda_{k,s}$	The set of nodes powered by the bus k
Power Grid Variables	
φ_k	The real power in a bus k
δ_k	The base apparent power and voltage angle (in radians) in bus k
h_{km}	The power flow in transmission line from bus k to bus m
$Z(\varphi_k)$	The total cost of generating φ_k amount of electricity at bus k

VITA

Xiasen Wang is a Ph.D. in transportation engineering at the University of Washington. He got his MS degree in transportation engineering from the University of Illinois at Urbana Champaign in 2014 and BS degree from the Tongji University in 2013. His research interests mainly focus on deployment of charging infrastructures, especially the DC fast charging stations and dynamic charging lanes. In particular, he is interested in car sharing, optimization algorithms, and intelligent transportation systems to explore how they could support the transportation system and lifes.